Faculty
Engineering

Development of a basic design tool for Multi-Effect Distillation plant evaporators

H Bogaards BEng

Dissertation submitted in partial fulfilment of the requirements for the degree *Master of Engineering (Nuclear)* at the Potchefstroom Campus of the North-West University

Supervisor: Dr BW Botha

May 2009

NORTH-WEST UNIVERSITY
YUNIBESITI YA BOKONE-BOPHIRIMA
NOORDWES-UNIVERSITEIT

Executive Summary

A need was identified for a set of basic design tools for Multi-Effect Distillation (MED) plant evaporators. This led to an investigation into the different types of evaporators as well as further research on horizontal falling film evaporators as used in the MED process. It also included the theory on these types of evaporators. In order not to duplicate existing design tools, an investigation was also performed on some of the tools that are currently available.

The first set of tools that were developed were tools, programmed in EES (Engineering Equation Solver), for the vacuum system and the evaporator. These programs can be used to simulate different parameters (like different mass flows and temperatures). That enables the correct selection of components for the vacuum system and can be used to address sizing issues around the evaporator. It can also be used to plan the layout of the plant.

The second of the design tools was developed by designing and building a flow pattern test section. From the flow pattern test section a set of curves for the wetted length under different conditions was obtained which can be used in order to design the sieve tray. This set of curves was found to be accurate for municipal as well as seawater and can be used in the design of the sieve tray of the evaporator.

Further development can be done by implementing the figures of the wetted length into a simulation package like, for example, Flownex (a system CFD (Computational Fluid Dynamics) code that enables users to perform detail design, analysis and optimization of a wide range of thermal-fluid systems). The background gained from the study done on the evaporator can also be implemented into such a package. This could solve the problem of different design packages by creating a single design package with all of the above mentioned options included.

Acknowledgements

I would like to thank the following people and organizations.

- THRIP and M-Tech Industrial for providing the much needed financial support to pursue this work.
- Riaan de Bruyn at M-Tech Industrial for his problem-solving skills and his help on the test section.
- Philip de Vos at M-Tech Industrial for his help on the EES program
- Dr Barend Botha for his valuable advice.
- My lovely fiancé who had to listen to my continuous ramblings. Thank you for all the support.
- My parents who stood by me through all the troublesome times. Thank you for the love and always believing in me.
- My Creator to whom I will forever be in indebted.

Declaration

I, the undersigned, hereby declare that the work contained in this project is my own original work.

_____

Henk Bogaards

Date: 8 May 2009

Potchefstroom

TABLE OF CONTENTS

LIST OF FIGURES

LIST OF TABLES

List of Symbols

A	Area [m^2]
A_i	Inner surface area of tube [m^2]
a_L	Thermal diffusivity of the liquid [m^2/s]
A_m	Mean surface area [m^2]
A_o	Outer surface area of tube [m^3]
BPE	Boiling point elevation
C	Brine specific heat [J/kg K]
C_{max}	Maximum value of specific heat [J/kg K]
C_{min}	Minimum value of specific heat [J/kg K]
Cp_{brine}	Brine specific heat [J/kg K]
c_{pL}	Liquid specific heat [J/kg K]
C_{pL}	Liquid specific heat [J/kg K]
Cp_L	Liquid specific heat [J/kg K]
C_r	Ratio constant
D	Evaporator diameter [m]

d_i	Tube inner diameter [m]
d_o	Tube outer diameter [m]
d_p	Droplet detachment diameter [m]
f	Friction factor
$f_{DW,i}$	Darcy Wisebach factor
FF	Fouling factor
g	Acceleration due to gravity [9.81 m/s^2]
H	Entropy
h	Height [m]
H_c	Enthalpy of condensate [J/kg]
H_f	Enthalpy of fluid [J/kg]
hfg	Heat of vaporization
	Average heat of vaporization [J/kg]
h_i	Heat transfer coefficient for vapour condensation inside the horizontal tubes [J/kg]
h_{LG}	Latent heat of vaporization [J/kg]
h_o	Heat transfer coefficient for horizontal falling film boiling of the brine [J/kg]
H_s	Enthalpy steam [J/kg]
h_u	Heat transfer constant [J/kg]
H_v	Enthalpy vapour [J/kg]
Ja	Jacob number
K_1	Constant
K_2	Constant
k_f	Fluid thermal conductivity [W/m K]
k_g	Vapour thermal conductivity [W/m K]
k_L	Liquid thermal conductivity [W/m K]
L	Length [m]
L_{dev}	Developing length [m]
m	Mass [kg]
m_b	Mass of condensate [kg]
m_e	Mass of brine at exit [kg]
m_f	Mass of ingoing recycled brine [kg]

m_g	Mass of vapour [kg]
m_i	Mass of flowing in [kg]
m_l	Mass of liquid [kg]
m_m	Mass of flashing steam [kg]
m_s	Mass flow rate of steam [kg/s]
m_{si}	Mass flow rate of steam flowing in [kg/s]
m_{so}	Mass flow rate of steam flowing out [kg/s]
	Mass flow of steam [kg/s]
m_v	Mass flow rate of vapour [kg/s]
n	Exponent
n	Number of tubes
NEA	None-equilibrium allowance
NTU	NTU – Method (Number of Transfer Units)
Nu	Nusselt number
p	Pressure [kPa]
p_b	Pressure of condensate [kPa]
p_c	Center pitch [m]
p_e	Pressure of brine at outlet [kPa]
p_g	Pressure of recycled brine at outlet [kPa]
p_h	Pressure of flashing steam from brine pool [kPa]
p_l	See figure
p_m	Pressure of flashing steam from condensate pool [kPa]
Pr	Prandtl number
q	Heat transfer [W]
Q	Volume flow rate [m^3/hr]
q_0	Heat transfer [W]
Q_l	Heat transfer at steam side [W]
	Heat transfer [W]
q_s	Heat transfer at steam side [W]
Re	Reynolds number
Re_{steam}	Reynolds number for steam
Re_Γ	Film Reynolds number
R_f	Fouling resistance

s_e	Entropy of outgoing brine [J/K]
s_g	Entropy of recycled outgoing brine [J/K]
T	Temperature [K]
$T_{brine,i}$	Inlet brine temperature [K]
T_c	Temperature of produced steam [K]
$T_{c,i}$	Temperature of outgoing flow of condensate from the effects [K]
$T_{c,i-1}$	Upstream temperature of condensate [K]
T_g	Temperature of vapour [K]
T_h	Temperature of flashing steam from brine pool [K]
T_l	Temperature of recycled condensate at outlet [K]
T_m	Temperature of flashing steam from condensate pool [K]
T_s	Surface temperature [K]
T_{sat}	Saturation temperature [K]
$T_{steam,i}$	Inlet steam temperature [K]
T_w	Wall temperature [K]
U	Overall heat transfer coefficient
UA	Heat transfer duty
V	Velocity [m/s]
v	Kinematic viscosity [m^2/s]
v_{steam}	Steam kinematic viscosity [m^2/s]
We	Weber number
x	Mass fraction
x_f	Mass fraction of fluid
Z	Constant
α_i	Inner effective heat transfer per unit area
α_{mean}	Mean heat transfer coefficient [W/m^2 K]
α_{nb}	Nucleate boiling heat transfer coefficient [W/m^2 K]
α_o	Outer effective heat transfer per unit area
α_Γ	Falling film heat transfer coefficient [W/m^2 K]
$\alpha_{\Gamma,dev}$	Developing region falling film heat transfer coefficient [W/m^2 K]
$\alpha_{\Gamma,lam}$	Laminar falling film heat transfer coefficient [W/m^2 K]
$\alpha_{\Gamma,turb}$	Turbulent falling film heat transfer coefficient [W/m^2 K]
Γ_L	Liquid flow rate per unit length on plate or one side of tubes [kg/m

	s]
$\Gamma_{L,trans}$	Transition liquid flow rate per unit length on plate or one side of tube [kg/m s]
δ	Liquid film thickness [m]
Δp	Pressure drop [kPa]
$\Delta p_{steam,max}$	Maximum steam pressure difference [kPa]
ΔT_f	Temperature difference of fluid [K]
ΔT_{max}	Maximum temperature difference [K]
Δx	Change in mass fraction
ε	Heat exchanger effectiveness
λ_s	Latent heat
λ_T	Taylor wavelength
μ_L	Liquid dynamic viscosity [Ns/m^2]
μ_{steam}	Steam dynamic viscosity [Ns/m^2]
v_g	Vapour kinematic viscosity [m^2/s]
v_L	Liquid kinematic viscosity [m^2/s]
ρ	Density [kg/m^3]
ρ_f	Fluid density [kg/m^3]
ρ_g	Gas density [kg/m^3]
ρ_L	Liquid density [kg/m^3]
ρ_{steam}	Steam density [kg/m^3]
σ	Surface tension [N/m]
σ_i	Inner free flow area
σ_o	Outer free flow area
χ	Vapour mass fraction

1. Introduction

1.1 Introduction

High Temperature Reactor (HTR) development has proven to be very suitable for generating process heat. This heat can be employed in various ways to increase cycle efficiency or to expand the market for such HTR technology. One such possible application is that of desalination.

Roughly 70% of the earth is covered with water of which only 2.5% is fresh water (Anon, 2006). The fast growing global population, as well as industrial development, is increasing the demand for fresh water globally, therefore putting increasing pressure on the supply thereof. People are becoming more aware of the critical limitations to ensure the availability of fresh water. This increasing demand may therefore soon result in an inadequate amount of fresh water. The problem is intensified by an increase in both salinity and pollution of the resources. It is therefore important to look at the conservation and preservation of existing sources as well as finding alternative water resources. One major potential source is using desalination to produce fresh water from seawater. The question thus is: which option exists that enables one to practise desalination as cost effectively as possible? In their attempt to gain knowledge and assist in addressing the growing need, the North-West University has identified a number of projects to investigate the different aspects of desalination. One such identified need is a tool or set of tools for the basic design of desalination plant components.

The most important step in this process is to identify which components are essential for performing a basic sizing (to determine the size of the required components) of a desalination plant. For this, some knowledge is required of the different desalination processes and their essential components.

1.2 Background

The Pebble Bed Modular Reactor (PBMR) is an advanced helium-cooled graphite moderated high-temperature nuclear reactor of which the heat can be used to produce electricity or it can be applied to a variety of process heat applications. The 165 MWe PBMR Demonstration Power Plant (DPP) under development rejects about 220 MW of waste heat through the pre- and inter-cooler at about 70°C and is well suited for coupling with a desalination plant. This waste heat is well suited to be used for desalination because heat is needed in the process. It can even improve the overall energy efficiency of the PBMR because less energy is wasted resulting in a higher overall efficiency. A PBMR can therefore be useful to produce electricity and clean and fresh water for areas in need by having a desalination plant coupled to it.

Striving towards finding the optimum desalination process has resulted in a number of desalination techniques being available currently. These techniques can all be sorted according to the saline process separation, namely membrane filtration or evaporation. Currently, techniques based on evaporation are the most widely used and of these, the two most common processes are the Multistage Flash (MSF) and Multi-Effect Distillation (MED) processes (Anon. 2006). Both these processes utilize heat as energy source. The most common technique for membrane filtration is Reverse Osmosis (RO), which, although not limited to it, mainly utilizes electrical energy. These processes can be summarized as follows:

1.2.1 Multi-Effect Distillation (MED)

Multi-Effect Distillation is one of the oldest evaporative processes. In each stage (or effect) heat is transferred from condensing water vapour on one side of a tube bundle to the evaporating brine on the other side of the tubes. This is a process which is repeated continuously in each of the stages by pumping the brine from stage to stage. This happens at progressively lower pressure and temperature. In the last effect (at the lowest pressure) the vapour condenses in the heat rejection heat exchanger, which is cooled by seawater. The condensed distillate is then recovered. Major components found in this

process include heat exchangers, pumps (normal and vacuum) and pipeline networks (for the brine and the distillate) (Anon. (2006)).

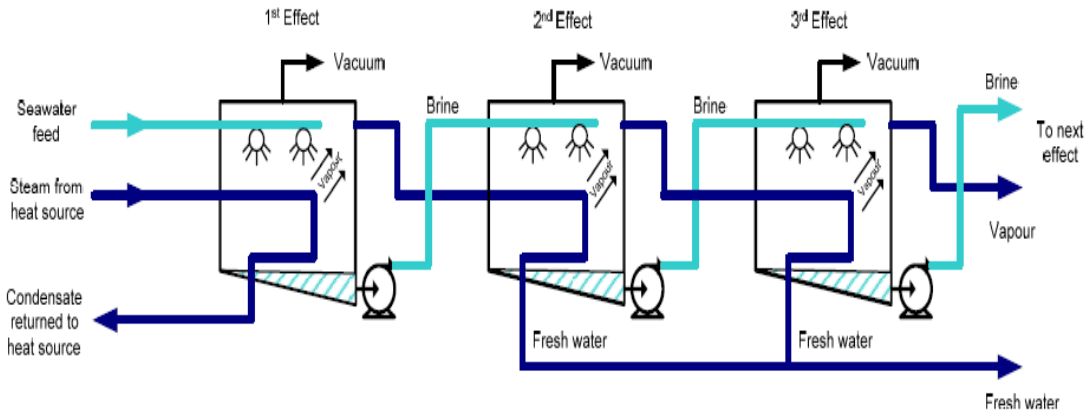

Figure 1.1: *Schematic representation of the Multi-effect Distillation process (Anon. (2006))*

1.2.2 Multi-Stage Flash (MSF)

In Multi-Stage Flash, seawater is passed through tubes in each evaporation stage where it is progressively heated. Final heating of the seawater takes place in the brine heater, which is a steam heat exchanger. The heated brine flows into the first stage through nozzles. The stage is kept at a pressure lower than the pressure of the incoming steam. As a result, a small fraction of the brine flashes forms pure steam. The heat to flash the vapour comes from the cooling of the remaining brine flow. This lowers the temperature of the brine. Vapour is passed through a mesh demister in the upper chamber of the evaporation stage. Here it condenses on the brine tubes and is then collected in a distillate tray. The transferred heat warms the incoming seawater as it passes through. Now the remaining brine passes successively through the stages at progressively lower pressures. The hot distillate is pumped from stage to stage. It is cooled by flashing a portion into steam, which then re-condenses on the outside of the tubes (Anon (2006)). Typical components found in this process are once again pumps, heat exchangers (evaporators) and pipeline networks (for the brine and the distillate).

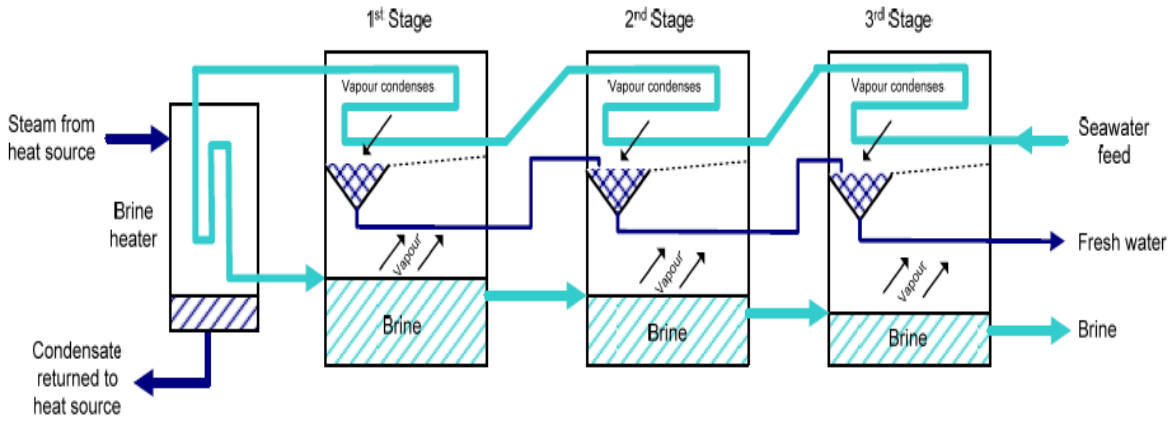

Figure 1.2: *Schematic representation of the Multistage Flash Desalination Process (Anon. 2006)).*

1.2.3 Reverse Osmosis (RO)

Reverse Osmosis (RO) is a process in which a semi-permeable membrane forms the core of the desalination process. Pure water passes from the high-pressure seawater side of a semi-permeable membrane to the pure water side of the membrane. In order to overcome the natural osmotic process, the seawater side of the system has to be pressurized to create a sufficiently high net driving pressure across the membrane. RO systems require stringent feed water pre-treatment in order to protect the membranes from effects such as scaling and fouling (Anon. (2006)). Components found in this process are pipeline networks, high pressure pumps, and pressure regulating devices and membranes modules.

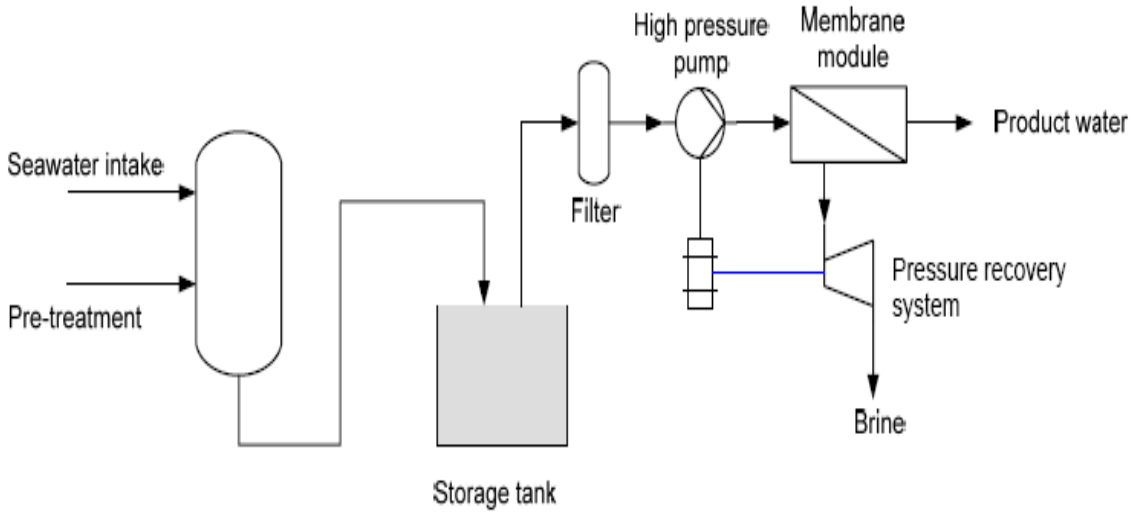

Figure 1.3: *Schematic representation of the Reverse Osmosis Process (Anon. (2006))*

It can be seen from these processes, the most suitable one for use with the PBMR (for the case of utilization of waste heat) is the MED process. This is due to the fact that there is a huge amount of waste heat available at low temperatures which is ideal for use with the Low Temperature MED (LT-MED) process. The MED process, which was discussed earlier, further consists of various subsystems such as the pre-treatment, post-treatment, evaporator and vacuum system.

1.3 Problem Statement

From the above it can be seen (because of the heat available at low temperatures) that the use of the different processes described will be influenced by the available energy source. When large amounts of waste heat is available, such as is common with a power generating plant for example, the option exists to use one of these processes in combination with the generator, thus increasing the overall cycle efficiency for utilizing the input energy of the system. The potential of the MED process to be applied in such conditions, especially when the waste heat temperature is not too high, makes it an option to consider. It was subsequently decided to focus, for the purpose of this study, on improving the ability for performing basic sizing of MED components.

The MED process consists of various subsystems such as the pre-treatment, post-treatment, evaporator and vacuum system. Each of these has sufficient complexity that they can be the subject of an independent study. As groundwork for further research, the need to do basic sizing of the evaporator was identified to be one of the key elements to doing basic plant sizing.

1.4 Objective

The purpose of this study is therefore to develop a design tool or a set of tools that can be used for basic sizing of an evaporator to be used in an MED desalination plant given the process and operating conditions. In this study, important parameters will be identified and effects such as the wetted length (the length of the tube that is covered by water) and tube layout will be addressed.

1.5 Method of Approach

A detailed literature study was performed to identify previous work performed on developing similar tools or identifying the important parameters. Hereafter a suitable platform for developing the tool was chosen. A case study was then implemented using the tool to show its ability. A test bench was also developed to confirm the impact of fresh water versus salt water on the wetted length and required layout of the tube bundles experimentally.

1.6 Chapter Lay-out

Chapter 1 gives an overview of the problem to be addressed in this project. In the next chapter a literature survey is done. This is executed by investigating previous work and the problems that were encountered before. Also discussed are the different types of evaporators currently available. In Chapter 3 evaporator modelling and falling film evaporation are investigated. The theory on falling film evaporators is also discussed in

this chapter. Furthermore, the MED stage component and MED stage thermodynamics are explained in this chapter.

In Chapter 4, the EES (Engineering Equation Solver) simulation for the evaporator is explained step by step and the theory behind it is also clarified. This approach is also followed in the explanation of the EES simulation of the vacuum system. For a better understanding of these simulations, a case study for both the evaporator system and vacuum system is done. The case studies clearly show what the input parameters will be and give an indication of the output parameters. Information obtained from the simulations can then be used to address design issues.

Chapter 5 details how a flow pattern test section was designed and used to obtain data regarding the wetted length and the flow over the tubes. The tests, which were done using the flow pattern test section, were done at different temperatures and different pressures. Another parameter that can be changed in the test section is the tube diameter and layout. From the tests, figures were obtained that can be used when designing the sieve tray for the evaporator.

In Chapter 6 some conclusions regarding the study are drawn and recommendations are made for future work.

1.7 Conclusion to Chapter 1

The increasing need for fresh water has resulted in increased effort in finding alternative methods of obtaining this. One such an effort is that of desalination. The availability of waste heat from various processes offers a potential to use the MED process to produce fresh water and increase process efficiency. The aim of the study is therefore to develop a tool which can be used in creating a basic design of the evaporator for an MED desalination plant. Such a tool or tools will enable the designer and manufacturer to design the evaporator components and will also be of great value to the concept design of the plant. Designing a desalination plant is necessary to address the shortage of fresh

water. It is therefore essential to develop a tool or set of tools which will aid these studies by giving perspective on certain critical issues.

2. Literature Survey

In Chapter one, it was stated that the MED process would be the best option to utilize energy which is available at low temperatures. It was found that the evaporator is one of the critical components of an MED plant. There is a need for the development of a tool or set of tools in order to do a concept design of the MED plant. In order to create such a tool or set of tools the background of evaporators in an MED environment must be investigated and work done previously must also be taken into consideration.

Because of the lower temperatures found in the evaporator, the pressure has to be regulated in order for steam to form. This is normally done using a vacuum system, which necessitates some background on vacuum systems. This will enable the development of a realistic set of tools for designing an evaporator for a MED plant. This chapter presents information on research already done in the field. Relevant research includes research on different types of evaporators, boiling point research, and vacuum pump research, all of which are interrelated in their influence on the effectiveness of a desalination plan. The chapter also mentions available simulators and explains why their shortcomings necessitate the design of a new system.

2.1 Evaporators

Since the evaporator plays such an important role in the MED process, background knowledge of its working principles is necessary. It would also be good to consider briefly the different types of evaporators and how they work. From this, the best evaporator for the application in the MED process can then be chosen and further investigations can be done for this type of evaporator.

2.1.1 Evaporator Basics

In an evaporator, heat is transferred from a heating medium to a solution by conduction through a solid surface (a surface without holes). This means heat transfer takes place through the material to the surface. Heat is now transferred to the vapour as boiling of the liquid (for example water) takes place. In order to determine the heat transfer a model can

be developed for the evaporator. The model consists of heat transfer equations, overall material balance, component material balances, and energy balances.

In order to be able to develop a model to do the modelling of the evaporator, heat transfer effects have to be taken into account. These heat transfer effects include:

1. the heat transfer from condensing steam vapour to the interior of the tube wall;
2. the heat transfer through the tube wall;
3. the heat transfer through scaling or fouling on the interior wall of the tube;
4. the transfer through fouling on the exterior of the tube wall, and
5. the heat transfer to the boiling liquid.

To ensure an accurate model, all of these effects should be considered when calculating the overall heat transfer.

2.1.2 Evaporator Types

Currently, various types of evaporators are available for different purposes. The types mostly used today are the natural/forced evaporators, falling film evaporators, plate evaporators, and multiple effect evaporators. Each of these will be explained briefly.

Natural/forced evaporator:

Natural/forced evaporators are also called flooded evaporators. They work on the concept of the natural circulation of the liquid. In this type of evaporator, which uses tubes that are flooded, the liquid starts boiling, causing circulation. This boiling of the liquid facilitates the separation of the liquid and the vapour. Separation of the liquid and vapour causes natural circulation in the evaporator. In order to determine the amount of vapour (amount of evaporation) in circulation, the temperature difference between the vapour and the solution is used (Smook, 1990).

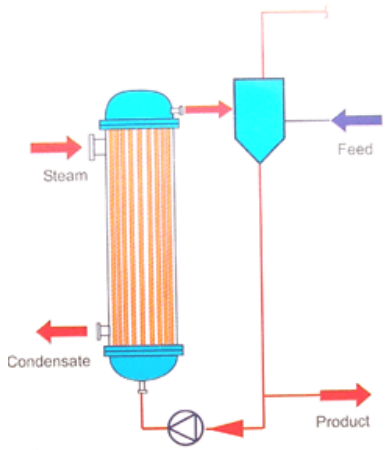

Figure 2.1: *Natural/forced evaporator (Smook, 1990)*

Falling Film Evaporators:

According to Roque and Thome (2007), falling film evaporation takes place when liquid is flowing as a film on a heated surface. This heated surface transfers the heat to the liquid causing vapour to be created. The vapour is then created at the liquid-solid interface or the liquid-vapour interface depending on the conditions and these effects can also occur simultaneously. In comparison to other evaporation processes, falling film evaporators present advantages like a reduced amount of liquid (meaning less liquid is needed to achieve a certain amount of evaporation) compared to a flooded pool, and also a pressure drop which is so low as to be negligible.

According to Chun and Seban (1971) falling film evaporators consist of tubes surrounded by steam jackets. Falling film evaporators can be divided into vertical and horizontal falling film evaporators. Chun and Seban (1971) indicate that when using these evaporators it is important that the distribution of the water over the tubes should be uniform.

Vertical falling film evaporators:

Falling film evaporators are generally built vertically. Liquid is fed on top of the arranged tube bundle and the liquid then flows down the tube walls as a film under gravity (see figure 2.2). In the majority of the designs the liquid, which has to be vaporized, flows inside the tubes. In order to balance the high heat transfer of the evaporating film,

condensing steam is often used as a heating medium. In most cases, the vapour that is generated flows concurrent with the liquid film. The pressure and the vapour flow direction are dictated by the location and temperature level of the applied condenser. In general, the liquid and vapour are separated at the bottom of the unit (Anon, 2007).

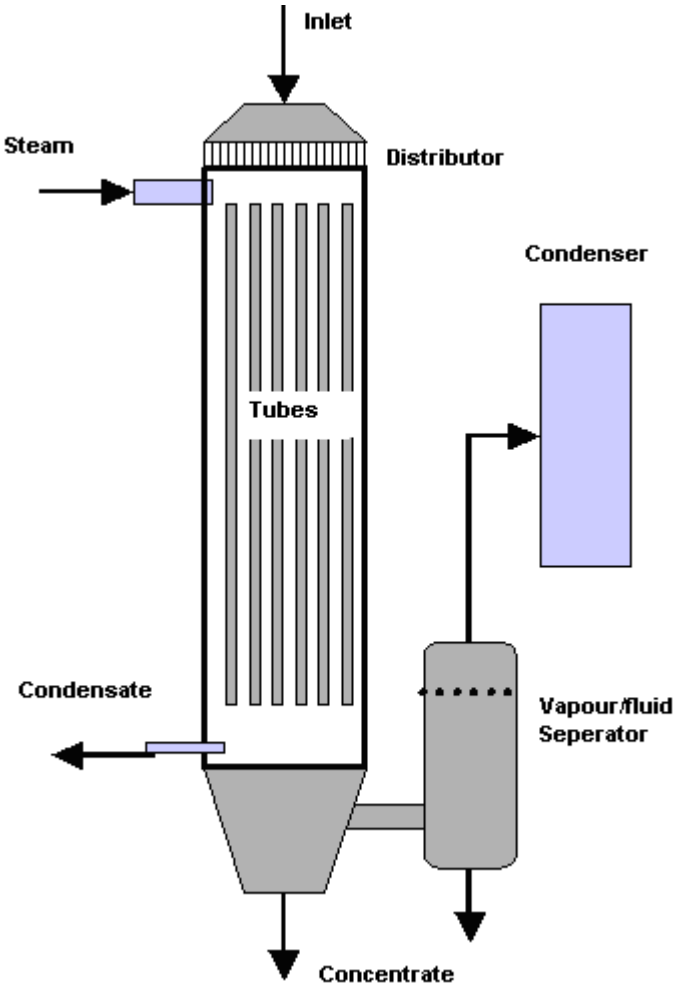

Fig 2.2: *Vertical falling film evaporator (Anon, 2007)*

Horizontal falling film evaporators:

Horizontal falling film evaporators are used mainly in applications for seawater desalination or refrigeration technology. The liquid is evaporated at the outside of the tubes. It flows from one tube to the other in the form of droplets, jets or as a continuous sheet. Due to the impinging effect when flowing from one tube to the other, the heat transfer is higher compared to vertical falling film evaporators. In addition, this type of

evaporator can be operated with lower pressure drops than vertical falling film evaporators. It is also possible to design a higher heat transfer area for a given shell in comparison with the vertical evaporators. Therefore, horizontal falling film evaporators are often used in the desalination industry (Anon, 2007).

Even distribution over the tubes is an important aspect to prevent the formation of dry patches on the tubes. Therefore perforated plates or nozzles can be used in order to obtain an even liquid distribution for each tube.

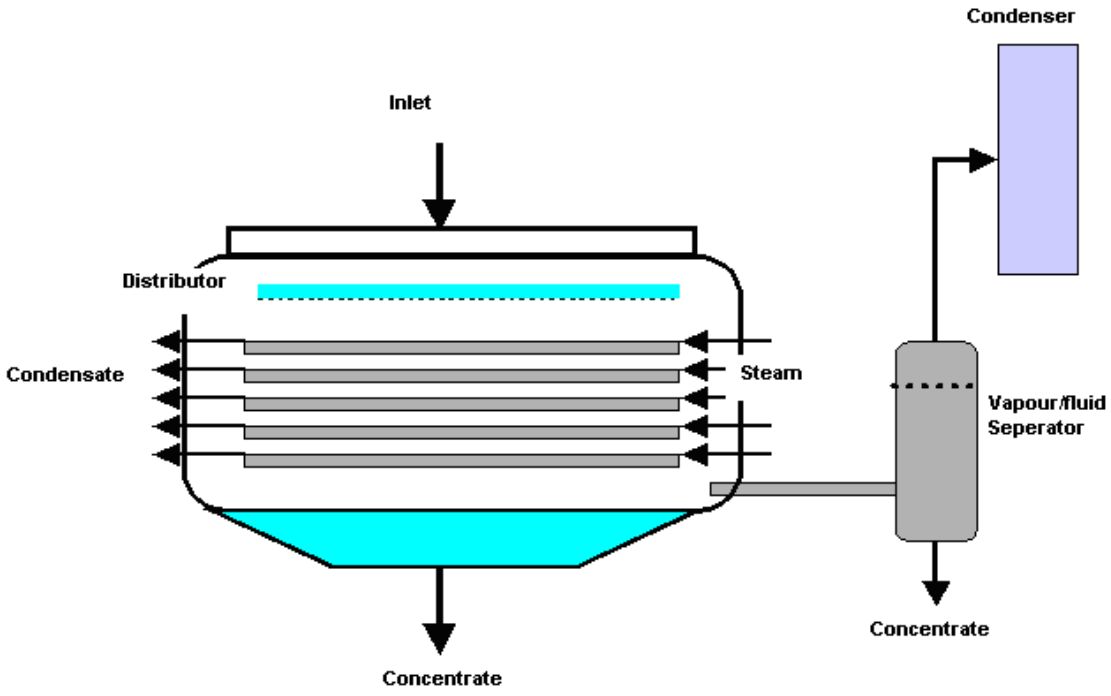

Figure 2.3: *Falling film evaporator (Anon, 2007)*

Plate evaporators:

Plate evaporators consist of corrugated plates supported by a frame. Vapour flows through the channels between the corrugated plates. The concentrate and vapour is then fed into a separation stage from where the vapour is sent to a condenser where it is condensed and the product collected. An advantage of these evaporators is that they have a large surface area, which means it has a large heat transfer area that will give good heat transfer efficiencies. A disadvantage is that the large surface area increases the setup cost

of the evaporator. A further disadvantage of plate evaporators is that they are limited in their ability to accommodate viscous products, which means it will not be suitable for the use of the evaporator in the MED process (GEA Process Engineering Inc., 2008).

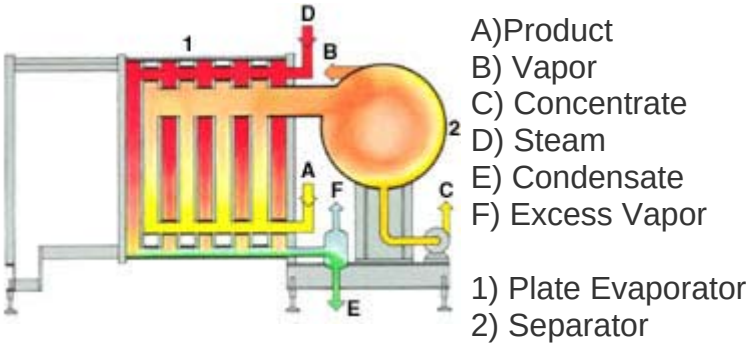

Figure 2.4: *Plate evaporator (GEA Process Engineering Inc. 2008)*

Multiple-effect evaporators:

Multiple-effect evaporators are made up of stages (effects). It has the advantage that when a combination of single evaporators is used it will require less energy. The number of effects for these evaporators is normally restricted to seven because of equipment cost.

According to the University of Michigan (2007) there are two configurations that can be used for the effects i.e. a forward feed configuration or a backward feed configuration. In a forward feed configuration, the product enters the first effect where the highest temperature is found. Here the product is partially concentrated and steam is formed and carried away. The second stage then uses the steam as heat source. In the backward feed configuration, the diluted product is fed into the last effect. In other words, in the backward feed the product enters the last effect with the lowest temperature. From here it is moved from stage to stage (University of Michigan, 2007). The advantage obtained from the stage-to-stage movement is that the heat is used over and over again which means that the system has a high heat economy. Therefore, a forward feed configuration would be suitable to use in the MED process because of the lower energy requirements than that required for a backward feed configuration.

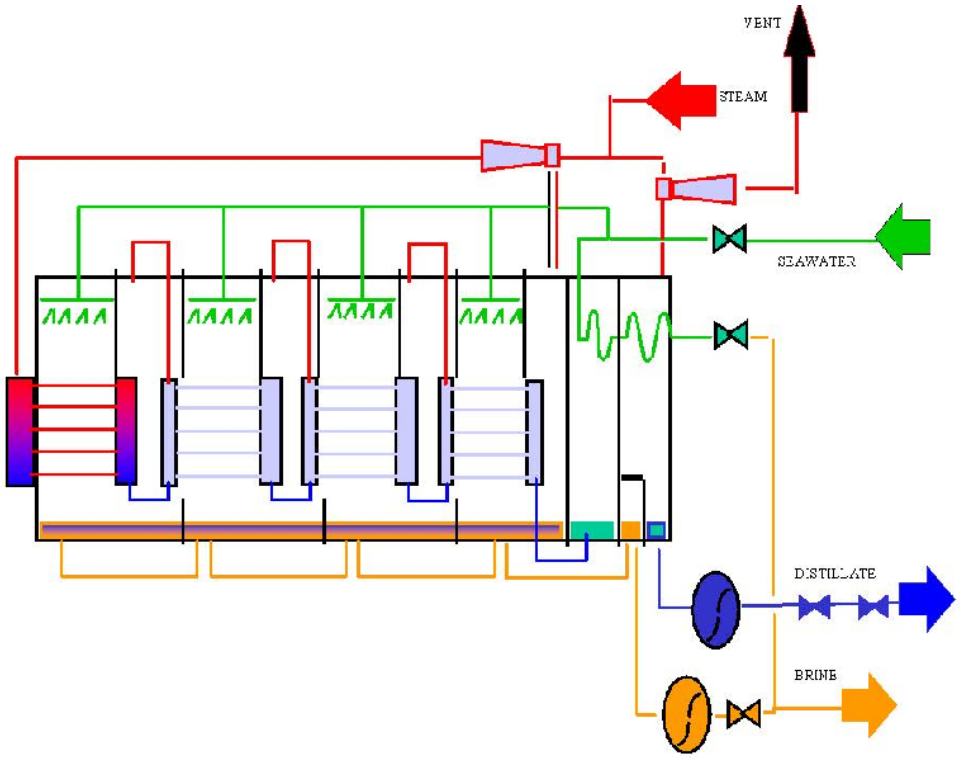

Figure 2.5: *Multiple-effect evaporator (forward feed configuration) (University of Michigan, 2007)*

Another feed configuration used in the MED process is that of parallel feed. In the parallel feed configuration multiple feed streams are created by separating the main seawater feed. Therefore the seawater flows in parallel into each effect. In the first effect vapour and liquid forms and the liquid is then collected as the product and the vapour is then used as the heat source in the next effect. The condensed vapour in each effect forms the product and the seawater not evaporated forms the brine. In the final condenser seawater is used to condense the vapour to produce fresh water. The advantage of this configuration is that the salinity concentration occurs at low temperatures which cause less fouling on the components of the desalination plant (Greyvenstein, 2007).

In order to obtain the best results using the MED process, the desalination industry mainly focuses on multiple effect evaporators with a falling film (Chun and Seban, 1971).

2.2 Falling Film Evaporation

As discussed in Chapter 1, the MED process is the most suitable for utilizing waste heat from the PBMR. Chun and Seban (1971) points out that the MED process mostly uses horizontal falling film evaporators because of the better heat transfer in comparison with the other evaporators. Considering these two findings, horizontal falling film evaporators appear to be the most applicable to this research project and will consequently be investigated further in this study.

Horizontal shell-side falling film evaporators have significant advantages, which include a higher heat transfer and a smaller need for refrigerant. This results in smaller evaporators, which is a great advantage and a better option than previous systems such as vertical tube-side falling film evaporators (Chun and Seban, 1971).

Having established that falling film evaporators are best suited for the purposes of this project, the most critical aspects of their design will now be discussed.

2.2.1 Advantages and Disadvantages

According to Thome (2004:14-3), falling film evaporators have the following **advantages**:

- They have a high heat transfer.
- Their overall heat transfer coefficient (U) is uniform.
- They have a close temperature approach.
- The design of the evaporator is compact.

Thome (*ibid.*) further indicates that the following **disadvantages** are applicable:

- There is less design experience available for falling film evaporation units than for the other types that are available.
- Distribution of liquid on the top row is not uniform.
- Tolerances for undercharging are smaller.

These advantages mean that falling film evaporators would be most suitable for use with the MED process. Further work, however, has to be done to ensure good distribution of the liquid on top brine and experiments will have to be done to address these design issues.

2.2.2 Design Consideration

Less experience and know-how is available for the design of falling film evaporators than for the other mentioned evaporator types and, according to Thome (2004:14-4), the following challenges should be considered:

- The selection of the tubes for the fluid in terms of material and diameter to ensure good heat transfer;
- The selection of the layout of the tube bundle (factors such as number of tubes, tube length, bundle width, bundle height, tube pitch, number of passes and layout of the tubes), this must be done in order to obtain optimum flow and heat transfer;
- The choice of placement for nozzles, sprinklers or distribution trays for uniform distribution of the liquid on the top rows of tubes in the bundle to ensure complete wetting of the tubes in order to prevent dry patches;
- The escape of vapour from the bundle to determine the best solution to facilitate the escape of vapour from the bundle;
- The modelling of heat and mass transfer coefficients and their effects for an optimum design.

In summary, there are numerous aspects to be considered and some of them, like the distribution system, can only be resolved with experimental tests. Therefore further tests will have to be performed in order to design the distribution system.

Various thermal mechanisms and flow characteristics should also be kept in mind. For falling film evaporation on horizontal tubes, Thome (2004:14-4) stated that the following should be considered to ensure a good design:

- Liquid modes of flow transitions between tubes should be predicted;
- Shear effects of vapour in a tube bundle on film flow of the liquid;
- Cross-flow effects of vapour on film flow;

- Nucleate boiling in the film and its onset;
- Prediction of heat transfer coefficients;
- Prediction of formation of dry patches on tubes;
- Heat flux for nucleate boiling;
- Enhancement geometry effects for the above mentioned.

All of these have an important influence on the proper operation of these units and their thermal optimisation, and essentially all require further study.

2.2.3 Modes of Falling Film

The inter tube flow modes can be classified into droplet, droplet-columns, column, column-sheet and sheet mode of which the three principle modes are droplet, column and sheet (Thome, 2004:14-6). According to Roques and Thome (2003), two intermediate transition modes (droplet-columns and column-sheet) can also be observed. The modes are defined and described by them as follows:

- The *droplet mode* is when only droplets are falling between the tubes.
- The *droplet column mode* is an intermediate mode where both droplets and columns can be found flowing side to side between the tubes.
- The c*olumn mode* is a mode where only liquid columns are flowing between the tubes.
- The *column sheet mode* is another intermediate mode where both columns and sheets can be found next to each other between the tubes. Small sheets are formed by the merging of two neighbouring columns.
- *Sheet mode* occurs when fluid flows uniformly between the tubes as a liquid film. The surface of the sheets can be disturbed by ripples and waves.

Flow progresses from droplet to sheet mode with an increase in the mass flow rate. Figure 2.5 illustrates the different modes of flow (also see Figure 2.6.). In order to allow for good movement of the vapour inside the evaporator, the required flow will have to be column or column-sheet for the purpose of desalination, since steam has to be formed and collected where after it will be condensed.

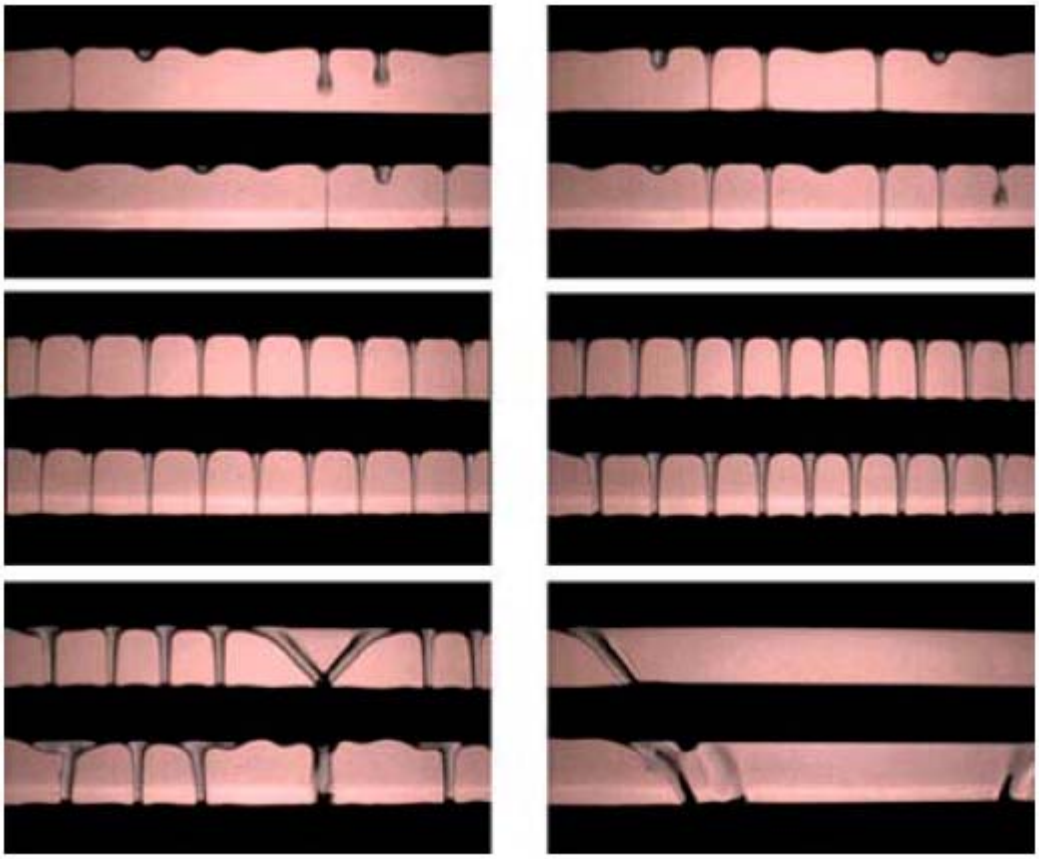

Figure 2.6: *Photographs of flow modes on plain tubes (from left to right, top to bottom): droplet, droplet-column, column (inline), column (staggered), column-sheet, and sheet. Note that the black areas represent the tubes and the light areas the gaps between the tubes (Thome, 2004)*

2.2.4 Film breakdown

Roque and Thome (2007) has highlighted the formation of dry patches on the heated surface as an important aspect of falling film evaporation. These dry patches do not transmit heat to the liquid and therefore reduces the thermal performance. Consequently, the prediction of the onset of dryout is an important design variable for this condition to be avoided. In the case for a film without nucleate boiling, dryout takes place when the film is very thin while in the case of films with nucleate boiling, dryout is caused by dry patches formed under quick growing bubbles. The following forces are listed by Gross (1994) as being involved in the formation of dry patches in thin films without nucleate boiling:

- Liquid inertial forces. The rewetting of a dry patch is favoured by the pressure created by the deceleration of the liquid at the stagnation point.
- Surface tension forces. The size of a dry patch is enlarged by the interfacial surface tension.
- Marangoni effect. A dry patch is created because of the temperature gradient in the film which causes liquid to be transported away from the thin film layer.
- Vapour inertial forces. Dry patch sizes are increased by the vapour flow that creates a suction force when going around the liquid.
- Interfacial shear stress. The effective surface coverage is increased by the vapour that tends to equalize the liquid film thickness around the tube perimeter.

2.2.5 Falling film evaporator studies

According to Roque and Thome (2007), the design of horizontal falling film evaporators composed of a horizontal tube bundle with evaporation on the shell side of the evaporator needs significant advances to be made in order to be able to do accurate sizing and to optimise these units. In large refrigeration systems, flooded evaporators are normally used for the evaporation of the refrigerants. These flooded evaporators are equipped with enhanced boiling tubes, which enhance nucleate boiling pool contribution. It is also useful to use externally enhanced boiling tubes in horizontal falling film evaporators in order to have a compact design.

Further work done on falling film evaporators:

Roque and Thome (2007) stated that an expression can be derived for laminar flow falling film evaporation on horizontal tubes that is equivalent to the Nusselt theory for film condensation. This, however, does not describe experimental results as well as it does condensation. Therefore, empirical methods are often suggested.

Most of these existing methods were developed for a single fluid (due to the lack of experimental data) and most are for plain tubes. The first method that is widely used is that of Chun and Seban (1971). They have provided correlations in order to predict heat

transfer and the threshold between laminar and turbulent flow in non-nucleate boiling conditions.

Evaporation on a horizontal tube bundle was studied by Danilova et al. (1976). This tube bundle was six rows deep and had one or three columns of plain tubes. Danilova et al. correlated their data from this tube bundle with two equations. The one equation was for vaporization-dominated heat transfer and the other one was for nucleate boiling dominated heat transfer. Roque and Thome (2007) criticises Danilova et al. According to Roque and Thome (2007), Danilova et al. did not propose a transition equation to link the two expressions and the correct value according to Danilova et al. is the larger value of the result from the two equations. This however, may lead to inaccuracies.

A simple and more complete analytical model was presented by Lorenz and Yung (1978) for falling film evaporation on a plain tube. In their model the liquid flow around the tubes are split into two regions. The two regions are a thermal developing region (region at the top in which heat is only employed to superheat the liquid) and a fully developed region (region where evaporation takes place). By adding a boiling heat transfer coefficient, they included all the nucleate boiling contributions for the entire tube. Roque and Thome (2007) state that the agreement of the method used by Lorenz and Yung compared to their (Lorenz and Yung's) own measurements with water and data from other studies were relatively good.

Numerous studies on falling film evaporation for horizontal tubes were done by Fujita and co-workers, according to Roque and Thome (2007). Further heat transfer was obtained by Fujita and Tsutsui (1994) for a pressure of 2 MPa with 25 mm horizontal tubes, a vertical tube pitch of 50 mm and R11 refrigerant. The falling film modes observed by Fujita and Tsutsui included droplets, columns, disturbed columns, and sheets. In order to determine the distribution (modes of flow) on the lower tubes they used various combinations and layouts. Fujita and Tsutsui (1994) proposed a more detailed multi-zone model than Lorenz and Yung (1978). The multi-zone model they proposed consisted of a stagnation region, impingement flow region, thermally

developing region and fully developed region. For simplicity, they have ignored the impingement region. The three-zone model can be seen in Figure 5.

One of the assumptions made by them was that the thermal boundary layer grows from the stagnation point on the top of the tube around the tube. Sensible heat is absorbed by the liquid film in the thermally developing region ($0 < \Phi < \Phi_d$). The end of this region is where the growing thermal boundary layer reaches the interface of the liquid film. In the fully developed region ($\Phi_d < \Phi$) the temperature profile changes from a 3^{rd} order polynomial profile at the beginning to a linear profile. For the larger angles up to $\Phi = \pi$, heat conducted into the film is assumed to evaporate at the interface of the film.

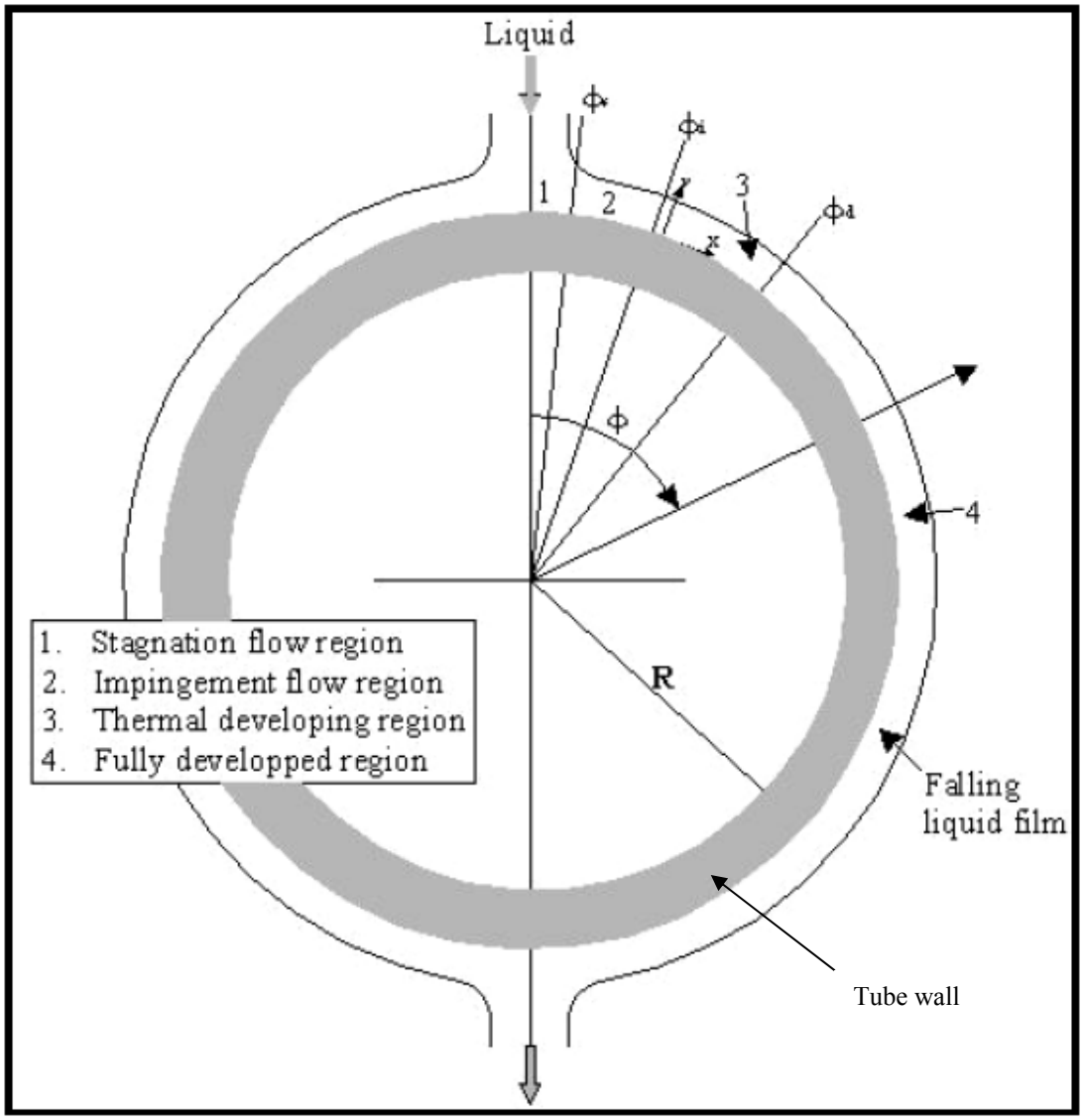

Figure 2.7: *Three-zone model of Fujita and Tsutsui (1994)*

In their study, Roque and Thome (2004) proposed that there are six parameters which have an influence on the heat transfer coefficients:

- The Reynolds number of the liquid flowing that characterizes the quantity of the liquid flow.
- The flow mode of the liquid (as was discussed in section 2.2.4 of this study).
- The heat transfer coefficients of nucleate boiling when occurring in the liquid film.

- The force that accelerates the flow of the liquid is controlled by the tube pitch between the tubes. This also controls the impingement velocity at the top of the tubes. It also has an indirect effect on the liquid flow mode.
- The threshold of breakdown of the film. When the film breaks up dry patches appear. These dry patches will reduce the heat transfer coefficients.
- The placement of the tubes should be such that it will prevent the formation of dry patches on top of them. It should be placed such that it is fully wetted.

Roque and Thome conclude that the heat transfer coefficients above the onset of the dryout threshold are almost insensitive to the film Reynolds number. It only has an influence of 3% or less on average.

Based on their new method, Roque and Thome proposed that it is possible to use an incremental approach. In this approach, the local heat transfer coefficient depends on the local film Reynolds number of the liquid arriving on the top of the particular tube in the array at the axial location. Their results further show that there is a transition to partial dryout as the film Reynolds number is reduced, marked by a sharp decrease in heat transfer. Except for this transition, the heat transfer coefficient is nearly insensitive to the film Reynolds number as was discussed earlier.

Roque and Thome provide no method to predict the onset of dry patches for horizontal falling films over the tubes. This means that there is a need for experiments to be done in order to be able to design the distribution system so that the formation of dry patches is prevented. This thus means that there is a need for a tool which can determine the wetted length of the tubes caused by the brine distribution system.

2.2.6 Brine distribution system

The method of distributing the brine over an evaporator is important to ensure that the tubes are completely wetted in order to prevent scaling. The brine can be distributed over the tubes by sieve trays or by nozzles Anon (1990:12).

If nozzles are used, there will be a higher pressure drop, which would require more pumps. In order to minimize the number of pumps a sieve tray design can be used as it allows for a design with only one major pump in the brine distribution system (discussion with Mr. R. de Bruyn, 2007). Brine will flow through the further evaporation stages under gravitational force. This section will give a short summary of these two techniques.

2.2.6.1 Brine distribution by sieve trays

Sieve trays have two functions:

- It provides for good distribution of the brine; and
- it helps to compensate for the trans-stage difference in pressure to avoid vapour blow-through.

The ratio between the total area of the sieve hole and the sieve tray is small (Anon., 1990:12).

The wetted length of the tube for each hole is a function of liquid properties, pressure difference, and the diameter of the tube and the hole. Figure 2.8 shows the wetted length for a 38 mm tube diameter as a function of temperature. It also indicates the effect of the diameter of the hole and pressure difference. This type of figure can be used to determine the number of holes as well as the spacing of the holes.

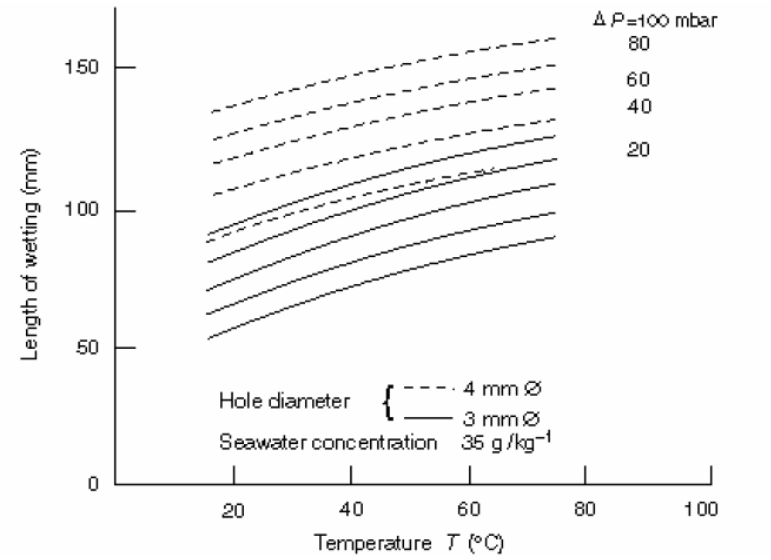

Figure 2.8: *Wetting lengths for a single hole for a horizontal tube (38 mm) (Arzt, 1984)*

Placement of the holes must be above the centre-line of the tubes of the bundle. The wetted length of a hole must be used to determine the spacing of the holes. Spacing of the holes should be equal to (or less than) the wetted length. Figure 2.9 shows an arrangement of a sieve tray above a tube bundle (Anon., 1990:13).

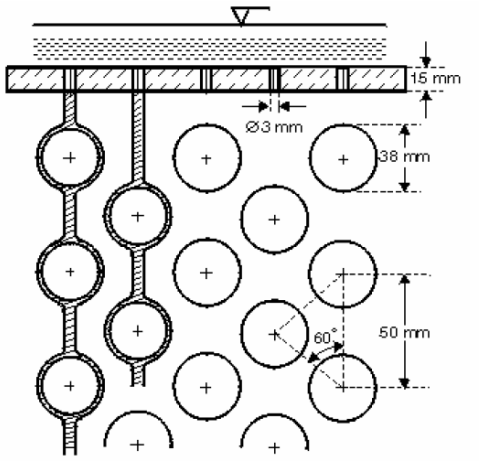

Figure 2.9: *Typical arrangement of a sieve tray above a tube bundle (Anon., 1990:14)*

2.2.6.1 Brine distribution by nozzles

A certain amount of overspray is present when nozzles are used because of their circular spray pattern. This results in an improper distribution of the brine on the top of the bank of tubes. This is a problem especially in large evaporators, although a large number of nozzles would minimize the problem. However, the number of nozzles must be minimized in order to obtain a simple distribution system. The distribution is good for all the tube rows except for the top row. A countermeasure that can be taken is to plug the top row and use these tubes only for distribution and not evaporation (Anon., 1990:14).

2.2.7 Discussion of falling film evaporation

Two mechanisms control the falling film heat transfer, evaporator film coefficient and nucleate boiling heat transfer coefficient if present. Vapour at the surface of the liquid is created by film evaporation while liquid in the film is evaporated by nucleate boiling. The flow is laminar or turbulent with or without interfacial ripples. Intense nucleate boiling could cause dry patches to form on the tubes.

Experiments have been done for different fluids to determine the heat transfer for horizontal tubes. The tubes that were used in these experiments are plain, low finned, enhanced boiling, and enhanced condensation tubes. Single tubes as well as tube bundles were investigated to determine models for heat transfer coefficients.

Numerous methods have been proposed for the design of falling film evaporators. For these methods, various heat transfer correlations have been proposed but these methods can only predict a few influences. One of the models that are used by the Camel Pro simulation package is that of Chun and Seban (1971) and it is very accurate. The problem, however, is that the user has to enter some of the parameters of which some are still unknown at this point. A need therefore exists for a tool that can be used in order to determine these unknown parameters.

Another important influence that has to be kept in mind is the pressure in the evaporator. The pressure is important because it determines the temperature at which evaporation will occur. As the pressure drops, a lower temperature is required for the liquid to evaporate. There is a good possibility that this could result in vacuum conditions being required. These vacuum conditions are regulated by a vacuum system.

2.3 Vacuum System

Another important system in an MED plant therefore is a suitable vacuum system. The purpose of the vacuum system is to generate the required vacuum when the pressure required for vaporization drops below atmospheric pressure due to the low temperatures. In selecting the system, it is important to remember that it will be subjected to cost issues. An optimum point must therefore be found between cost and size (de Bruyn and du Plessis, 2007).

2.3.1 Normal Vacuum System

As was discussed with de Bruyn and du Plessis (2007), the normal vacuum system is a relatively simple commercial system using a commercial normal vacuum pump that can be bought off-the-shelf. No further investigation is therefore required. Larger vacuum plants will also be required as the size of the plant increases. For a small plant like a demonstration plant, for instance, a normal vacuum plant would seem to be the cheaper option. However, when a full-scale plant is built, the cost of normal vacuum pump systems will be much higher than that of a jet vacuum pump system. It will therefore not be investigated further for the purpose of this study.

2.3.2 Basics of jet vacuum pumps

According to GEA Jet Pumps GmbH (2008**a**), jet vacuum pumps are used to create vacuums in applications using evaporators, driers, distillation and rectification plants, processes of freeze drying, polycondensation, degassing and deodorizing. These types of equipment will basically consist of jet pumps and condensers, but can also make use of a combination with other vacuum plants.

2.3.3 Advantages of jet vacuum pumps

According to GEA Jet Pumps GmbH (2008**a**), jet vacuum pumps have the following advantages in comparison to normal vacuum pumps:

- They have a relatively simple construction.
- They are safe to operate.
- They have relatively low wear and tear and require the minimum of maintenance.
- They are available in all the material types that are used in the equipment.
- They are available for suction flows from 10 m^3/h up to 2 000 000 m^3/h.
- They can be used for vacuums up to 0.01 mbar.
- They are driven by water vapour or other vapour, with vapour pressure above and below atmosphere.
- They can be used in conjunction with mechanical vacuum pumps.

These advantages contribute to the fact that liquid jet vacuum pumps are widely used in the desalination industry (GEA Jet Pumps GmbH 2008**a**). In order to improve the selection of a suitable evaporator it would be useful to have a tool that can help in the selection of the pump that will be required. Such a tool can then also be used to do an analysis on the vacuum system.

2.4 Boiling point elevation

Atkins (1994) describes the boiling point elevation as the phenomenon where the boiling point of a liquid will be higher when a compound substance is added (see Figure 2.10). This happens when, for example salt (which is a non-volatile solute), is added to water (which is a pure solvent).

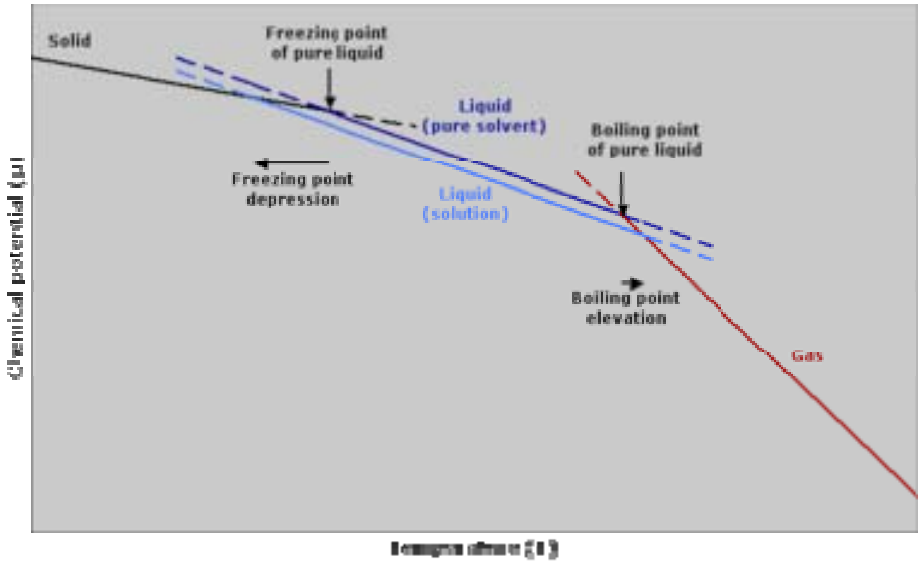

Figure 2.10: *The change in chemical potential of a solvent when a solute is added explains why boiling point elevation takes place (Atkins, 1994).*

The boiling point elevation is dependent on the presence of the particles that are dissolved as well as their number, but not their identity. This is known as a colligative property and can be expressed in vapour pressure terms. When expressed in these terms it means that the boiling of a liquid occurs when its vapour pressure is equal to the surrounding pressure. For the solvent, the vapour pressure is reduced by the presence of the solute. A non-volatile solute has a vapour pressure of zero, so the vapour pressure of the solution and the vapour pressure of the solvent are equal. Therefore in order to reach the surrounding pressure, a higher temperature is required and thus the boiling point is increased as well (Atkins, 1994).

In order to calculate the extent of the boiling point elevation, according to Atkins (1994), the Clausius-Clapeyron relation and Raoult's law are applied. They are applied along with the assumption of the non-volatility of the solute. The Clausius-Clapeyron relation characterizes the phase transition between two states of matter. On a pressure-temperature (P-T) diagram, the line that splits the phases is called a coexistence curve and the slope of this curve is given by the Clausius-Clapeyron relation (Kenneth, 1988). Furthermore, McQuarrie and Simon (1997) points out that Raoult's law states that the

vapour pressure of an ideal solution is dependent on the vapour pressure of each chemical component and the mole fraction of the component present in the solution. By applying these, (the Clausius-Clapeyron relation and Raoult's law) the boiling point elevation of a solution can by found by means of:

$\Delta T_b = K_b.m_b$

where

- ΔT_b is the boiling point elevation ($T_{b(solution)} - T_{b(pure\ solvent)}$),
- K_b is the ebullioscopic constant which is dependent on the properties of the solvent, and
- m_b is the molarity of the solution.

This is according to Atkins (1994) and the effect can be seen in Figure 2.11. Since seawater has a high salt content, the effect of the boiling point elevation can come into play.

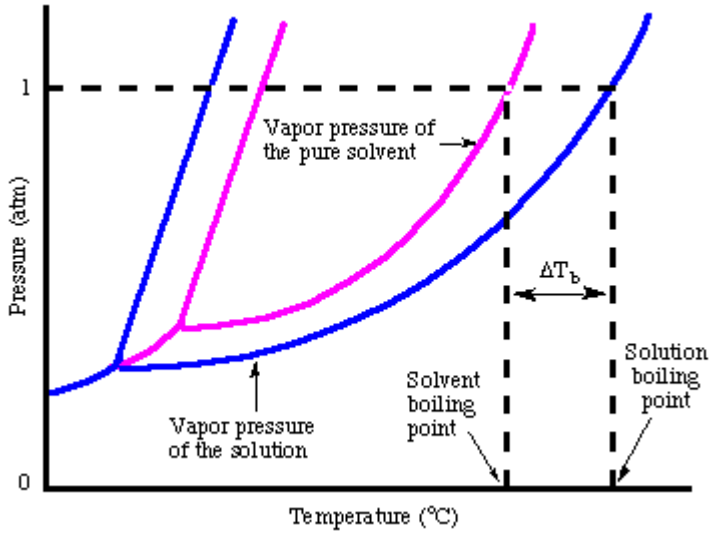

Figure 2.11: *Showing ΔT_b (Atkins (1994))*

For purposes of this study, however, the boiling point elevation will not be such a big issue and will therefore not be taken into consideration. It is not taken into account because it has an effect on ΔT which is a parameter that is an input parameter which could easily be changed. (It will be easy to enter, for example, a ΔT of 5.5 K instead of a ΔT of 5 K to allow for the boiling point elevation should it be required.)

2.5 Simulation tools

Although simulation tools are available commercially, they do have some shortcomings. Some of the simulation tools currently used are MEE Simulator, the DEEP Code and Camel Pro.

2.5.1 MEE Simulator

The tool, MEE Simulator, is a program that was developed by the Middle East Desalination Research Center or MEDRC. It requires inputs such as the length of the evaporator tubes and the length of the condenser. This is a tool that simulates the entire evaporation process with all the stages and does not do the detail design of a single evaporator and therefore requires these inputs from the user. It can give the user the shell diameter, evaporator heat transfer and the number of tubes. Another problem with this simulation software is that it is for MEE (referred to in this text as MED) with thermal vapour compression (TVC) process and not just normal MEE (Multi-Effect Evaporation). It can thus not be used for this study because it is not a tool that can be used in the design of a single evaporator along with its parameters. It is also difficult to use because it requires the input of unknown parameters, like for instance the tube length.

2.5.2 DEEP Code

Another software package that is available commercially is the DEEP Code. This package, however, is primarily for examining the economics of seawater desalination. It is used for making a comprehensive evaluation of cost comparison between nuclear and fossil energy sources with the selected desalination process, including regional studies and sensitivity analyses. This means that the DEEP code will not be investigated further for purposes of this study, since it does not touch on design issues – only economic issues (IAEA, 2000**a**).

2.5.3 Camel Pro

From Sciubba (2007) it can be seen that Camel Pro is an excellent simulation tool for an entire MED plant, but it also has its shortcomings. The problem with Camel Pro is that it requires inputs from the user such as the length of tubes, number of tubes and heat transfer coefficient. All these parameters, however, are unknown and somehow need to be determined to be able to use this simulation tool.

2.6 Conclusion

From the literature, it is evident that the evaporator, together with its vacuum system, is the main component or sub-system of an MED plant. Different models have been developed for different studies, but there still are certain aspects that require more attention. Although a number of tools exist, a need was identified for a tool that can determine the unknown parameters as well as a tool that can help with the sizing issues for a liquid jet vacuum pump system. A tool also needs to be developed to determine the wetted length of the tubes since the entire tube needs to be covered with water for an accurate Reynolds number.

This means that there is a need to develop a simulation tool that can determine parameters such as tube length, evaporator diameter, number of tubes, and the heat transfer coefficients. A need also exists for the creation of graphs that will help in designing the sieve tray in such a way that it can provide the wetted lengths for specific conditions. The current study will therefore focus on the development of simulation tools that will be able to determine the unknown parameters required by the existing simulation packages. The wetted length for various conditions will also have to be determined in order to prevent the formation of dry patches on tubes.

3. Theoretical Background

From chapter 1 and 2 it can be seen that the theory behind the evaporator and its vacuum system will have to be investigated. The investigation needs to include research into evaporator modelling. Furthermore, the theory on falling film evaporation will be discussed and following this, an in-depth study will be conducted on the heat transfer coefficients. An accurate model can then be created from the theory, which will help in designing an MED stage that basically is an evaporator. From this, a tool can then be developed which will assist in singling out important parameters.

3.1 Heat transfer

Heat transfer needs to be investigated since the heat transfer coefficients play an important part in the design of an evaporator. As indicated in Chapter 2, there are numerous heat transfer effects that must be considered when modelling an evaporator.
All these effects should be considered while calculating the overall heat transfer. If the interior scaling is neglected, the following heat transfer expressions are obtained from Incropera (2002):

$$q_0 = \frac{T_s - T}{\frac{1}{h_i A_i} + \frac{\Delta x}{k A_m} + R_f + \frac{1}{h_o A_o}} \tag{3.1}$$

This can be expressed in terms of an overall heat transfer coefficient (U):

$q_0 = UA\Delta T$

To create a better understanding on how heat transfer fits in with the evaporator with falling film, falling film evaporation needs to be investigated.

3.2 Falling Film Evaporation

Horizontal, shell-side falling film evaporators have significant advantages over other types of evaporators such as higher heat transfer and less refrigerant. According to Thome (2004) it is therefore a great advantage and a better option to use than the previous system such as vertical tube-side falling film evaporators.

Falling film evaporation is controlled by thin film evaporation, which is a heat transfer mechanism. This is controlled by conduction and/or convection across the film. Phase change is at the interface and is related to film thickness and to whether the flow is turbulent or laminar. The film flows downward under the influence of gravity and the film thickness determines the heat transfer. Heat transfer to the film is further increased by nucleate boiling in the falling evaporating film. Furthermore, the formation of dry patches on the tubes should be avoided; otherwise, it will cause the heat to be transferred to the vapour phase on those parts of the surface (Thome, 2004).

A schematic illustration of the falling film evaporation with nucleate boiling can be seen in Figure 3.1. Both thin falling film evaporation and nucleate boiling play a role in the heat transfer process. A horizontal array of tubes is used with the liquid falling from tube to tube as can be seen in the figure.

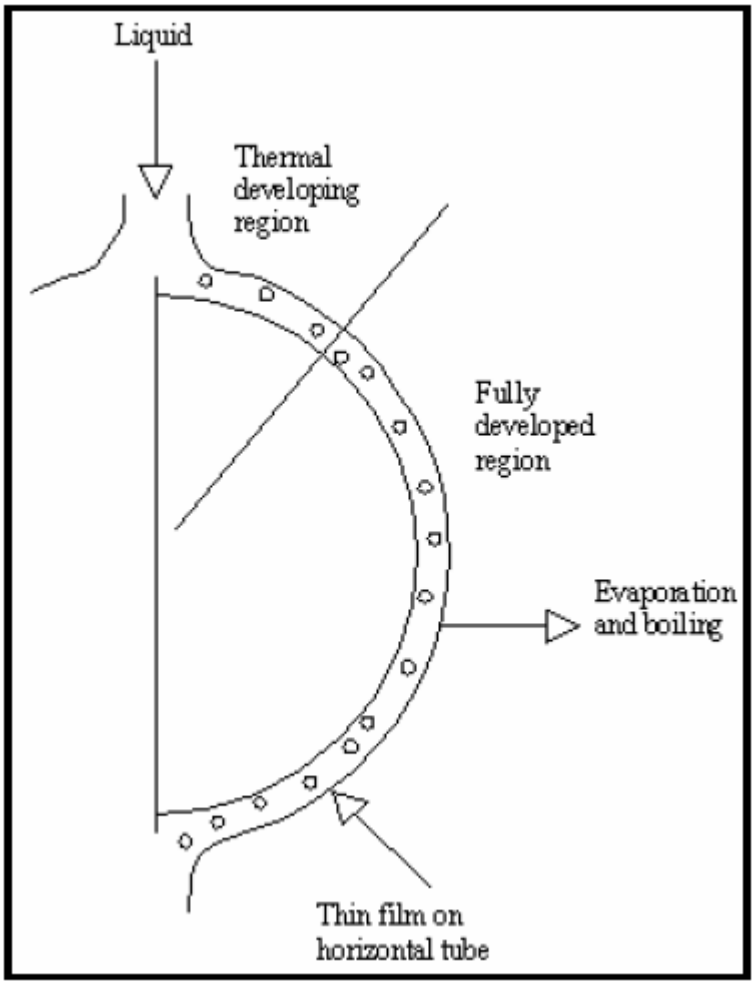

Figure 3.4: *Falling film evaporation on a heated horizontal tube with nucleate boiling (Thome, 2004).*

Falling film evaporation is utilized by large heat pump systems and is also used widely in the desalination industry with the use of tube bundles. Furthermore falling film evaporation will also allow for closer temperature approaches and energy savings.

The reduction of liquid charge is a significant advantage of the falling film evaporators. Falling film evaporators are somewhat similar to kettle type steam generators. Liquid is fed by sprinklers or trays overhead to the bundle. All that is different from kettle type steam generators is that the liquid hold-up in the shell is minimized and the flow rate of the liquid is limited to the required flow rate to wet the bundle without the formation of dry patches and without flooding the shell. This is done to achieve a falling film. A

nozzle can be placed at the bottom of the shell to remove the un-evaporated liquid as illustrated in Figure 3.2.

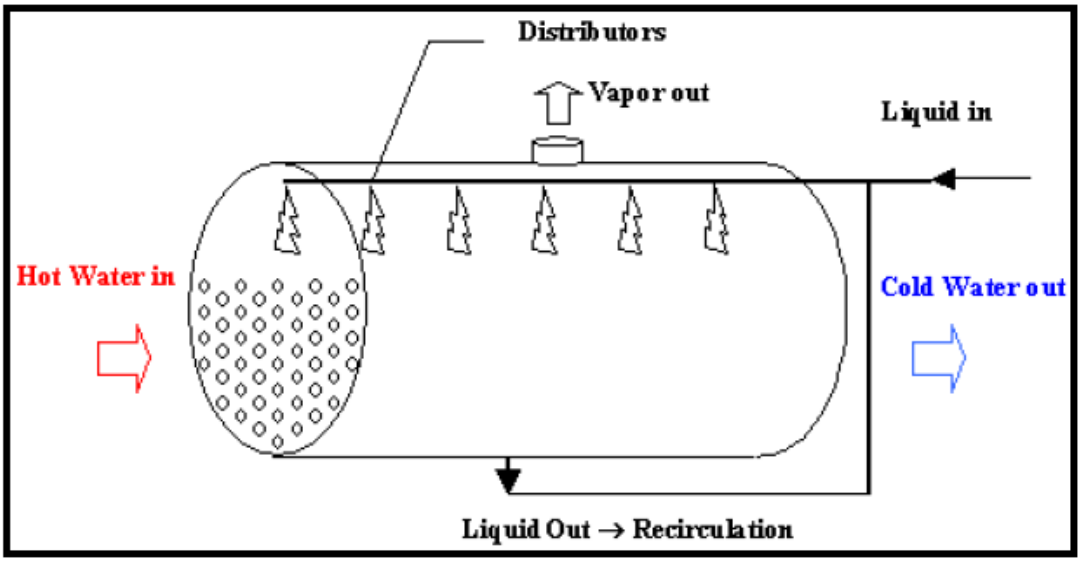

Figure 3.5: *A horizontal shell-and-tube falling film evaporator (Thome, 2004).*

3.3 Stage Model and Heat Transfer Coefficients

In this section, the semi-empirical formulae used for the calculation of the overall heat transfer coefficient will be discussed (see the list of symbols). It is necessary to determine the heat transfer coefficient to do a design. Engineering literature indicates that the following steps can be followed in the process of simulating the evaporator:

1. Firstly, the inlet properties (mass flow, pressure, and temperature) of the steam and the brine have to be specified and selected. Then the tube layout (inner and outer diameter as well as the pitch) and geometry have to be specified and the number of tubes selected, as well as the ratio (F) of the net cross-sectional area covered by the tube bundle. Geometry calculations can then be done by the following generic relationships as proposed by Rousseau (2006:61):

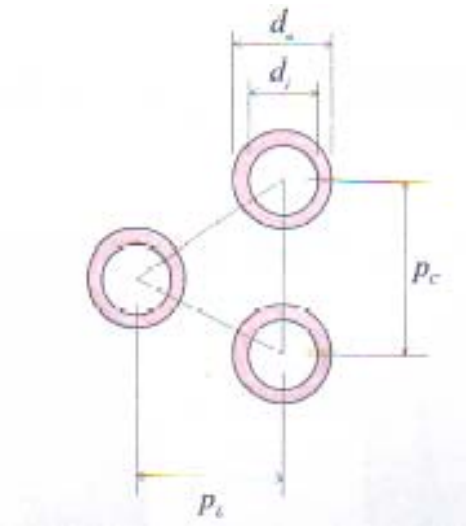

Figure 3.3: *Typical layout of tubes in staggered arrangement (Rousseau (2006:61)).*

$$p_l = p_c \cos(\theta)$$

$$\sigma_i = 0.908(\frac{d_i}{p_c})^2$$

$$\sigma_o = 1 - \frac{d_o}{p_c} \qquad (3.2)$$

$$\alpha_i = 3.628(\frac{d_i}{p_c^{\,2}})$$

$$\alpha_o = 3.628(\frac{d_o}{p_c^{\,2}})$$

2. Steam and brine properties then have to be determined from the steam tables (available in Incropera, 2002).
3. Once the properties for the steam and the brine have been obtained, the total heat transfer can be determined from the mass flow rate of the brine using the following formula from Sciubba, 2005):

$$m_b = \frac{\dot{Q}_H}{Cp_{brine}\Delta T_f} \qquad (3.3)$$

4. To determine the effectiveness of the heat exchanger (the evaporator), Rousseau (2006:63) proposed that the required heat exchanger effectiveness (ε) can be calculated by using

$$C_r = \frac{C_{\min}}{C_{\max}}$$
$$\Delta T_{\max} = T_{steam,i} - T_{brine,i} \tag{3.4}$$
$$\varepsilon = \frac{\dot{Q}_H}{C_{\min}\Delta T_{\max}}$$

5. Using the C_r and ε as is shown above, the required UA (heat transfer duty) value can be calculated by using the NTU-Method as was proposed by Rousseau (2006:63). For the purpose of this study it will be done for a single tube pass (when the tubes only pass through the evaporator once) and UA is determined by using

$$NTU = (\frac{1}{C_r - 1})\ln(\frac{\varepsilon - 1}{\varepsilon C_r - 1}) \tag{3.5}$$
$$UA = C_{\min} NTU$$

6. The overall shell dimensions, the evaporator diameter (D) and length (L), are now determined to ensure compliance with heat transfer duty (UA) and pressure drop (Δp) requirements. It is determined by using the following constants:

$$K_1 = 1.273 \cdot \frac{UA}{F \cdot \alpha_i \cdot U}$$
$$K_2 = 0.864 \cdot \sigma_i^2 \cdot F^2 \cdot d_i \cdot \rho_{steam} \cdot \Delta p_{steam,\max} \cdot \frac{1000}{f_{DW,i} \cdot \dot{m}_{steam}^2}$$
$$D = \sqrt{n}(\frac{K_1}{K_2})^{\frac{1}{6}} \tag{3.6}$$
$$L = \frac{K_1}{D^2}$$
$$\mathrm{Re}_{steam} = \rho_{steam} \cdot v_{steam} \cdot \frac{d_i}{\mu_{steam}}$$
$$v_{steam} = 1.273 \cdot \dot{m}_{steam} \cdot \frac{n}{F \cdot \rho_{steam} \cdot \sigma_i \cdot D^2}$$

(The process for determining K_1 and K_2 can be seen in Appendix B while D, L, Re_{steam} and v_{steam} is calculated as was done by Rousseau, 2006:66)

7. In order to determine the length and diameter of the evaporator, the heat transfer coefficients for horizontal falling film evaporation needs to be calculated and evaluated.

8. To evaluate the heat transfer coefficients (h_i) for vapour condensation inside the horizontal tubes, the Shah (1978) formula was used according to Sciubba (2005). The vapour mass fraction (χ) is assumed as average (0.5) in the tube. Next, the heat transfer coefficients (also see list of symbols) in the tubes can be determined from:

$$h_i = h_u\left(1+\frac{3.8}{Z^{0.95}}\right)$$

$$Z = \left(\frac{1}{\chi}-1\right)^{0.8}\cdot \mathrm{Pr}_{steam}^{0.4}$$

$$h_u\, 0.023\cdot \mathrm{Re}^{0.8}\cdot \mathrm{Pr}_{steam}^{0.4}\cdot\frac{k_L}{d_i}\cdot(1-\chi)^{0.8} \qquad (3.7)$$

$$\mathrm{Re} = \rho_L\cdot v\cdot\frac{d_i}{\mu_L}$$

$$\mathrm{Pr} = \mu_L\cdot\frac{Cp_L}{k_L}$$

9. To determine the overall heat transfer coefficients, the heat transfer coefficient of the brine also has to be established. To evaluate the heat transfer coefficient (h_o) for the horizontal falling film boiling of the brine, the Nusselt expression has been used where the subscripts f and g respectively refer to the fluid and gas brine phase. These parameters (see list of symbols) are determined by using the following formulas according to Sciubba (2005):

$$
\begin{aligned}
\nu &= 0.62 \cdot \left[g \cdot (\rho_f - \rho_g) \cdot \overline{hfg} \cdot \frac{d_o}{\nu_g \cdot k_g \cdot (T_w - T_{sat})} \right]^{\frac{1}{4}} \\
T_w &= 0.5 \cdot (T_s + T_{sat}) \\
\overline{hfg} &= hfg \cdot (1 + 0.34 \cdot Ja) \\
Ja &= C \cdot \left(\frac{T_{sat} - T_w}{hfg}\right) \\
\nu &= h_o \cdot \frac{d_o}{k_f}
\end{aligned}
\tag{3.8}
$$

where the symbol T_w represents the wall temperature, Ja the dimensionless Jacob number, and hfg the heat of vaporization.

10. To determine the overall heat transfer coefficient (U), the heat transfer coefficients (h_i) for vapour condensation inside the horizontal tubes as well as the heat transfer coefficient (h_o) for the horizontal falling film boiling of the brine is calculated as was shown earlier in this section. By using these two parameter, h_i and h_o, the overall heat transfer coefficient can be calculated with the following equation:

$$
\frac{1}{U} = \frac{1}{h_i \cdot \frac{d_i}{d_o}} + \frac{1}{h_o} + FF \tag{3.9}
$$

In this equation, the parameter FF indicates the fouling factor (Sciubba, 2005).

3.4 Vacuum System

To create the required vacuum, it is important to investigate a suitable vacuum system. The reason for the investigation into the vacuum system is that pressures lower than atmospheric pressure has to be created to allow the vaporization of the water. Various types of vacuum systems are available. In the selection of the specific type of vacuum system, it is important to remember that selection will be subject to cost issues. An optimum point must therefore be found between cost and size (du Plessis, 2007).

3.4.1 Normal Vacuum System

The normal vacuum system uses a commercial normal vacuum pump that can be bought off the shelf, as it is a relatively simple commercial system that does not need any further investigation. In addition, larger vacuum plants will be required as the size of the plant increases. For a small plant like a demonstration plant, for instance, a normal vacuum plant would seems to be the cheaper option, but when a full-scale plant is built, the cost of normal vacuum pump systems will be much higher than that of a jet vacuum pump system. It will therefore not be investigated further in this study (du Plessis (2007)).

3.4.2 Basics of jet vacuum pumps

Vacuums are created by jet vacuum pumps in applications such as evaporators, driers, distillation and rectification plants, processes of freeze drying, polycondensation, degassing and deodorizing.

These types of equipment basically will consist of jet pumps and condensers or it can make use of a combination with other vacuum plants.

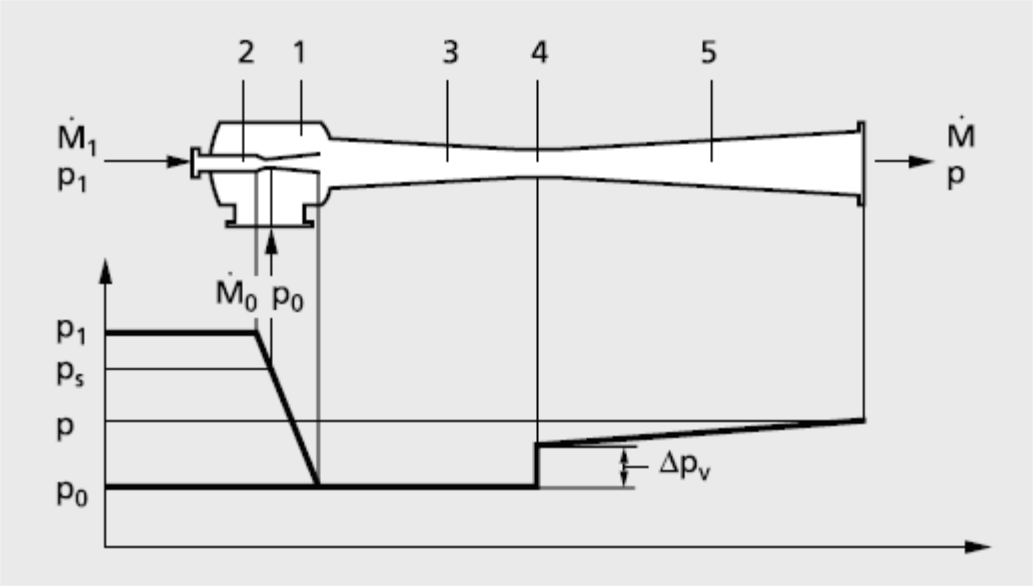

1	*head*		p_1	*motive steam pressure*
2	*motive nozzle*		p_0	*suction pressure*
3	*inlet cone*	*mixing nozzle*	p	*counter pressure*
4	*throat*		p_s	*pressure at sound velocity*
5	*diffuser*		Δp_v	*compression thrust*
			$\dot{M}_1$	*motive steam flow*
			$\dot{M}_0$	*suction flow*
			$\dot{M}$	*mixing vapour flow*

Figure 3.4: *Working principle of a steam jet pump and the pressure differences over the flow path (GEA Jet Pumps GmbH, 2008**a**).*

3.4.3 Working principles

The expansion work of a motive (moving) medium is used by jet pumps to create the vacuum. In the motive nozzle a high velocity jet is created and at a low suction pressure the suction medium is entrained by this jet and it accelerates its path. Through transformation of the kinetic energy, this mixture is brought up to a higher pressure level in the throat and the diffuser of the ejector.

Three connections are available for jet pumps:

- A connection for the moving medium with the highest pressure p_1.

- A connection for the suction medium with the lowest pressure p_0.
- A connection that is used to discharge the motive and suction media with a medium pressure p.

With a sufficient high expansion ratio of p_1/p_0 a compression ratio, p/p_0, of up to 20 can be achieved by a single stage jet pump. Less moving medium will be required for a higher expansion ratio, and a higher compression ratio on the other hand will require more motive medium.

In most cases for suction under 100 mbar, multi-stage vacuum pumps are used. The motive medium and condensable compounds are condensed between the stages to most effectively utilize the energy.

The temperature of the cooling medium, as well as the characteristics of the motive medium, determines the condensation pressure.

To avoid the contamination of the cooling water with the suction, medium surface condensers are preferred as inter-condensers.

According to GEA Jet Pumps GmbH (2008**a**), the following data is required for the optimum design of a jet vacuum pump:

For the suction medium:

- Composition, mol mass [kmol/kg]
- $\dot{M}_0$ (Suction flow) [kg/s]
- Absolute suction pressure p_0 [mbar]
- Temperature T_0 [°C]
- Absolute counter pressure p [mbar]

For the motive medium:

- Absolute pressure p_1 [bar]
- Temperature T_1 [°C]

For the cooling medium:

- Temperature [°C]
- Head pressure

This data is required to determine the arrangement, number of stages and consumption of the motive and cooling medium (GEA Wiegand GmbH, 2008).

3.4.4 Advantages of jet vacuum pumps

According to GEA Jet Pumps GmbH (2008**a**), jet pumps have the following advantages:

- They have a relatively simple construction
- They are safe to operate
- They have relatively low wear and tear and require the minimum of maintenance
- Available in all materials that are used in the equipment
- Available for suction flows from 10 m^3/h up to 2 000 000 m^3/h
- Can be used for vacuums up to 0.01 mbar
- Driven by water vapour or other vapour, with vapour pressure above and below atmosphere
- Can be used in conjunction with mechanical vacuum pumps

3.4.5 Vacuum plants for sea water desalination

The vacuum system with a liquid jet vacuum pump is widely used in the desalination industry. It is a system which is slightly more complex than a normal vacuum system (which uses a vacuum pump to create the required vacuum), but there is an optimum point where the cost of this system will be lower than that of a normal vacuum system. This system (which uses liquid jet vacuum pumps) generally uses water as the flow medium. Normal pumps can also be found in the system and they are used to pump the water through the liquid jet vacuum pump to create the required vacuum. The liquid jet vacuum pump consists of a head, diffuser and flow nozzle. Figure 3.5 shows a liquid jet vacuum pump (GEA Wiegand GmbH, 2008).

Figure 3.5: *Liquid jet vacuum pump with flanged connection (GEA Jet Pumps GmbH, 2008**c**).*

The operation of these liquid jet vacuum pumps is based on the liquid jet from the motive nozzle emerging at a higher velocity, entraining air or gas in the head and compressing it to atmospheric pressure.

Liquid jet vacuum pumps can be directly coupled to the water when water is used as the motive medium. If, however, the water consumption has to be as economical as possible, the operating water may be circulated. This is also true for all cases where other liquids are used as the motive medium.

The layout of the vacuum system with the liquid jet vacuum pump is illustrated in Figure 3.6. Note that the liquid jet vacuum pump will still operate satisfactorily if the outlet pipe is below the liquid level or if a reducing piece is connected to the liquid outlet.

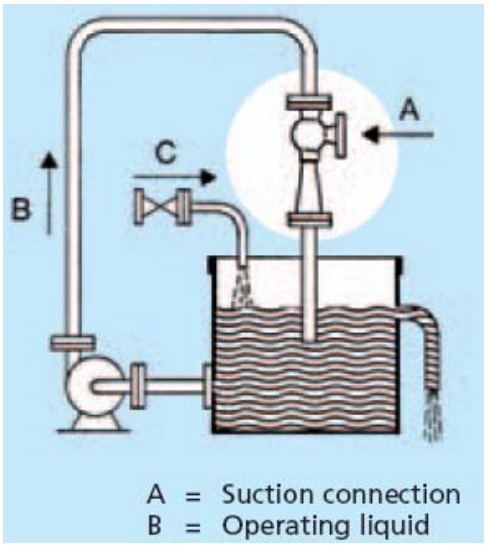

Figure 3.6: *Layout of a Vacuum System with a liquid jet vacuum pump (GEA Jet Pumps GmbH, 2008**b**)*

For this type of system it would be useful to have a tool that can help when selecting the pump size and doing an analysis on the vacuum system.

3.4.6 Vacuum system modelling

The vacuum system is responsible for the evacuation of the system and for maintaining a certain pressure in the vacuum manifold. To select the correct vacuum system the required parameters needed are:

- For the vacuum system (the vacuum vessel that acts as a buffer of some kind in the system) the length and diameter (L_{vacves} & D_{vacves}) needs to be known.
- For the pipes in the auxiliary pumping system the diameter, length and roughness (D, L & e) needs to be available.
- The pressure and volume flow rate in and through the system are required for the liquid jet vacuum pump (P_1 & Q).
- The Losses for the components in the auxiliary system such as the elbows and valves also have to be specified (k_{elbows} & k_{valves}).
- Likewise the water temperature of the auxiliary system has to be specified (T_1).

- Furthermore the static height (h_s) in the auxiliary system has to be specified to be able to determine the total height in the system.

These parameters can then be used to do further calculations as is shown in principle in Shames (2003).

1. The first step in further calculation are to calculate the parameters which are needed to determine the mass flow rate and this is done by using the following equation:

$$\dot{m} = Q \cdot \frac{\rho}{60 \cdot 60} \tag{3.10}$$

2. Then the mechanical losses caused by valves and elbows in the auxiliary system can be calculated by adding up the lost factors of the mentioned components:

$$k_m = k_{valves} + k_{elbows} \tag{3.11}$$

3. Since the diameter and the length of the vacuum vessel are known, the volume of the vacuum vessel can be calculated using:

$$Vol_{VacVes} = \frac{\pi}{4} \cdot D_{VacVes}^2 \cdot L_{VacVes} \tag{3.12}$$

4. Now the friction factor (f), which is a function of the Reynolds number and relative roughness (RR), can be determined. This is done by using the Moody chart (Figure 3.7), a graph in non-dimensional form. The graph relates the friction factor, Reynolds number (ratio of inertial to viscous forces in the velocity boundary layer) and relative roughness for fully developed flow in a circular pipe. To select the correct value, the Reynolds number, as well as the value for the relative roughness, has to be calculated. It is done by using the following as is shown in Shames (2003):

$$A = \frac{\pi}{4} \cdot D^2$$

$$\dot{m} = \rho V A$$

$$\mathrm{Re} = \frac{\rho V D}{\mu} \tag{3.13}$$

$$RR = \frac{e}{D}$$

$$f = f(\mathrm{Re}, RR)$$

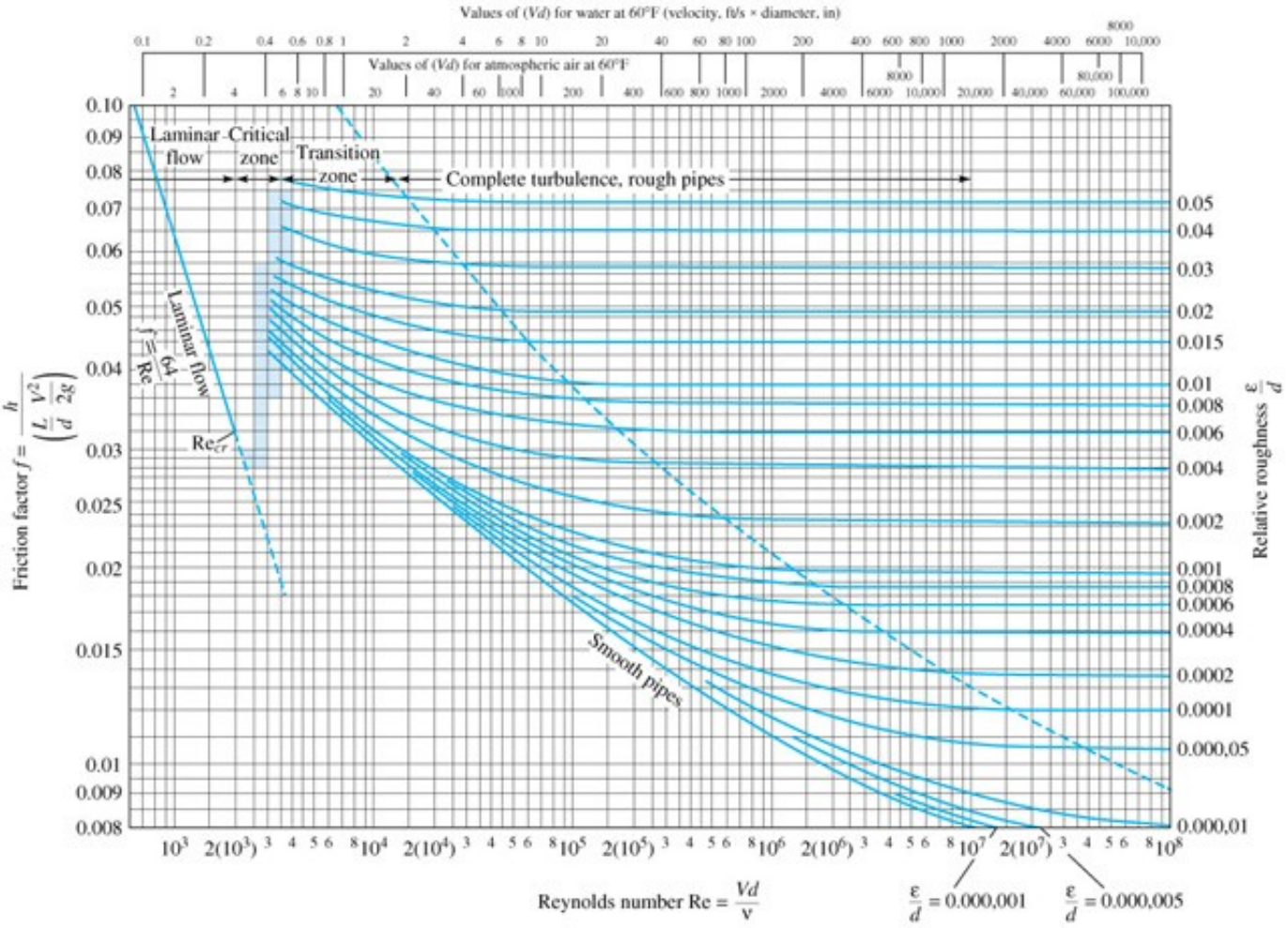

Figure 3.7: *Moody Chart (Shames (2003))*

5. Now the total losses due to friction and mechanical losses can be calculated by using the friction factor that has just been calculated. This is done by the calculation of the following constant:

$$k = f \cdot \frac{L}{D} + k_m \tag{3.14}$$

6. From this constant (k), which has just been calculated, the head (or in other words the height) that needs to be pumped due to the losses in the system, can be determined. It can be calculated by using:

$$h_l = k \cdot \frac{V^2}{2 \cdot g} \tag{3.15}$$

7. Now that the head caused by the losses in the pipe is known, the total height (H) that has to be pumped by the water system can be calculated using:

$$H = h_s + h_l + \frac{P_1}{10} \tag{3.16}$$

The method explained above provides the information required to create a simulation tool for the vacuum system of an MED plant. From this a simulation tool can now be developed.

3.5 Conclusion

The above-mentioned theory can be used and implemented in a simulation tool or set of tools for an MED plant and will help to determine the important unknown parameters of the evaporator and vacuum system. These parameters can typically be the length of the tubes or the diameter of the evaporator (for the purpose of this study it will be assumed that the evaporator will be circular) as well as the heat transfer coefficients. For the vacuum system it will help to determine the required head and volume flow rate in order to be able to do the selection of the correct pump for the system. Using the theory discussed in this section, simulation and design tools can now be developed.

4. Simulation tools

4.1 Introduction

In Chapter 2, it was concluded that there is a need for a tool which will be able to address sizing issues of the evaporator as well as a need for a tool that will help in the design of the vacuum system. In order to be able to investigate the sizing issues of evaporators as used in MED desalination plants, a tool were required that would aid in determining the size of an evaporator and its vacuum system. Such a tool was then able to enable the user to determine the size and layout of the plant as well as determining the quantity of materials required. This in turn assists in determining the material costs and will therefore be useful in the case of a cost analysis. The acquired data can also involve parameters such as the evaporator diameter, tube length and the number of tubes. Another parameter that can be determined with the aid of such a tool is the heat transfer coefficients. These are important parameters because some of the existing desalination plant design software (like Camel Pro) requires them as input should the need arise to use one of the existing tools that were discussed in Chapter 2. In order to determine these parameters, EES (Engineering Equation Solver) were used to create a basic tool that can calculate and determine these parameters.

EES was used to create a program to do the calculation for the vacuum system. For purposes of this study a vacuum system that utilizes a liquid jet vacuum pump will be investigated. The vacuum system will interface with the rest of the desalination plant via a vacuum manifold. The importance of the vacuum system is that it is responsible for maintaining a certain pressure level within the vacuum manifold. The user can then use this program to do a pump selection for the vacuum system. The tool can also assist in designing the auxiliary pumping system – normal as well as liquid jet. The vacuum requirements for a vacuum system of a specific size can also be calculated.

What must be made clear is that the tools that were developed were not meant to be detail design tools; they rather give the user a good indication of the order size of the parameters. These parameters can then act as a starting point in the detail design process

using the more advanced tool available, which requires these size parameters as input. It also enables the user to do a quick cost analysis and help in determining the order size of a desalination plant. This can be used to design the layout of the desalination plant. To keep the design tools small and simple, separate EES programs were developed for the evaporator and the vacuum system.

4.2 EES Simulations

The EES programs that were developed will be subsequently discussed briefly in this section.

4.2.1 Sizing of the evaporator

The EES program that was developed for the simulation of the evaporator (which will help to determine the size and heat transfer coefficients) functions in the following manner:

1. Firstly the inlet properties (mass flow, pressure and temperature) of the steam and the brine are specified and selected. Then the tube layout (inner and outer diameter as well as the pitch) and geometry are specified. Next, the number of tubes is selected together with the ratio (F) of the net cross-sectional area covered by the tube bundle. Geometry calculations can now be done as was discussed in Chapter 3 (see equation set 3.2).
2. Steam and brine properties are then specified and calculated from the steam tables, which are a built-in function of EES for the steam. The brine properties, however, have to be specified because there are no tables in EES available for seawater properties.
3. Once the properties for the steam and the brine have been obtained, the total heat transfer is determined from the mass flow rate of the brine using the equations provided in Chapter 3 (see equation 3.3).

4. Now the heat exchanger (evaporator) effectiveness (ε) can be calculated by the set of equations that were given in the theoretical section of Chapter 3 (equation set 3.4) by using the parameters that were determined as mentioned above.
5. Using the C_r and ε values that are now known, the required UA value can be calculated by using the NTU-Method as was discussed in Chapter 3 (equation set 3.5). For purposes of this study it is done for a single tube pass (when the tubes only passes through the evaporator once), where the parameter n (number of tube passes) equals one.
6. The overall shell dimensions, the evaporator diameter (D) and evaporator length (L), are now determined by using the parameters that were calculated earlier to ensure compliance with heat transfer duty (UA) and pressure drop (Δp) requirements. The shell dimensions are determined by using constants K_1 and K_2. The process for determining K_1 and K_2 can be seen in Appendix B while diameter (D), length (L), Reynolds number for the steam (Re_{steam}), and the velocity of the steam (v_{steam}) is calculated as is shown in Chapter 3 (see equation set 3.6).
7. In order to determine the length (L) and diameter (D) of the evaporator, the heat transfer coefficients for horizontal falling film evaporation now needs to be calculated and evaluated by using the theory in Chapter 3 (equation set 3.6) regarding the design of the evaporator.
8. In order to calculate the heat transfer coefficients (h_i) for vapour condensation inside the horizontal tubes, the Shah (1978) formula was used as was indicated in chapter 3. The vapour mass fraction (χ) was assumed as average (0.5) in the tube. From this the heat transfer coefficients in the tubes can now be determined by the equations as is shown in Chapter 3 (see equation set 3.7).
9. To determine the overall heat transfer coefficients, the heat transfer coefficient of the brine also has to be established. To evaluate the heat transfer coefficient (h_o) for the horizontal falling film boiling of the brine, the Nusselt expression was used where the subscripts f and g refer to the fluid and gas brine phases respectively. These parameters are determined by using the set of equations given in Chapter 3 (equation set 3.8). In this set of equations, the symbol T_w represents

the wall temperature, *Ja* the dimensionless Jacob number, and *hfg* the heat of vaporization (for purposes of this study taken as 2260 J/kg).

10. To determine the overall heat transfer coefficient (*U*), the heat transfer coefficients (h_i) for vapour condensation inside the horizontal tubes as well as the heat transfer coefficient (h_o) for the horizontal falling film boiling of the brine, as was calculated earlier, can then be used. The overall heat transfer coefficient is determined by substituting h_i and h_o into the equation given in Chapter 3 (equation 3.9) in which the parameter *FF* indicates the fouling factor which, for purposes of this study, is assumed to be 0.18 m^2K/kW (Sciubba, 2005). This now enables the tool (EES program) to determine the length and diameter of the heat exchanger (as was discussed earlier in this section) as well as determining the heat transfer coefficients.

4.2.2 Sizing the vacuum system

The vacuum system is responsible for the evacuation of the system and for maintaining a certain pressure in the vacuum manifold. The EES tool is also able to assist the designer in sizing the auxiliary pumping system of the vacuum system. It will also help the designer to study the effects that different vacuum pumps will have on the auxiliary system. Figure 4.1 gives a schematic illustration of a pilot desalination facility that was investigated by M-Tech Industrial in Potchefstroom and it indicates where the vacuum system in such a system will be situated.

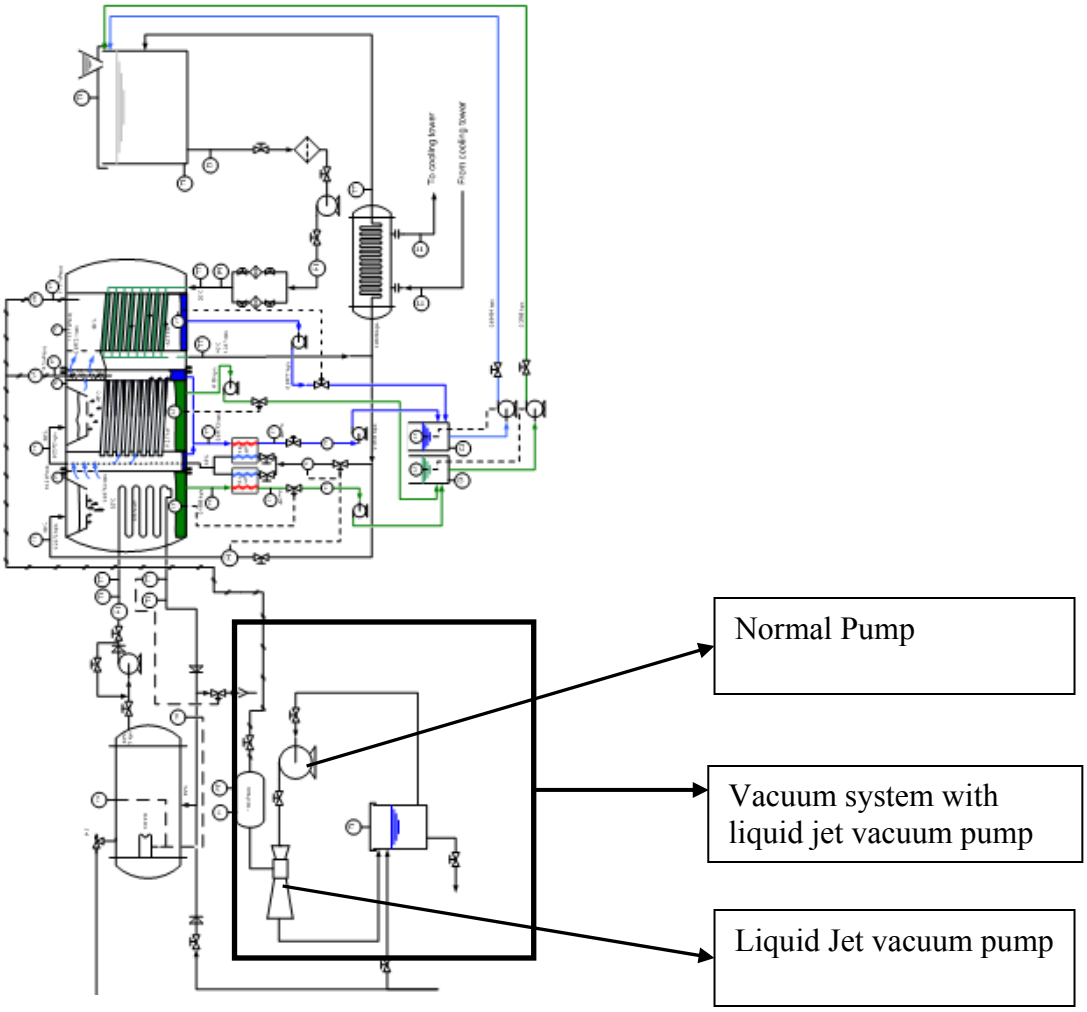

Figure 4.1: *Pilot desalination facility flow diagram indicating the use and position (possible location) of a vacuum system (du Plessis and de Bruyn (2007)).*

The EES Program for the vacuum system works by taking the following parameters as input:

1. For the vacuum system (the vacuum vessel that acts as a buffer of some kind in the system) the length and diameter is required (L_{vacves} & D_{vacves}).
2. For the pipes in the auxiliary pumping system the diameter, length and roughness is required (D, L & e).
3. The pressure and volume flow rate in and through the system are required for the liquid jet vacuum pump (P_1 & Q).
4. Losses for the components in the auxiliary system, such as the elbows and valves also have to be specified (k_{elbows} & k_{valves}).

5. Likewise the water temperature of the auxiliary system has to be specified (T_l).
6. Furthermore the static height (h_s) in the auxiliary system has to be specified to be able to determine the total height in the system.

The EES Program then utilizes these parameters to execute calculations.

1. The first step in this process of determining the parameters is to determine the mass flow rate and this is done by means of the equation for mass flow given in Chapter 3 (equation 3.10).
2. Then the mechanical losses caused by valves and elbows in the auxiliary system can be calculated by adding up the loss factors of the mentioned components as is shown in Chapter 3 by equation 3.11.
3. Since the diameter and the length of the vacuum vessel are known, the volume of the vacuum vessel can be calculated using the equation for the calculation of the volume given in Chapter 3 (equation 3.12).
4. Now the friction factor (f), which is a function of the Reynolds number and relative roughness (RR), can be determined. This is done by using the Moody chart (which is a built-in function of EES and is shown in Figure 3.7) and selecting the correct value for the Reynolds number as well as the value for the relative roughness. For this the equations (equation set 3.13) provided in Chapter 3 are used.
5. Now the total losses due to friction and mechanical losses can be calculated by using the friction factor that has just been calculated. This is done by calculating a constant (k) for the total losses as can be seen in the theory on the vacuum system in Chapter 3 (see equation 3.14).
6. From this constant (k) that has been calculated, the head (h_l) of the water, or in other words the height that needs to be pumped due to the losses in the system, can be determined by the equation given in Chapter 3 (as is shown be equation 3.15).
7. Now that the head losses in the piping is known, the total head (H) that has to be pumped by the water system can be calculated by the formulas provided in Chapter 3 (equation 3.16).

From the results obtained from the program as discussed above, a selection can be made concerning the correct liquid jet vacuum pump and the auxiliary pumping system for the liquid jet vacuum pump.

4.3 Case Studies

To show how the programs function, as well as to show the parameters the two separate EES-tools calculate, a case study will be performed for each of the programs. Thus, for purposes of this section, some parameters will be selected and assumed and from this it becomes clear what the output parameters will be for those conditions. To investigate the specified conditions the case studies will also be divided into two, namely one case study for the evaporator and one for the vacuum system.

4.3.1 Sizing of the Evaporator

The first tool, or EES program, that will be investigated in the case studies is the tool for the design of an evaporator which will help in solving sizing issues (evaporator diameter, tube length and number of tubes).

- For purposes of this case study the following values were selected as input parameters for the EES program:

Table 4.1 Evaporator – Input parameters

$\dot{m}_{steam}$	2 kg/s
p_{steam}	160000 Pa
$T_{steam,i}$	350 K
$T_{brine,i}$	303 K
$p_{brine,i}$	101000 Pa
$\dot{m}_{brine}$	2.5 kg/s
$\Delta p_{steammax}$	2000 Pa
d_o	0.03 m

d_i	0.028 m
p_c	0.05 m
e	30 x 10^{-6}
θ	30°
ΔT	5 K
n	1
F	0.5

- Using the above-mentioned parameters, the following values for the output parameters were obtained from the EES program that was discussed earlier in this chapter. *(Please note that these are only the most important parameters and not all of those that were calculated. The other parameters can be seen in the results of the EES-program for the evaporator in Appendix B.)*

Table 4.2 Evaporator – Some EES results

N_L	8
D	0.50 m
L	2.79 m
UA	1367 W/K
U	121.9 W/m^{2}K
V_{steam}	1.59 m/s
$\dot{Q}_H$	52500 W

From the simulation for the given input parameters the results as in Table 4.2 above were obtained. The results compare well (5% was selected as acceptable for the purpose of this study and the results differ by 3% in the end) with the case study in Rousseau (2006:59). The study by Rousseau was done for a shell-and-tube design and shares many similarities with the design that was used here. The EES program was also checked and approved by Mr. P de Vos (Mechanical Engineer) from M-Tech Industrial in Potchefstroom.

By varying the input variables, different observations can be made. For example, when the temperature of the steam is increased it causes a higher overall heat transfer coefficient. This means that a smaller evaporator will be needed because of a smaller heat transfer area being required. A further observation that can be made is when the mass flow of the brine is reduced, the overall heat transfer coefficient also increases. This will mean that less product (fresh water) will be produced over a certain time.

These results can now be applied to determine the layout of the plant. With this layout known and the placement of the evaporators determined, it will then allow for the design of the auxiliary systems and their placement. Furthermore, the results can also be used to do a cost analysis of the materials of the evaporators since the size is known. Another way the results can be used is by implementing the results in a simulation program like Camel Pro, for instance.

4.3.2 Vacuum System

In the following case study the effects of different liquid jet vacuum pumps, pipe diameters, pipe lengths and the effects of losses caused by the valves and elbows were investigated. The input and output parameters are as follows:

- Input parameters that were specified and selected for purposes of this case study (see Table 4.3):

Table 4.3 Vacuum system input parameters

D	0.065 m
e	0.00003
L	10 m
L_{VacVes}	2 m
D_{VacVes}	1 m
P_1	500 kPa
Q	24 m^3/hr
k_{elbows}	2

k_{valves}	1
T_1	25 °C

- The following output parameters were obtained from the calculations by the EES program that was created for the vacuum system (Table 4.4):

Table 4.4 Vacuum system EES results

V	2.01 m/s
A	0.00332 m^2
$\dot{m}$	6.65 kg/s
Vol_{VacVes}	1.57 m^3
H	52.23 m

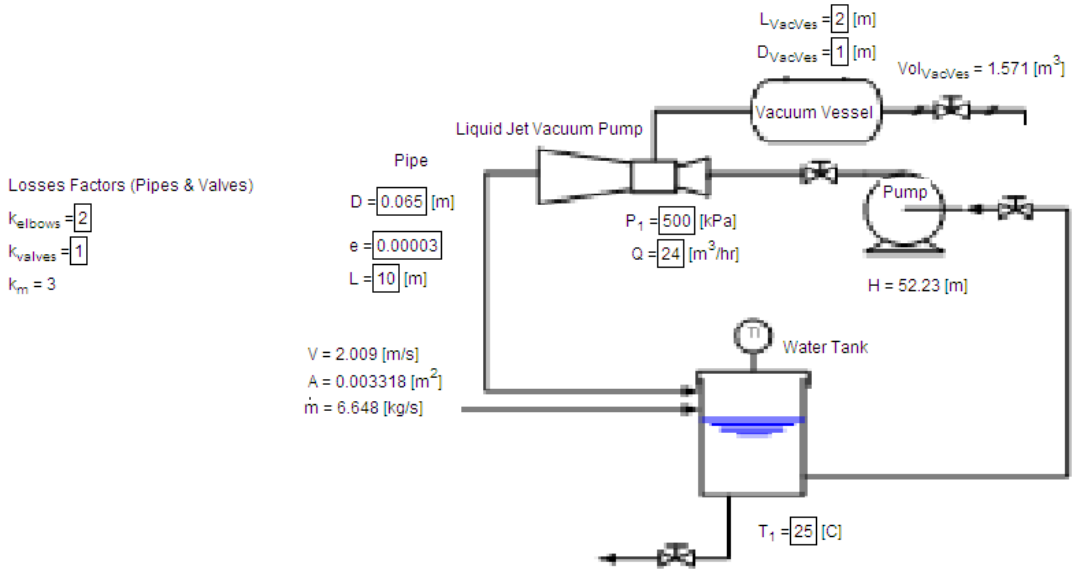

Figure 4.2: *Interface of the EES program for the vacuum system*

From the results obtained in this case study it can be seen that for a liquid jet vacuum pump to create a vacuum with a volume of 1.571m^3, a water pump is required with a volume flow rate of 24m^3/hr and a head of 52.23m.

The results were compared to the results from a study that was done by myself for M-Tech Industrial on a pilot desalination facility and presented to du Plessis and de Bruyn (2007) and it was approved by them. For this facility a vacuum system was also considered. The results obtained were within 2% of each other and therefore suggest that the EES simulation offers a valid tool for sizing of vacuum systems.

Varying the parameters has shown that a smaller vacuum pump (therefore a lower volume flow rate) will produce a smaller head and therefore will require a smaller vacuum pump. This means that the size of the vacuum required will play a vital role in the selection of a vacuum pump. The selection of a vacuum pump for a certain vacuum size can be done from the data sheets provided by the manufacturer of the vacuum pump. A further observation that can be made is that the required head will be lower for the pump if the losses in the pipes are minimized.

The results that were obtained from this EES program can now be used to select the correct water pump for a specific liquid jet vacuum pump. It can be done because the head (the height of the fluid that needs to be pumped) and the volume flow rate to obtain the required vacuum, are now known. Further information for the liquid jet vacuum pump, for example the time needed to obtain the required vacuum, can be found in the datasheet from the manufacturer of the liquid jet vacuum pump system (see datasheet of liquid jet vacuum pump in the Annexure D). This information can then be combined to design a complete vacuum system for the evaporator of a desalination plant.

4.4 Conclusion

First of all it should be noted that the purpose of this EES program was not to do a detailed analysis on horizontal falling film evaporators or the vacuum system, but merely

to provide the user with good indicative values (or guess values) which can be used, for example, for initial guess values for a simulation programme such as Camel Pro. These values can typically be for the heat transfer coefficients, evaporator diameter or area, and the tube length.

As can be seen in the EES programs, it allows for the variation in almost all parameters. The fluid property parameters can be changed as well as the input parameters such as temperature, pressure and mass flow. These parameters can then be taken and, as discussed earlier, be implemented in other software simulation packages.

Another advantage of the EES-programs is that it can be used later to develop a more complete desalination plant simulation tool for a simulation program like Flownex for example. Furthermore, the EES program for the evaporator provides a better understanding of the heat-transfer coefficients of horizontal falling film evaporators. The second EES program is also a handy tool for the selection of liquid jet vacuum pumps and normal pumps in the vacuum system.

5. Flow Pattern Test Section

In order to create graphs for determining the wetted lengths, as was discussed in Chapter 2, a flow pattern test section was designed and built to investigate the flow pattern and associated behaviour as a function of numerous geometric parameters.

5.1 Wetted Length Test Section design

The parameters that were used in the design were obtained from discussions with Mr. R de Bruyn (2007) from M-Tech Industrial. These parameters came from unpublished work done by Mr. R de Bruyn as well as studies and previous work and investigations done by him for M-Tech Industrial.

5.1.1 Overview

For the design of the evaporator, a detail design was done on the perforated plate for the seawater design. This ensured that the tubes were completely wetted and prevented the formation of dry patches on the tubes. This was vital because of the fact that corrosion and scaling would occur at the spots that were not covered with water. It means that there must be an optimal water distribution over the length of the tubes. In order to ensure that the tubes of the heat exchanger are completely wetted to prevent dry patches, a detail design needs to be performed on the perforated plate for the seawater.

To prevent dry spots through successful design, design curves were required for the perforated plate feeder system. A large collection of these curves was required to cover the spectrum of plates available. Design curves are required to design a perforated plate feeder system as can be seen in Figure 5.1. One thus needs a large collection of perforated plate design curves.

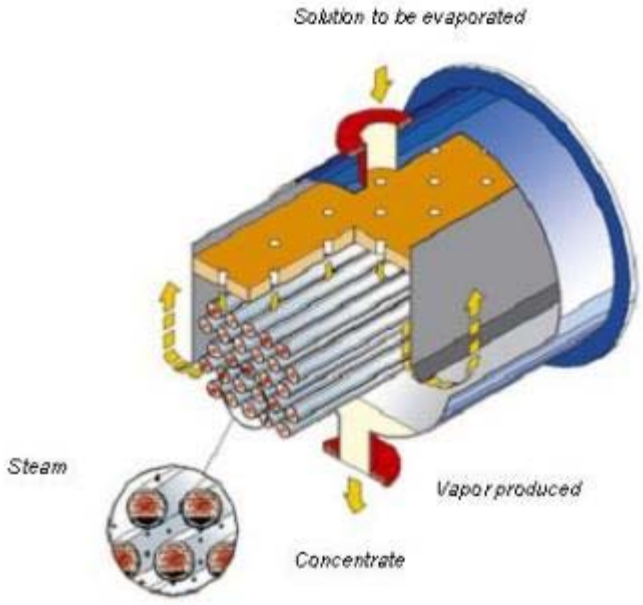

***Figure 5.1**: Evaporator with perforated plate (Anon (2007)).*

Parameters that are important to consider due to the fact that the wetted length is a function of them, are the following:

- Diameter of tubes
- Temperature of seawater
- Pressure difference
- Concentration of seawater
- Height of distribution

As these graphs were not available, a test section was required to generate them experimentally. It is important to create conditions similar to those expected. This meant that the tests had to be performed for at least the following conditions:

- Tube sizes:

Table 5.1: Tube sizes

Outer Diameter [mm]	**Wall Thickness [mm]**
19.1	1.22
22.2	1.22

25.4	1.22
31.8	1.62

- It was anticipated to perform the first test with only the 22.2 and 25.4 mm tubes.
- Temperature variation: 20ºC - 60ºC in 5ºC increments.
- Hole diameters: 3 mm / 4 mm / 5 mm
  Hole size in parameters were obtained from the previous smaller size.
- Pressure difference: 0 – 50 mbar
- Seawater concentration: The initial tests were performed with tap water, while a comparison test was done afterwards with seawater at 35 g/kg at 20ºC. The variation in wetted length for tap water and seawater will determine the necessity for further seawater tests.

It is foreseen that the above-mentioned should enable the design of a perforated plate for operation at specific Reynolds numbers and wetted lengths.

5.1.2 Geometry

The most important aspects to consider when designing the test section are the associated geometry with regards to the tube pitch and layout.

Tube pitch:

A triangular tube configuration will be used since it is more compact than a square tube arrangement and will therefore require fewer materials. Different tube pitches were also investigated as shown in Table 5.2 and Figure 5.2. According to the literature, the most common ratio is that found in the first row. The other configurations will be tested to provide some more space for a tube-to-tube-sheet fitting, while investigating whether it has any other effects on the flow pattern.

Table 5.2: Tube Pitch

B	S
$1.2 \cdot d_{ext}$	$1.3 \cdot d_{ext}$
$1.4 \cdot d_{ext}$	$1.3 \cdot d_{ext}$

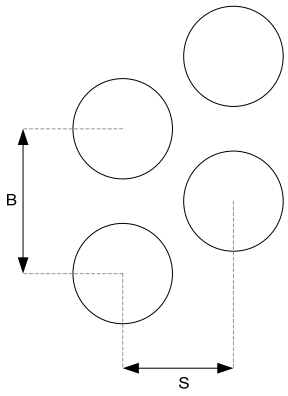

Figure 5.2

A matrix of tube arrangement as shown in Table 5.3, is created by these arrangements together with the different tube sizes. For the rest of the experiment the alpha numbering for the different configurations will be used for identification.

Table 5.3: Spacing of tubes

	Spacing	
Diameter	**$1.2 \cdot d_{ext}$ x $1.3 \cdot d_{ext}$**	**$1.4 \cdot d_{ext}$ x $1.3 \cdot d_{ext}$**
19.1	B1	B2
22.2	C1	C2
25.4	D1	D2
31.8	E1	E2

The effect of larger spacing will only be investigated once the complete graphs have been determined.

The following assumptions are made for the inputs to the system.

Assumptions/fixed inputs:

- Normal municipal water will be used to perform the tests, but seawater can also be used at a later stage if necessary and available.
- General aluminium tubes will be used in the test section. Although similar in dimension, this will not necessarily be the final grade as to be used in a possible final Pilot Desalination Facility (PDF).
- Normal water temperature is between 15°C and 25°C, while the actual temperature will be measured.
- A triangular tube arrangement will be used in the test section with the minimum number of vertical rows being 4 and always being an even number. This will allow for the examination of the flow pattern in both the higher and lower rows.

Parameters to be measured and investigated:

- Measurement of the mass flow [kg/s]
- Measurement of the wetted length of the tubes [mm]
- Investigation (visual inspection) of the flow pattern
- Measurement of the water temperature
- Sieve (distribution) tray height

5.1.3 Flow pattern test section

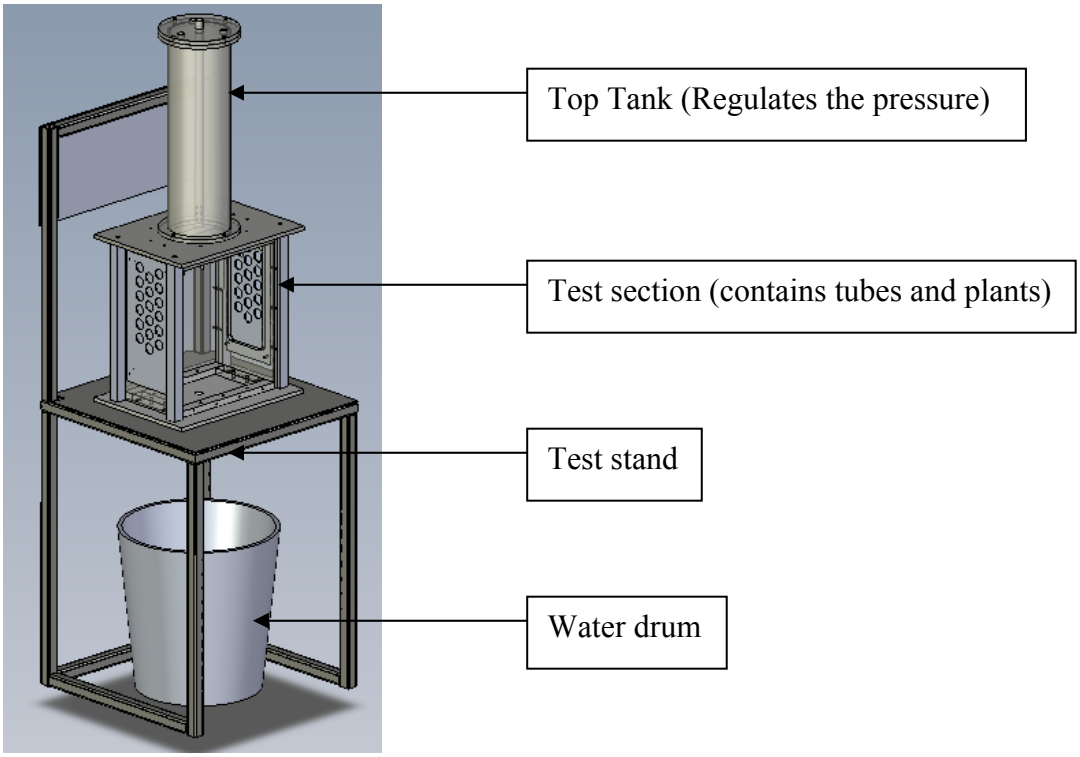

Figure 5.3: *Three-dimensional view of flow pattern test section with tubes removed*

The flow pattern test section that was designed can be seen in Figures 5.3 and 5.4. It consists of interchangeable parts such as sieve trays (perforated plates) with different hole diameters as was discussed earlier. The tube diameters can also be varied, as well as the layout and spacing of the tubes with the use of different side panels.

This flow pattern section was used to determine the wetted lengths and to investigate the flow patterns for different parameters.

Figure 5.4: *Flow pattern test section*

The flow pattern test section had to be able to test various conditions and geometries to determine the wetted length and flow patterns. It therefore needed to consist of different parts that could be removed and changed (substituted) with parts with other dimensions.

The test section consists of the following interchangeable parts:

- There were perforated plates with different hole diameters and spacing of the holes.
- There were various types of tube plates (also referred to as base plates) for the different tube sizes and spacing.
- The Aluminium tubes can be removed and they have different diameters to change the layout.
- The water level in the top tank can also be varied to change the pressure difference (Δp) of the water in the system.

For the water to be circulated continuously through the system, a pump is required. This meant that an auxiliary pumping system had to be designed.

The following formulas were used for the auxiliary pumping system to determine the pressure and the required flow rate:

$$p = \rho g h$$

$$\Delta p = \frac{1}{2}\rho V^2$$

$$m = \rho V A$$

$$Q = VA$$

This was done to determine the in- and outflow of water from the tank to keep the water in the tank at a constant level.

Implementation of these formulas gave the following results:

- For 50 mbar, the maximum volume flow rate is 1.072 m^3/hr (1072 l/hr) and the minimum flow rate was 0.319 m^3/hr (319 l/hr).
- At a pressure of 10 mbar it was found that the maximum volume flow rate was 0.479 m^3/hr (479 l/hr) and that the minimum flow rate was 0.143 m^3/hr (143 l/hr).

This information was then used to design the auxiliary pumping system for the test section.

5.2.1 Mass Flow

As discussed earlier in this chapter, one of the parameters that need to be investigated was the mass flow of the water through the holes. It was done by measuring the flow in the auxiliary pumping system with a flow meter. The water flow rate was controlled by means of a valve that was opened and closed to keep the water level in the top tank at a specific level to obtain a certain pressure difference. All the information gathered was then added to a table and from the table, the graph (Figure 5.5) was created that summarizes the results.

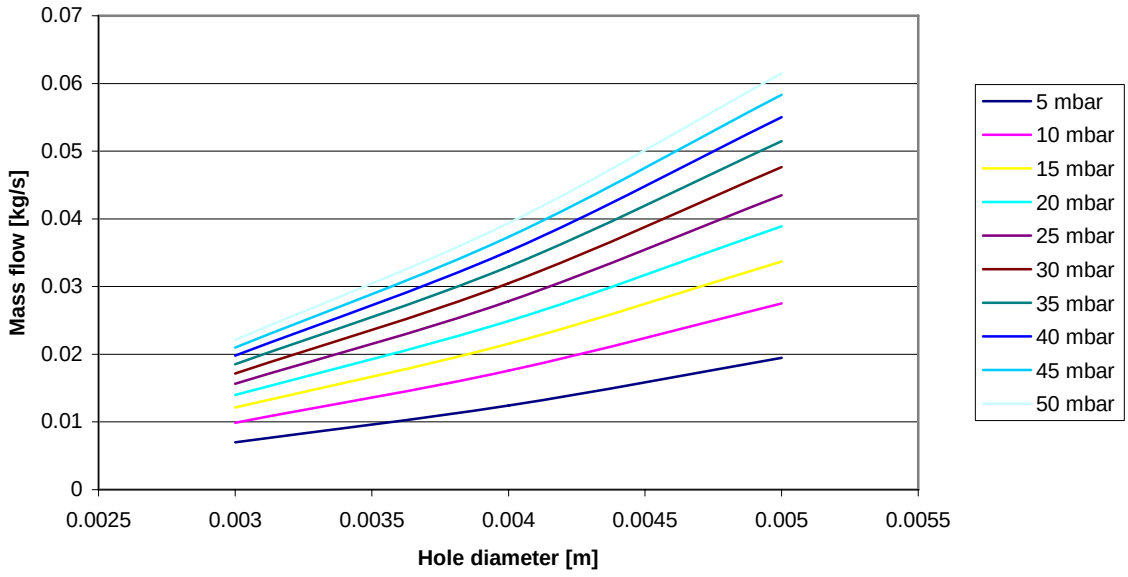

Figure 5.5: *Mass flow per perforated hole*

From Figure 5.5 it can be seen that the higher the pressure and the larger the hole diameter, the larger the mass flow and therefore the flow rate will be. This means that the water also flows onto the tubes with a higher mass flow and therefore a higher velocity. For example, it can be seen that for a pressure difference of 5 mbar and a hole diameter of 5 mm, the mass flow rate will be approximately 0.02 kg/s. To then calculate the total mass flow rate, the number of holes can be multiplied by the mass flow rate per hole.

This will help in the design process to do sizing of pumps in the system and to calculate the total flow for different geometries and pressures.

Once the mass flow was measured at different pressures, the rest of the experiment could be performed to determine the wetted length from a variety of pressures and at different temperatures.

5.2.2 Wetted Length

In order to measure the wetted length and to obtain accurate measurements, it was necessary to take down more than one measurement. In the end, readings at 4 different points were taken (2 in the front of the test stand and 2 at the back and it was measured by the use of a self-retracting pocket tape measure marked in millimetres) and the average value between the 4 readings was used in the further assimilation of the data that was obtained from the experiments. Measurements were taken for all the geometries and hole diameters as was proposed earlier in the chapter. Tests were done from 5 mbar up to 50 mbar. This was done by controlling the water level in the top tank by opening and closing a valve that controlled the flow of water into the tank. The water level in the top tank determines the head or pressure that was available for the water flowing over the tubes.

The following figures (Figure 5.6 up to Figure 5.9) show some of the results that were obtained from the data. Note that this is only the data for the 5 mm holes in some of the perforated plates and that the rest of the data for the 3 mm and 4 mm holes can be found in the Appendix to this report.

The figures for the 5 mm holes are displayed here to illustrate how the wetted length increases with an increase in temperature and pressures. Although it seems like a lot of figures, it is important to include them because it indicates how the wetted length changes along with the different conditions. It also illustrates the effect the tube layout and geometry has on the wetted length.

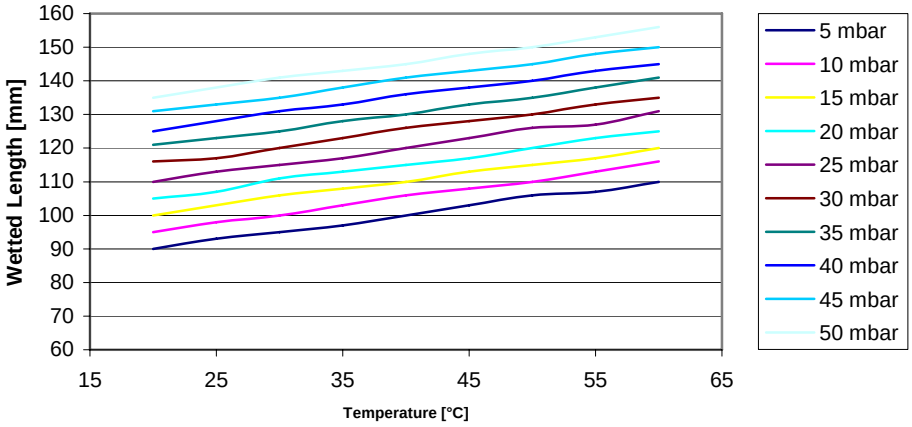

Figure 5.6: *Base plate E2 and perforated plate with 5 mm holes*

Figure 5.6 shows that as the temperature increases for a given pressure, the wetted length increases as well. In addition, it can also be seen that as the pressure (i.e. mass flow) increases, the wetted length also increases.

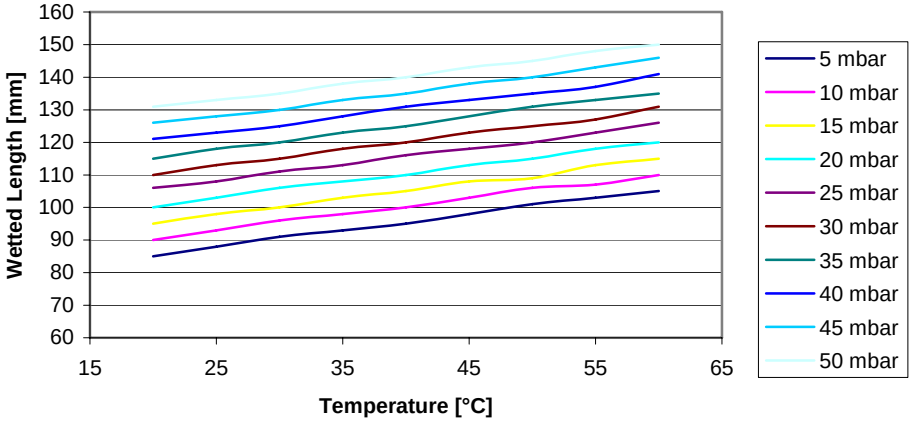

Figure 5.7: *Base plate E1 and perforated plate with 5 mm holes*

In figure 5.7 the same results can be seen as in Figure 5.6 except that the wetted length for the geometry of base plate E1 is smaller than that of E2. The difference between the geometry between E1 and E2 is that the tubes are spaced further apart in E2 than in E1.

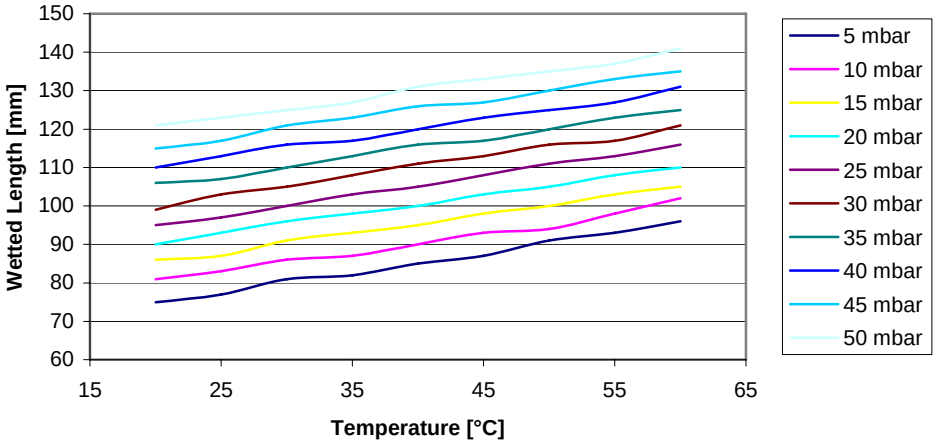

Figure 5.8: *Base plate B2 and perforated plate with 5 mm holes*

In Figure 5.8 the same can be seen as in Figure 5.6 except that the wetted length is smaller than in the case of Figure 5.6. In the case of Figure 5.8 the tube diameter for base plate B2 is smaller than the tube diameter for base plate E2.

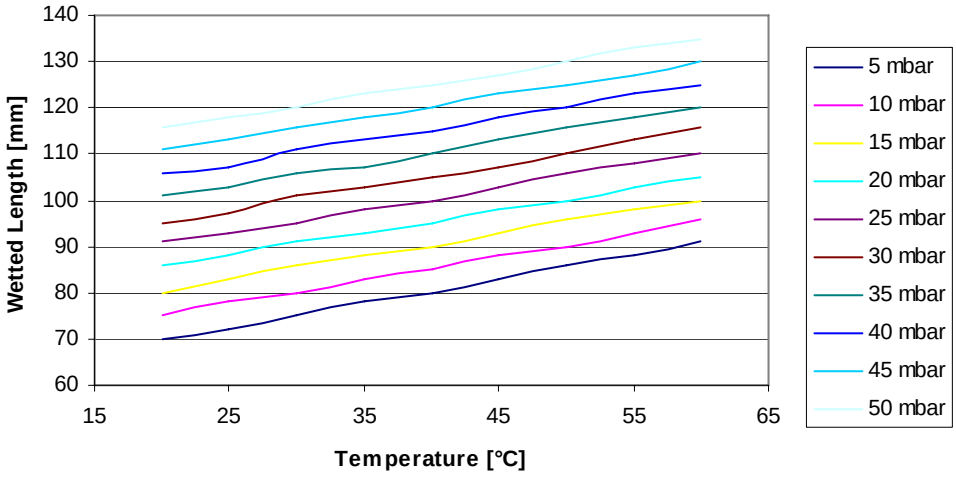

Figure 5.9: *Base plate B2 and perforated plate with 5 mm holes*

In this figure the same effects can be seen as was discussed for Figure 5.6 regarding the temperature, pressure and wetted length. As was the case for base plate E1 and E2 the same can be seen for base plate B1 and B2 regarding the spacing of the tubes.

The following observations can be made from these figures:

- Wetted length increases with an increase in pressure (meaning an increase in mass flow). This means that the higher the velocity of the water onto the tube, the better the wetted length will be. This can also be seen by doing the simple experiment of holding a pen under the water flowing out of a tap. As the flow from the tap is increased, more flowing water is covering the pen.
- Wetted length increases with an increase in temperature meaning that the decrease of the viscosity of the water plays a role because the viscosity decreases as the temperature increases. This means that a higher temperature (and lower viscosity) will lead to a better wetted length.
- A larger diameter tube also has a larger wetted length than would be the case for a smaller diameter tube at the same pressure and temperature.
- A wider spacing of the tubes also has a larger wetted length as would be the case if the tubes were spaced closer to each other. The reason for this is that the water can reach a higher velocity before reaching the next tube and, as discussed earlier, a higher velocity will lead to a better wetted length. (This will, however, cause a less compact evaporator and will therefore require more materials.)
- Finally it should be noted that wetting is primarily a function of the feed distribution, the falling film and heat transfer pattern, the evaporator tube bundle geometry and last but not least the seawater properties.

The results from the data, as shown in the figures, can now be used to design a sieve tray at a given temperature and pressure. It can now also be used to determine the size of the pump, for instance, because the required pressure is known and the cost of machining of the sieve tray can be calculated because the number of holes that need to be made in the sieve tray is now known. An optimum point between manufacturing cost and efficiency, or in other words the minimum wetted length required to prevent dry patches, can subsequently be determined.

It can for example be seen that, for a layout with base plate E2 with a 5 mm diameter hole with a Δp (pressure) of 10 mbar and a temperature of 40°C, the wetted length will be

105 mm. Hence the holes will have to be spaced 105 mm or less from each other for a tube above the centreline of the specific tube. In that manner the entire tube will be covered with a water film and there will be no dry patches where corrosion and scaling can develop.

The above-mentioned enables the designer to specify how many holes are required in a specific plate. From this, the machining cost can be calculated. Furthermore, parameters like the Reynolds number for instance, can be calculated accurately due to the fact that such a calculation requires the entire area of the tube to be wetted.

The following results regarding the minimum and maximum wetted lengths were gained from the experimental data. Similar tables and graphs were obtained for the other geometries and hole diameters and they can be seen in the appendix (Appendix A) to this report.

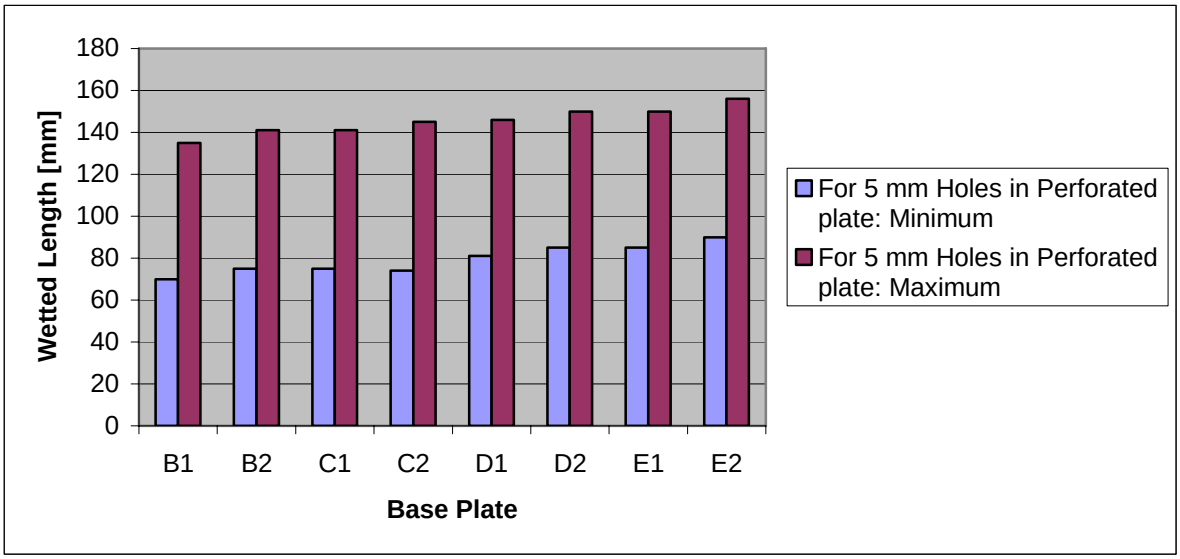

Figure 5.10: *Minimum and Maximum Wetted Lengths for pressure between 5 and 50 mbar.*

As has already been discussed, it can be seen from Figure 5.10 that the wetted length increases as the diameter increases. It can also be seen that the further the tubes are spaced from each other, the larger the wetted length would be. It can be seen that C2 and

D2 for example have the same wetted length although the diameter of the tubes for C2 is smaller than that of the tubes for D2. This, however, does not mean that the diameter does not make a difference. It only occurs because of the fact that the tubes of C2 are spaced farther apart than the tubes of D1. From this the conclusion can thus be made that the spacing of the tubes also plays a role in the design process. From the wetted length of C1 and D1 for example, which more or less have the same spacing, the conclusion can be drawn that a larger diameter tube will have a better wetted length than would be the case for a small diameter.

Comparison between seawater and municipal water:

Comparison tests were also done with seawater (35 g/kg) at 20°C and these results showed that the wetted length is basically the same as the results obtained with the municipal water. It can be seen that the difference is less than 2 % (the reason for the difference is that seawater is less viscous than municipal water due to a higher salt content) and for the purpose of this study a margin of 5 % at the most would be acceptable.. Therefore it was not necessary to repeat all of the tests for seawater because the small difference indicated that the results of the municipal water could be used for seawater as well. The results of the comparison tests are shown below.

Table 5.4: Difference between readings for seawater and municipal water.

Pressure [mbar]	**Difference [%]**
5	1.43
10	1.33
15	1.94
20	1.58
25	1.10
30	1.78
35	1.49
40	1.42
45	1.80
50	1.29

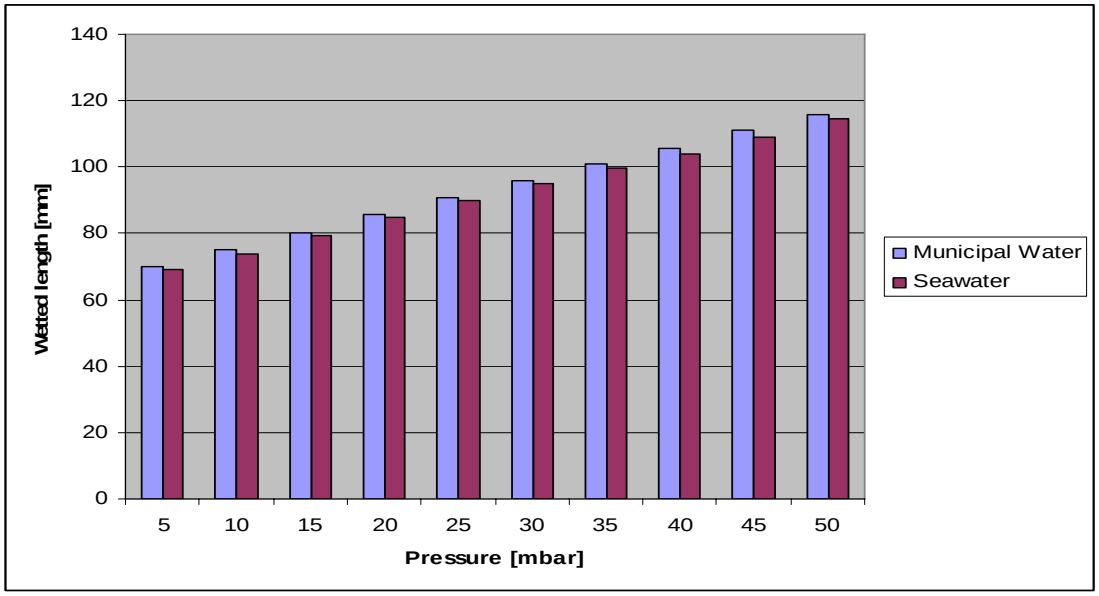

Figure 5.11: *Comparison on wetted length between municipal and seawater for setup B with tube plate B1 and 5mm holes in the perforated plate.*

5.2.3 Flow Pattern in test section

Investigation of the flow over the tubes showed that the flow varies from droplet column mode to column flow mode. Furthermore it can be seen that, for the most efficient flow over the tubes and tube bundles, the hole must be situated above the centreline of the tubes. The tests showed that larger diameter tube bundles will have better flow over them (meaning that they have a larger wetted length) than is the case with small diameter tube bundles.

For a larger spacing of the tube bundles the flow is also better and provides a larger and better wetted length than is the case if the tubes are grouped closer to each other. However, this will lead to a larger evaporator, which will mean that an optimum point has to be reached between efficiency and cost. The following figures (Figure 5.11 up to 5.14) show some of the flow over the tubes for the perforated plate with 5 mm holes and different base plates (with the different tube layouts and geometries). Note that the water had been coloured red for photographic purposes whereas the tests were performed with clear municipal water.

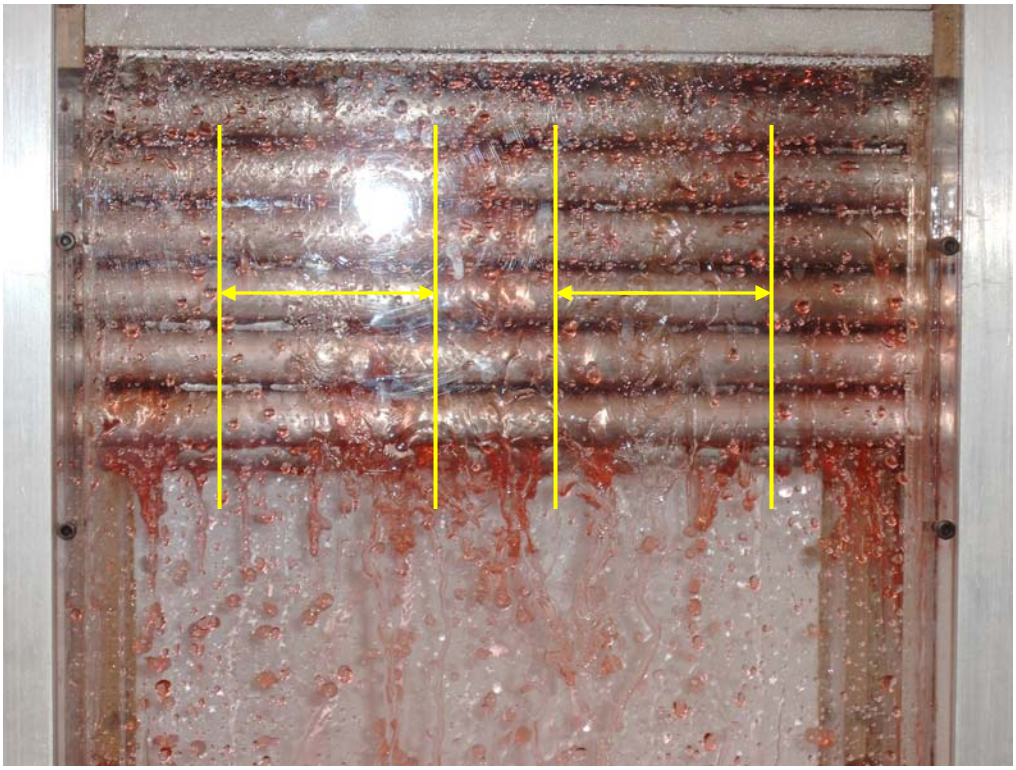

Figure 5.12: *Flow for B1*

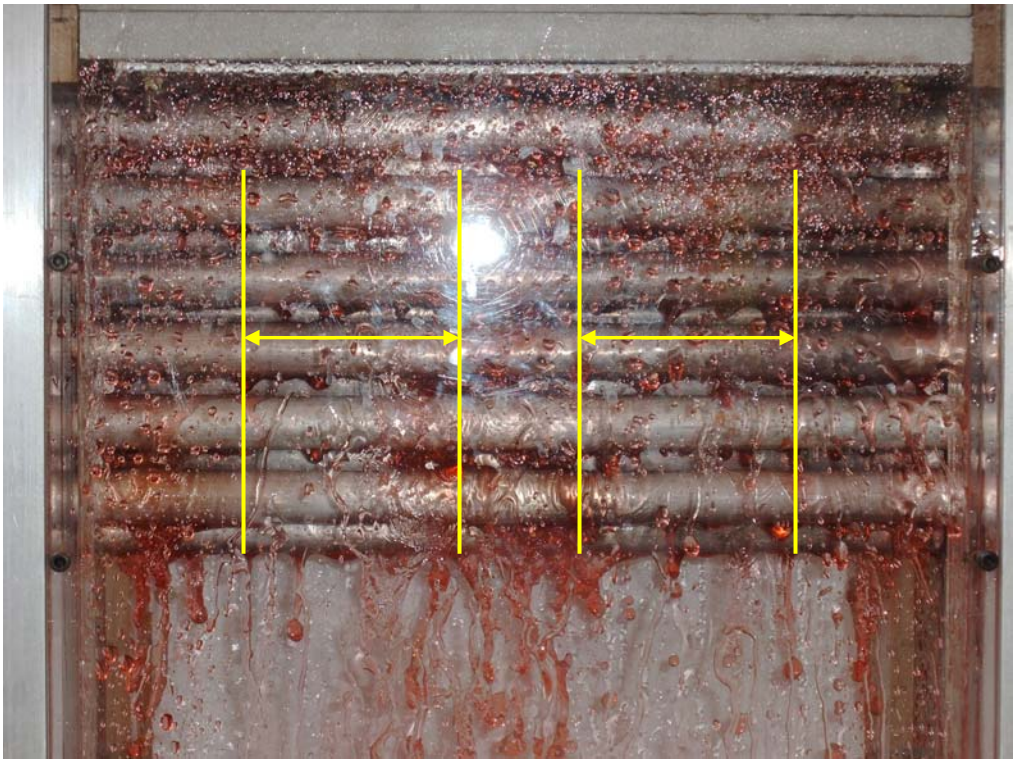

Figure 5.13: *Flow for B2*

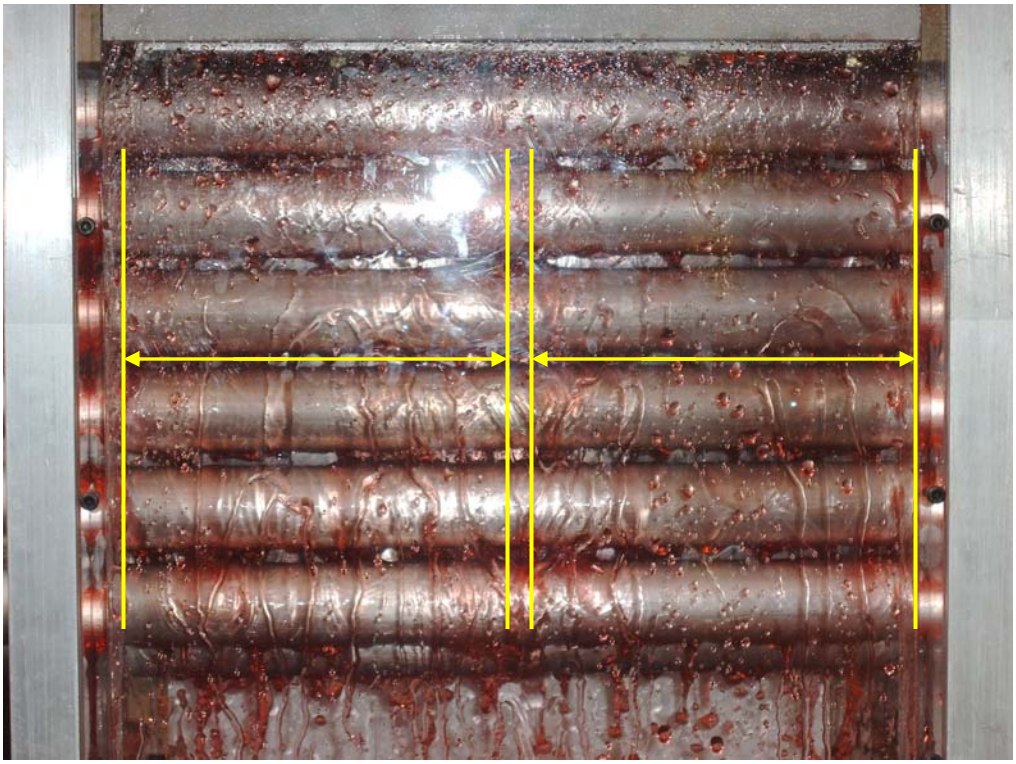

Figure 5.14: *Flow for E1*

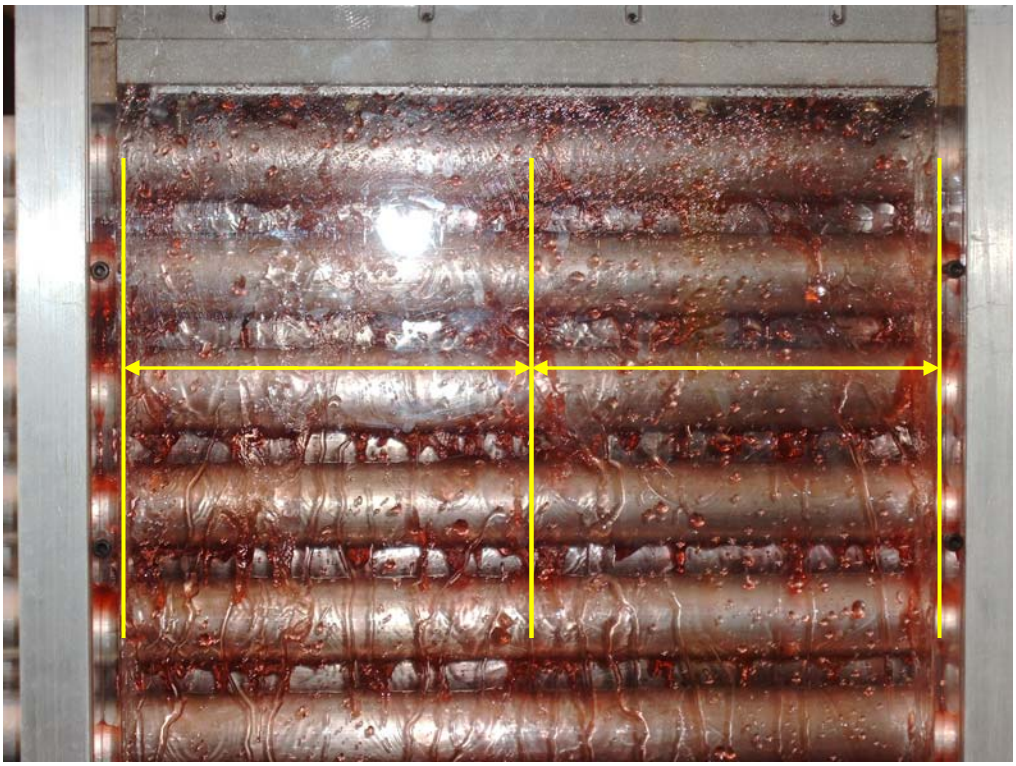

Figure 5.15: *Flow for E2*

From these figures it can therefore be concluded that the flow improves (better wetting and a larger wetted length as can be seen from the markings on the figures) with an increase in the tube diameter and a geometry that has the tubes spaced further apart from each other. Further tube spacing, however, can cause higher evaporator costs because, if the tubes were further apart from each other, it would mean that more materials would be required to manufacture the heat exchanger.

5.2.4 Uncertainty Analysis

To ensure that accurate results were obtained, readings at 4 different points were taken during the experiments as was stated earlier. The maximum deviation between the maximum and minimum value obtained on average were less than 2 % (between 1.5 and 2 %) as can be seen in Table 5.5 and Figure 5.16 below. As was stated earlier for the purpose of this study the maximum deviation was set at 5 % in order to be accurate. Therefore the deviation in the results is acceptable and the results from the tests can be assumed as accurate.

Table 5.5: % Difference between readings

Pressure [mbar]	**Difference between min and max value [%]**
5	1.90
10	1.73
15	1.81
20	1.69
25	1.58
30	1.83
35	1.76
40	1.91
45	1.63
50	1.66

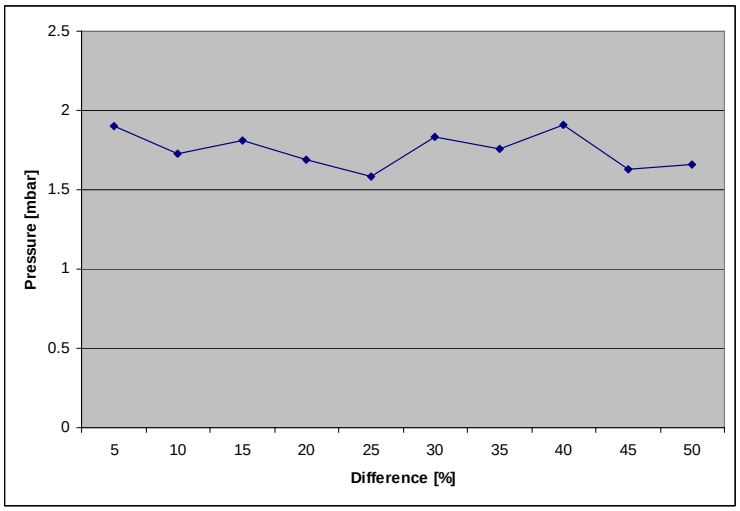

Figure 5.16: *Maximum difference between readings*

5.3 Conclusion

The results obtained from the experiments as discussed in this chapter, can now be used as a vital design tool that could be used in the design process of a sieve tray for an evaporator of a desalination plant. All the figures for the wetted length and mass flow that were developed from the experiments earlier in this chapter can now be used to make selections for given geometries and various conditions by selecting the correct spacing of the holes for a sieve tray. They can also be used as an important design tool to determine the effects of variations in the conditions such as the temperature (meaning viscosity as well) and the pressure (mass flow of the water). This means that they can now be used by the designer in the design process to design the best sieve tray (perforated plate) for the given conditions.

The results for seawater vary very little from those generated for municipal water. It therefore means that the results can be used for designing a sieve tray for both municipal water and seawater. The results that were generated also fall within acceptable limits and can therefore be accepted as reliable. It can also be considered in the future to implement these results into computer software to ensure a quick design of the sieve tray.

6. Conclusion and Recommendations for Further Work

In Chapter 1 and 2 it was indicated that there was a need for the design of a set of basic tools that could be used in the design process of evaporators to be used in Multi Effect Distillation desalination plants. Chapter 3 discussed the theory behind heat transfer in the evaporator as used for the development of the simulation design tools in Chapter 4. The tools can be used to investigate initial sizing issues and help to determine the heat transfer coefficient. The data obtained from the evaporator simulation design tool had a good comparison to a case study that was done by Rousseau (2006:66). Furthermore from the work done by others, as was discussed in Chapter 2, a study was launched which led to the development of an experimental test section (as was discussed in Chapter 5) which was used to study the flow over the tubes in the evaporator.

The detailed discussions and conclusions of the results are summarized in the following 3 sections:

6.1 EES program simulation

The following conclusions were made on the tools that were developed for the evaporator and the vacuum system (as was discussed in Chapter 4):

6.1.1 Evaporator

The simulation programs developed in EES were developed for the evaporator of an MED plant and are valuable in giving the initial order of magnitude for parameters like the heat transfer coefficient as well as the amount of heat transferred. Another advantage is that the program can also be used to address sizing issues of the evaporator by means of calculating the evaporator diameter and length as well as the number of tubes inside the evaporator. With the size known, a layout of the plant can be planned and a preliminary cost analysis can be done.

6.1.2 Vacuum System

During this study (Section 4.2.2) a simple approach was used in the development of a tool that can help in the selection of the components for the vacuum system. Therefore, for this study, a relatively simple tool was created that is easy and quick to use and can easily be modified or expanded.

6.2 Wetted length flow pattern test section

The graphs obtained from the experiments on the wetted length test section for different tube sizes and spacing that was done in Chapter 4, can be used as a convenient design tool which can be used in the design of the perforated plate of a horizontal falling film evaporator. An investigation into this prospect was important because, in order to prevent scaling and corrosion, the entire tube needed to be covered with a water film as was pointed out in Chapter 2. Therefore, this was an important study and the results can be implemented in a design tool.

6.3 Conclusion

As was discussed at the end of Chapters 4 and 5, the research performed during this study resulted in a set of tools that can be used in the initial design of an evaporator for a Multiple Effect Distillation (MED) plant. Information supplied can furthermore be used to develop a simulation package to do a detail in-depth design. A layout study can also now be performed to address sizing issues. The study further has shown that it is possible to develop a basic design tool with which an MED evaporator together with its vacuum system can be designed. The tool that was developed has shown that it is applicable on both municipal and seawater as a 1st order approach of the design. From the success of the method, it was proved that it is acceptable to include into a detail simulation package.

6.4 Recommendations and future work

6.4.1 Wetted Length

Since the experiments were initially carried out with normal municipal water, seawater comparison tests had to be done to verify that the municipal water gave realistic results. The results that were obtained from these tests showed good correlation between fresh and seawater indicating that the results regarding the wetted length was applicable to both normal municipal water as well as seawater.

The results (graphs) obtained can also be programmed into a simulation package, like for instance Flownex or other design software, to make the design of the perforated plate easier by using these curves. The correct curves for the various conditions (temperatures, pressures and geometries) can then easily be selected and implemented.

Another important suggestion that can be made is the design of a corrosion test section. This needs to be done in order to investigate the corrosion rate of the proposed aluminum tube together with the sealing methodology. It can form another important study because of the fact that seawater is highly corrosive.

6.4.2 Evaporator

The simulation program gives good initial design values for sizing purposes. However, for a more detailed design on the evaporator, the simulation program will have to be expanded in such a way as to include, for example, an incremental approach. From such an expansion a temperature profile over the evaporator, for example, can then be generated.

Another option that should be considered is to implement the information of this study regarding the evaporator into a simulation program like, for example, Flownex. The reason for this is that EES sometimes has its shortcomings in calculations. One of these

shortcomings is that when the values are changed it needs to be done in small steps in EES.

EES uses a solving technique to solve a number of equations and an equal number of unknown variables. In case of an explicit solution of a poorly earthed matrix, the system tends to be rather unstable and can therefore not solve the initial guess values and is too far from the solution. This means that for complex solutions, changes need to be done in small steps updating new guess values after each iteration. If this is not done, the program has some calculation instabilities. An example of this is when trying to increase the mass flow from 1 kg/s to 20 kg/s. Due to the instabilities, it cannot be done in one single step, but has to be done in smaller steps by gradually increasing the mass flow value. This is one reason for the small mass flow used in this study (it was also used to be comparable to the data in Rousseau, 2006:59). A simulation package like, for example, Flownex on the other hand uses a new generation solver rendering it very stable for solving similar systems even when taking significant steps. That is why it would be advisable to implement the information of this study into another simulation package or to create a new program.

6.4.3 Vacuum system

Further investigations needs to be done for the vacuum system in order to create a detail design tool seeing as a simple approach without too much detail was followed for this study. It would, however, be advisable to do a detail design on the vacuum system of the desalination plant as it plays such an important role in the regulation of the pressure in the evaporator.

Another aspect regarding the vacuum system that could be of value is the incorporation of a vacuum system design function into a simulation package. One option would be implementing it into Flownex (a systems CFD (Computational Fluid Dynamics) code that enables users to perform detail design, analysis and optimization of a wide range of thermal-fluid systems). However, an alternative would be to create a standalone program

in C++ or even Excel, as Flownex is not freely available to everyone. Another option is to do an in depth design in EES. It is therefore suggested to create an EES-program and to then carry the acquired knowledge over into the Flownex package.

This study attempted to solve the question of whether a basic design tool could be developed and sensibly employed in a commercial desalination process (MED for the purpose of this study). For the purposes of answering this question, new tools were developed to help with the design of an effective system. These tools proved that it is indeed possible and they bring us one step closer to utilizing these set of tools in the design of a MED plant.

7. References

ANON. 1990. Horizontal tube Multiple Effect – Stacked Design. pp 12 -17.

ANON. 1998. Falling film evaporation of single component liquids. International. Journal of Heat Mass Transfer, Vol. 41, No 12, pp 1623-1632.

ANON. 2006. Opportunity to use PBMR for Desalination and Dry-Cooling, *Ans Meeting 2006.*

ATKINS, P.W. 1994. Physical Chemistry. 4th ed. Oxford, pp 222-225.

CHUN, K.R. and SEBAN, R.A. (1971). Heat Transfer to Evaporating Liquid Films, *Journal of Heat Transfer,* Vol. 93, November, pp. 391-396.

DE BRUYN, R. 2007. Aural discussion concerning test section with author. M-Tech Industrial, Potchefstroom.

DU PLESSIS, G. and DE BRUYN, R. 2007. Aural discussion concerning vacuum system for pilot desalination test plant. M-Tech Industrial, Potchefstroom.

FUJITA, Y. and TSUTSUI, M. (1996). Experimental and Analytical Study of Evaporation Heat Transfer in Falling Films on Horizontal Tubes, Proc. 10th International Heat Transfer Conference, Brighton, Vol. 6, pp. 175-180.

GEA JET PUMPS GMBH 2008**a**. Jet Vacuum Systems. http://www.geajet.com/jetpump/en/cmsresources.nsf/filenames/strahl_vakuumsysteme_en.pdf/$file/strahl_vakuumsysteme_en.pdf [Date of access:: 3 Apr. 2008]

GEA JET PUMPS GMBH 2008**b**. Liquid Jet Vacuum Pumps with threaded connections. http://www.niro.de/jetpumps_ecatalogue/katalog_e/frame-produkte.htm [Date of access: 4 Apr. 2008]

GEA JET PUMPS GMBH 2008**c**. Liquid Jet Vacuum Pumps with flanged connections. http://www.niro.de/jetpumps_ecatalogue/katalog_e/frame-produkte.htm [Date of access: 4 Apr. 2008]

GEA PROCESS ENGINEERING INC 2008. Plate Evaporators. http://www.niroinc.com/evaporators_crystallizers/plate_evaporators.asp [Date of access: 5 Nov. 2007]

GEA WIEGAND GMBH 2008. Jet pumps. http://www.gea-wiegand.com [Date of access: 31 May 2008]

GREYVENSTEIN, F.S. 2007. Performance Prediction for Multi-Effect Distillation (MED) Plants. Potchefstroom : NWU (Dissertation – M.Ing) 128p.

IAEA. 2000**a**. Examining the Economics of Seawater Desalination using the DEEP Code. Printed by the IAEA in Austria, November.

IAEA. 2000**b**. Introduction of Nuclear Desalination. Vienna.

IAEA. 2002. Design Concepts of Nuclear Desalination Plants. Printed by the IAEA in Austria, November.

INCROPERA, F.P. and DE WITT, D.P. Fundamentals of Heat and Mass Transfer. 5th ed. New York: Wiley. 981 p.

INGERSOLL, D.T., BINDER, J.L., CONTI, D. and RICOTTI, M.E. 2004. Nuclear Desalination options for the International Reactor Innovative and Secure (IRIS) design.

5th International Conference on Nuclear Option in Countries with Small and Medium Electricity Grids. Dubrovnik, Croatia, 2004.

LORENZ, J.J. and YUNG, D. (1978). A Note on Boiling and Evaporation of Liquid Films on Horizontal Tubes, *J. Heat Transfer,* Vol. 101, pp. 178-180.

MACIVER, A., HINGE, S., ANDERSEN, B.J. and NIELSIN, J.B. 2005. New trend in desalination for Japanese nuclear power plants, based on multiple effect distillation, with vertical titanium plate falling film heat transfer configuration. Santa Margherita, Italy, 2005.

ROQUE, J.F. and THOME, J.R. 2007. Falling Films on Arrays of Horizontal Tubes with R-134a, Part I: Boiling Heat Transfer Results for Four Types of tubes. Heat Transfer Engineering, 28:5, pp. 398-414.

ROQUE, J.F. and THOME, J.R. 2007. Falling Films on Arrays of Horizontal Tubes with R-134a, Part II: Flow Visualization, Onset of Dryout, and Heat Transfer Predictions. Heat Transfer Engineering, 28:5, pp. 415-434.

ROQUE, J.F. and THOME, J.R. 2003. Falling Film Transitions between Droplet, Column, and Sheet Flow Modes on a Vertical Array of Horizontal 19 FPI and 40 FPI Low-Finned Tubes. Heat Transfer Engineering, 24:6, pp. 40-45.

SCIUBBA, E. 2005. Systematic Application of Exergo-Economic Methods to the Analysis and Optimisation of Desalination Processes – Final Report. Roma, Italy. 143p.

SHAMES, I.H. 2003. Mechanics of fluids. 4th ed. New York: McGraw-Hill. 822p.

SMOOK, G.A. 1990. Handbook of pulp and paper technology. Angus Wilde Publications.

THOME, J.R. 2004. Engineering Data Book III. Swiss Federal Institute of Technology Lausanne. Lausanne, Switzerland.

UNIVERSITY OF MICHIGAN (2007). Double Effect Evaporator. Department of Chemical Engineering. December 2007.

YUNG, D., LORENZ, J.J. and GANIC, E.N. (1980). Vapor/Liquid Interaction and Entrainment in Falling Film Evaporators, *Journal of Heat Transfer,* Vol. 102, No 1, pp. 20-25.

Annexure A – Figures and Drawings

Wetted Length Curves

In Chapter 4 tests and experiments were done on the flow pattern test section to determine the wetted length for different pressure and temperatures. In the chapter only some of the figures for the holes in the perforated plates were given. The figures for the 3 mm and 4 mm holes in the perforated plates, however, were not given. In this annexure the figures for the 3 mm and 4 mm holes for the different conditions are given. These are the figures, along with those in Chapter 5, which can be used in the design of the perforated plate in an evaporator for a MED desalination plant.

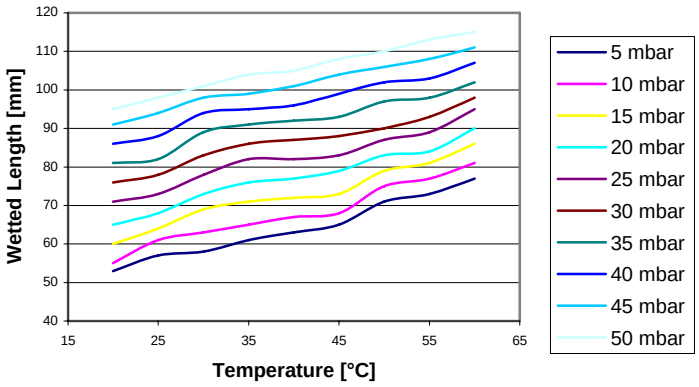

Figure A.4: Base plate B1 and perforated plate with 3 mm holes

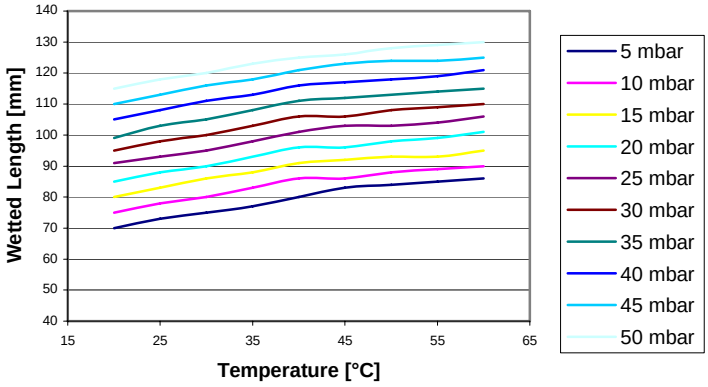

Figure A.5: Base plate B1 and perforated plate with 4 mm holes

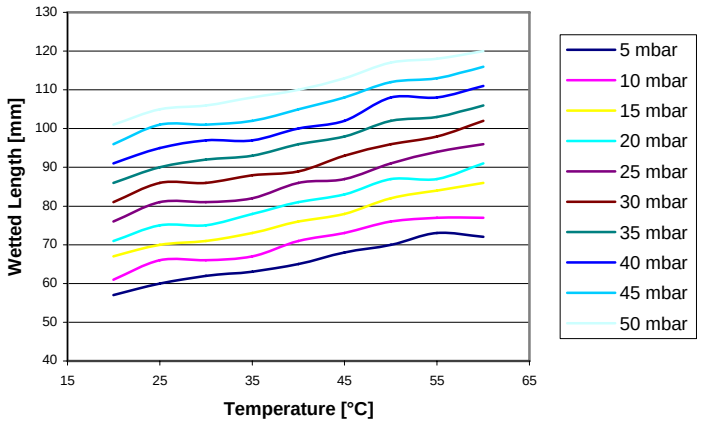

Figure A.6: Base plate B2 and perforated plate with 3 mm holes

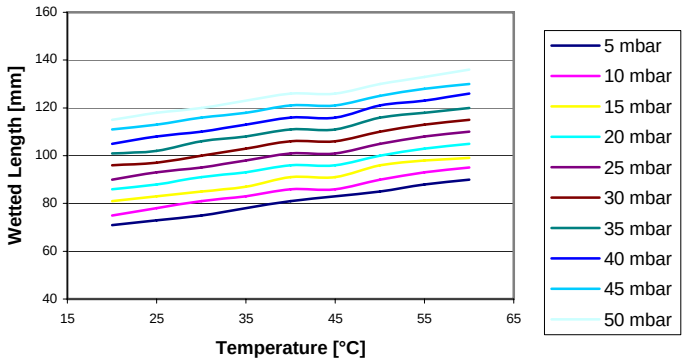

Figure A.7: Base plate B2 and perforated plate with 4 mm holes

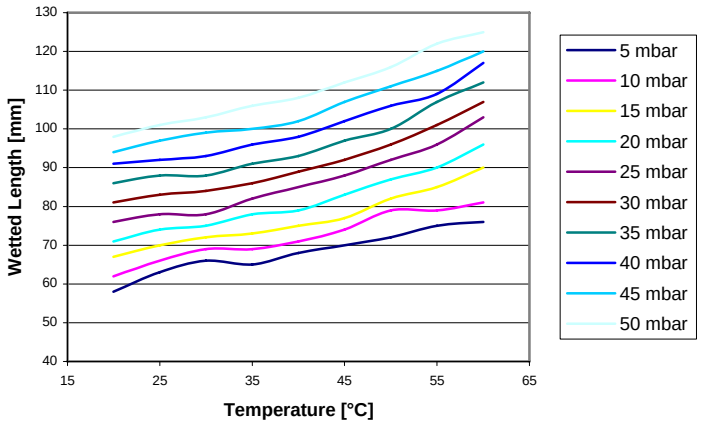

Figure A.8: Base plate C1 and perforated plate with 3 mm holes

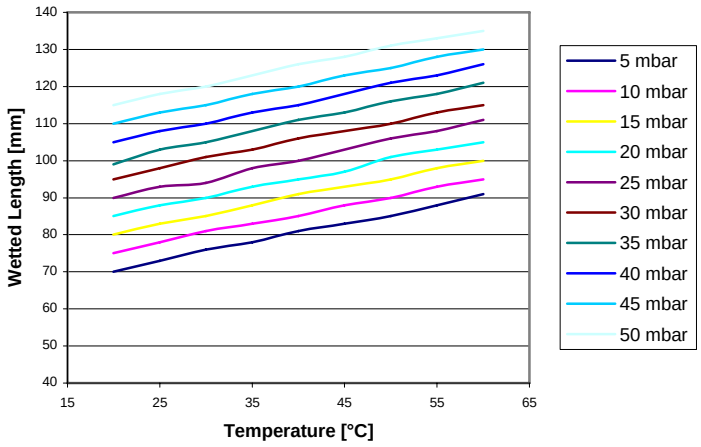

Figure A.9: Base plate C1 and perforated plate with 4 mm holes

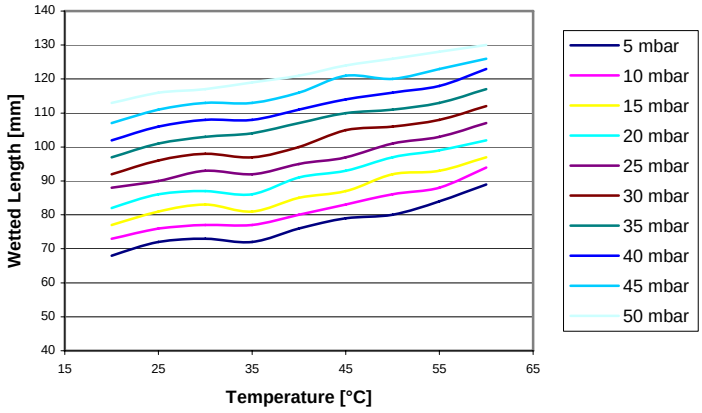

Figure A.10: Base plate C2 and perforated plate with 3 mm holes

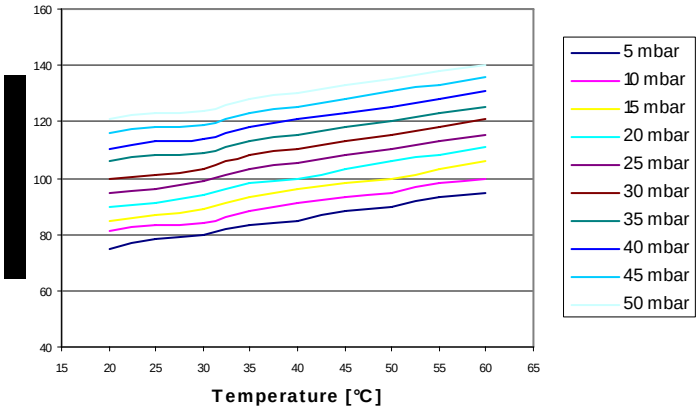

Figure A.11: Base plate C2 and perforated plate with 4 mm holes

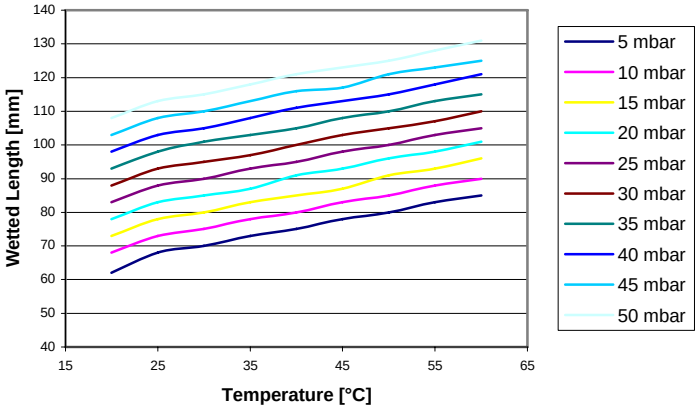

Figure A.12: Base plate D1 and perforated plate with 3 mm holes

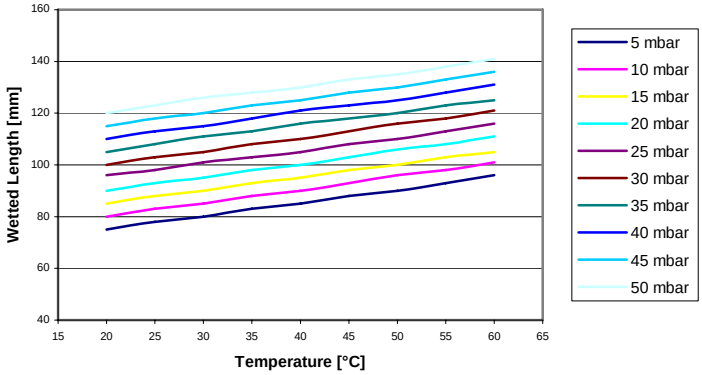

Figure A.13: Base plate D1 and perforated plate with 4 mm holes

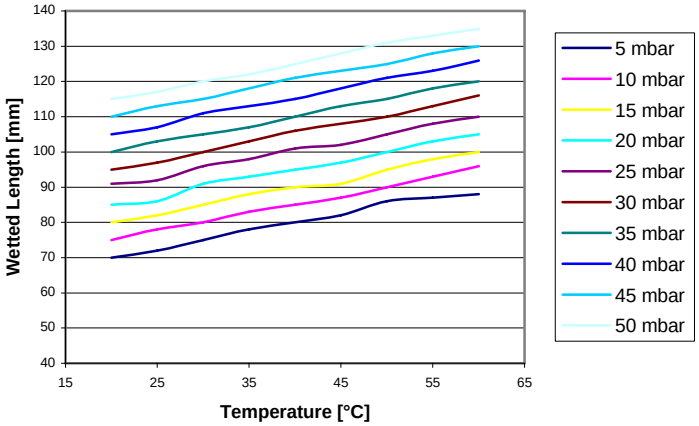

Figure A.14: Base plate D2 and perforated plate with 3 mm holes

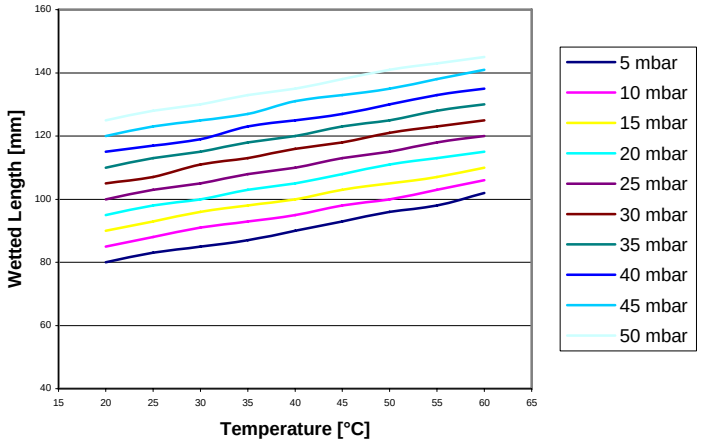

Figure A.15: Base plate D2 and perforated plate with 4 mm holes

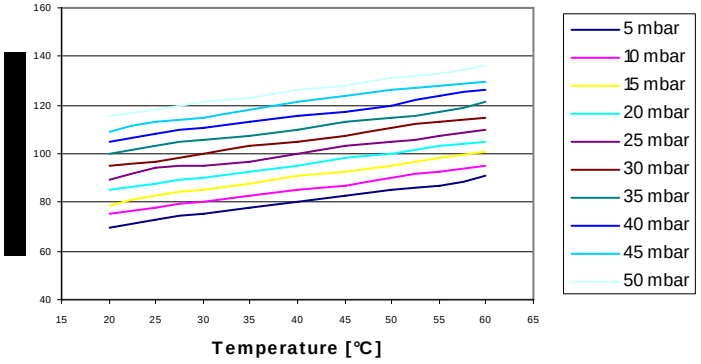

Figure A.16: Base plate E1 and perforated plate with 3 mm holes

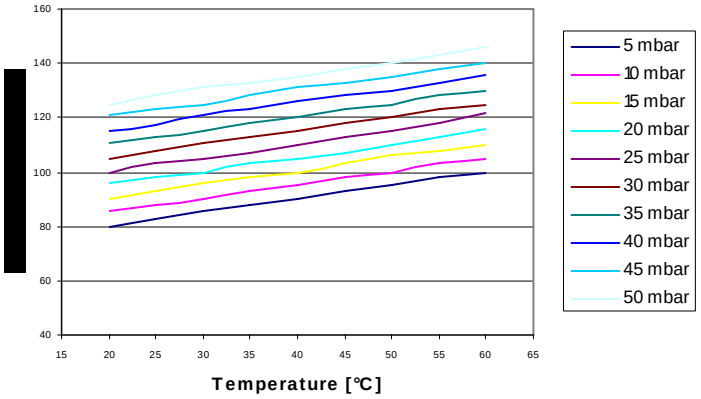

Figure A.17: Base plate E1 and perforated plate with 4 mm holes

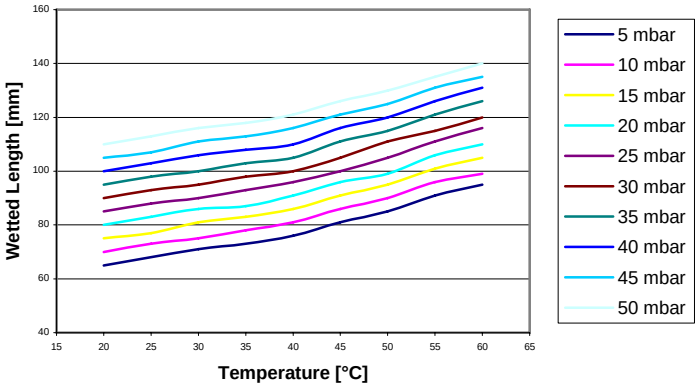

Figure A.18: Base plate E2 and perforated plate with 3 mm holes

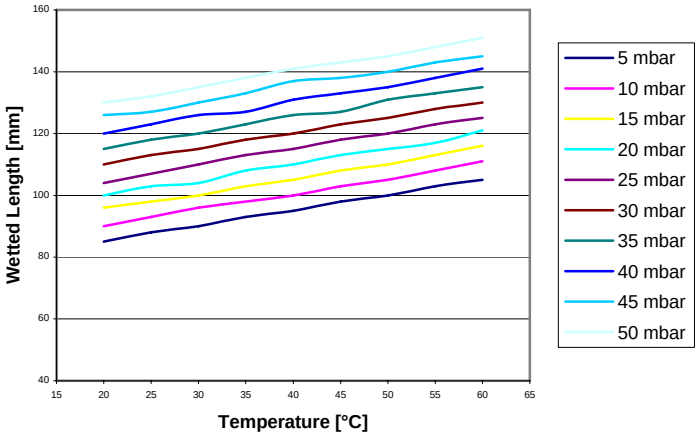

Figure A.19: Base plate E2 and perforated plate with 4 mm holes

Further from the results that were obtained in the experiments the following figures could also be drawn to give an indication of the minimum and maximum wetted lengths for the different base plates.

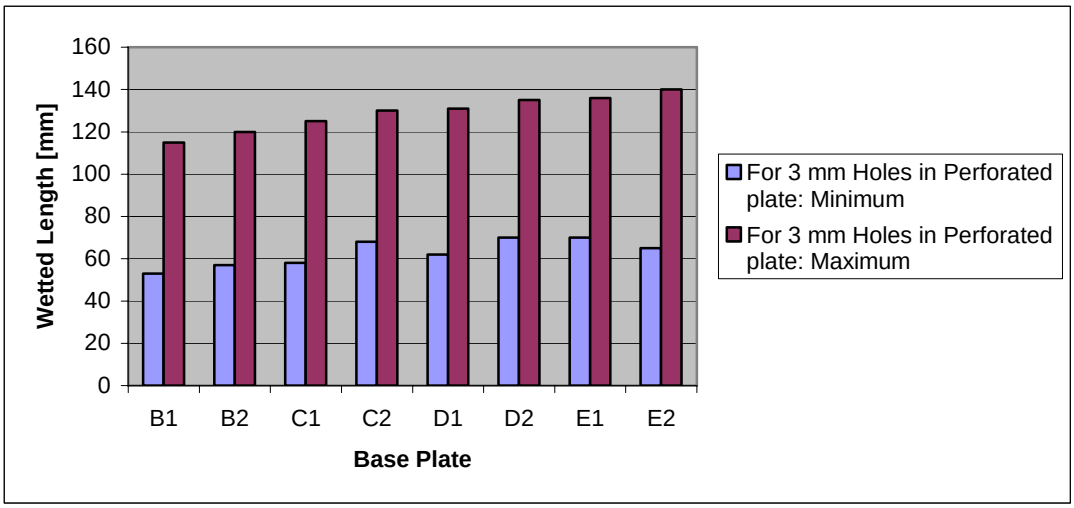

Figure A.20: Minimum and Maximum wetted lengths for 3 mm holes

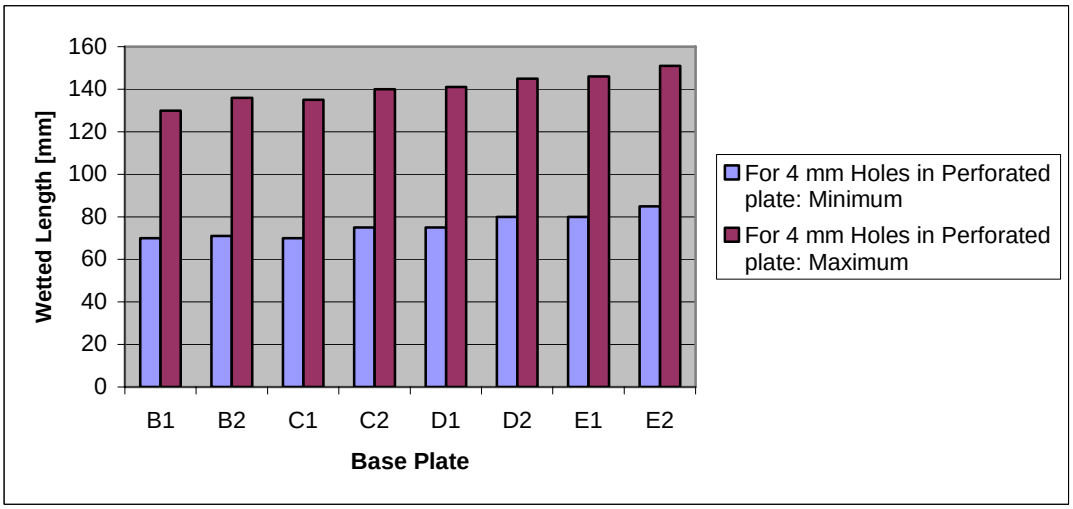

Figure A.21: Minimum and Maximum wetted lengths for 4 mm holes

Annexure B – Derivations

In order for the evaporator diameter and length to be determined the following derivations had to be. This was done by creating constants that would in the process of determining these parameters.

- Determine overall shell dimensions to ensure compliance to heat transfer duty (UA) requirement for both the single and multiple tube passes (n) arrangement:

$$UA = U_i \cdot A_{Hi}$$
$$UA = U_i \cdot \alpha_i \cdot F \cdot Vol$$
$$UA = U_i \cdot \alpha_i \cdot F \cdot \frac{\pi}{4} \cdot D^2 \cdot L$$
$$D^2 \cdot L = \frac{UA}{F \cdot \frac{\pi}{4} \cdot \alpha_i \cdot U_i}$$
$$L = \left[1.273 \cdot \frac{UA}{\alpha_i \cdot U_i} \right] \frac{1}{D^2}$$
$$\therefore K_1 = 1.273 \cdot \frac{UA}{\alpha_i \cdot U_i}$$

- Determine overall shell dimensions to ensure compliance to pressure drop (Δp_{max}) requirement for both the single and multiple tubes passes arrangement:

$$V = \frac{\dot{m}}{\rho \cdot \sigma_i \cdot \frac{1}{n} \cdot F \cdot \frac{\pi}{4} \cdot D^2}$$
$$V = 1.273 \frac{\dot{m} \cdot n}{\rho \cdot \sigma_i \cdot F \cdot D^2}$$
$$\Delta p = f_{DW} \frac{n \cdot L}{2 \cdot d_i} \rho \cdot V^2$$
$$\Delta p = 0.81 \frac{n^3 \cdot f_{DW} \cdot \dot{m} \cdot L}{\sigma_i \cdot d_i \cdot \rho \cdot F^2 \cdot D^4}$$

- To allow for inlet and outlet losses as well as bends etc. use only 70% of allowed pressure drops:

$$0.7 \cdot \Delta p = 0.81 \frac{n^3 \cdot f_{DW} \cdot \dot{m} \cdot L}{\sigma_i \cdot d_i \cdot \rho \cdot F^2 \cdot D^4}$$

$$L = \frac{1}{n^3} \left[0.864 \frac{\sigma_i^2 \cdot d_i \cdot \rho \cdot F^2}{f_{DW} \cdot \dot{m}^2} \Delta p_{\max} \right] D^4$$

$$\therefore K_2 = 0.864 \frac{\sigma_i^2 \cdot d_i \cdot \rho \cdot F^2}{f_{DW} \cdot \dot{m}^2} \Delta p_{\max}$$

K_1 and K_2 can now be used to determine the length as well as the diameter of the Evaporator as was shown in the theory and used in the EES-program for the evaporator.

Annexure C – EES Programs

The EES programs that were developed during this study as a design tool are displayed in this annexure. Also included in this section are the results of a run of the EES program. This is done to show how the calculations were done and to show which values were chosen for the purpose of this study.

C.1 Evaporator

In this section of the Annexure the EES program of the evaporator is shown together with a trial run to show the parameters involved and how they can be found in the equations.

```
"EES Program for Evaporator"
"Specifications:"
m_dot_steam = 2  [kg/s]
p_steam_i = 1600000 [Pa]
T_steam_i = 350 [K]

T_brine_i = 303 [K]
p_brine_i = 101000 [Pa]
m_dot_brine = 2.5 [kg/s]

DELTAp_steam_max = 2000 [Pa]

"Select:"
"Tube layout and Geometry"
d_o = 0.03 [m]                                  "Tube outer diameter"
d_i = 0.028 [m]                                 "Tube inner diameter"
p_c = 0.05 [m]
e = 30e-6 [m]                                   "Friction factor"
theta = 30 [°]

"Choose"
DELTAT_f = 5 [K]
n = 1                                           "Number of tube
passes"
F = 0.5                                         "Net cross-sectional
area ratio covered by tube bundle"

"Geometry Calculations"
p_l = p_c*cos(theta)
sigma_i = 0.908*(d_i/p_c)^2
sigma_o = 1 - d_o/p_c
alpha_i = 3.628*d_i/p_c^2
alpha_o = 3.628*d_o/p_c^2

"Calculation"
```

```
"Steam and water(brine) Properties:"
rho_steam =Density(Steam,T=T_steam_i,P=p_steam_i)
mu_steam = VISCOSITY(Steam,T=T_steam_i,P=p_steam_i)
k_steam = CONDUCTIVITY(Steam,T=T_steam_i,P=p_steam_i)
Cp_steam = CP(Steam,T=T_steam_i,P=p_steam_i)
C_steam = m_dot_steam * Cp_steam
Pr_steam = PRANDTL(Steam,T=T_steam_i,P=p_steam_i)

rho_brine = 1027
mu_brine = 1.056 * 10^(-6)
k_brine = 0.596
Cp_brine = 4200
C_brine = m_dot_brine*Cp_brine
Pr_brine = 7.2

m_dot_brine = Q_dot_H/(Cp_brine * DELTAT_f)

C_min = MIN(C_steam, C_brine)
C_max = MAX(C_steam, C_brine)

C_r = C_min/C_max

DELTAT_max = abs(T_brine_i - T_steam_i)
epsilon = Q_dot_H/(C_min * DELTAT_max)

NTU = (1/(C_r-1))*ln((epsilon-1)/(epsilon*C_r-1))
UA = C_min*NTU

f_DW_i =MoodyChart(Re_steam, e/d_i)                    "Darcy Wisebach factor"

K_1 = 1.273*UA/(F*alpha_i*U)
      "Calculation of a constant"
K_2 = 0.864*sigma_i^2*d_i*rho_steam*F^2*DELTAp_steam_max/(f_DW_i*m_dot_steam^2)
      "Calculation of a constant"

D = SQRT(n)*(K_1/K_2)^(1/6)                            "Diameter of
Evaporator"
L = K_1/D^2                                            "Length of tube"
N_L = 0.9*d/p_c*cos(30)                                "Number of
tubes"

Re_steam = rho_steam*V_steam*d_i/mu_steam
V_steam = 1.273*m_dot_steam*n/(N_L*F*rho_steam*sigma_i*D^2)


"To evaluate the heat transfer coefficient (h_i) for vapour condensation inside horizontal tubes,
the Shah (1978) formula has been used:"
CHI = 0.5                                              "Vapor phase mass
fraction, assumed as average in the tube"
k_L = Conductivity(Water,T=T_steam_i,P=p_steam_i )
mu_L = 0.00005
rho_L = 1000
Cp_L=Cp(Water,T=T_steam_i,P=p_steam_i )
V = V_steam
h_i = h_u*(1+ 3.8/Z^0.95)                              "Heat transfer
coefficient in tubes"
```

```
Z = (1/CHI -1)^0.8*Pr_steam^0.4
h_u = 0.023*Re^0.8*Pr_steam^0.4*(k_L/d_i)*(1-CHI)^0.8
Re = rho_L*V*d_i/mu_L
Pr = mu_L*Cp_L/k_L

"To evaluate the heat transfer coefficient (h_o) for the horizontal falling-film boiling of the brine the Nusselt expression has been used:"
"Subscripts f and g refer respectively to the fluid and gas brine phases"
g = 9.81 [m/s^2]
rho_f = rho_brine
rho_g = rho_steam
nu_g = 1.17e-6  [m^2/s]                                   "kinematic viscosity"
k_g = k_steam
k_f = k_brine
T_s = T_steam_i                                           "Temperature of vapor inside the tube"
T_sat = 343                                               "Temperature of produced steam at saturated conditions"
C = Cp_brine                                              "Brine specific heat"
Nusselt = 0.62*(g*(rho_f-rho_g)*hfg_bar*d_o/(nu_g*k_g*(T_w-T_sat)))^(1/4)
T_w = 0.5*(T_s + T_sat)                                   "Wall temperature"
hfg_bar = hfg*(1+0.34*Ja)
Ja = C*(T_s - T_sat)/hfg                                  "Dimensionless Jacob number"
hfg = 2260 [J/kg]                                         "Heat of vaporization"
Nusselt = h_o*d_o/k_f                                     "h_o = heat transfer coefficient of the brine on outside of tubes"

"Overall heat transfer Coefficient:"

1/U = 1/(h_i*(d_i/d_o)) + 1/h_o + FF
FF = 0.008
```

The results of the EES-program are as follows:

Unit Settings: [J]/[C]/[Pa]/[kg]/[degrees]

α_i = 40.63	α_o = 43.54	C = 4200
Cp_{steam} = 2193 [J/kg K]	C_{brine} = 10500	C_{max} = 10500
D = 0.5015 [m]	$\Delta p_{steam,max}$ = 2000 [Pa]	ΔT_f = 5 [K]
e = 0.00003 [m]	ε = 0.2547	F = 0.5
hfg = 2260 [J/kg]	$\overline{hfg}$ = 12256	h_i = 6567 [W]
K_1 = 0.7025	K_2 = 44.17	k_{brine} = 0.596
k_{steam} = 0.05068	L = 2.793 [m]	μ_{brine} = 0.000001056
$\dot{m}_{steam}$ = 2 [kg/s]	n = 1	NTU = 0.3117
Pr = 2.163	Pr_{brine} = 7.2	Pr_{steam} = 0.9638
$p_{steam,i}$ = 1.600E+06 [Pa]	$\dot{Q}_H$ = 52500 [W]	Re = 889150
ρ_g = 5.729 [kg/m^3]	ρ_L = 1000 [kg/m^3]	ρ_{steam} = 5.729 [kg/m^3]
$T_{brine,i}$ = 303 [K]	T_s = 350 [K]	T_{sat} = 343 [K]
UA = 1367 [W/K]	V = 1.588 [m/s]	V_{steam} = 1.588 [m/s]

$\chi = 0.5$	$Cp_{brine} = 4200$ [J/kg K]	$Cp_L = 2193$ [J/kg K]
$C_{min} = 4385$	$C_r = 0.4176$	$C_{steam} = 4385$
$\Delta T_{max} = 47$	$d_i = 0.028$ [m]	$d_o = 0.03$ [m]
$FF = 0.008$	$f_{DW,i} = 0.0318$	$g = 9.81$ [m/s^2]
$h_o = 25283$ [W]	$h_u = 1353$ [W]	$Ja = 13.01$
$k_f = 0.596$	$k_g = 0.05068$	$k_L = 0.05068$
$\mu_L = 0.00005$	$\mu_{steam} = 0.00002228$	$\dot{m}_{brine} = 2.5$ [kg/s]
$Nusselt = 1273$	$\nu_g = 0.00000117$ [m^2/s]	$N_L = 7.817$
$p_{brine,i} = 101000$ [Pa]	$p_c = 0.05$ [m]	$p_l = 0.0433$
$Re_{steam} = 11434$	$\rho_{brine} = 1027$ [kg/m^3]	$\rho_f = 1027$ [kg/m^3]
$\sigma_i = 0.2847$	$\sigma_o = 0.4$	$\theta = 30$ [°]
$T_{steam,i} = 350$ [K]	$T_w = 346.5$ [K]	$U = 121.9$
$Z = 0.9854$		

C.2 Vacuum System

In this section of the Annexure the EES program of the vacuum system is shown together with a trial run to show the parameters involved and how they can be found in the equations.

```
"EES program for the vacuum system"

m_dot = (Q*rho/(60*60))                          "Mass flow"

g = 9.81 [m/s^2]

k_m = k_valves + k_elbows                        "Losses"
h_s = 1 [m]                                      "Static height"

Vol_VacVes = pi/4*D_VacVes^2*L_VacVes            "Volume of vacuum vessel"

rho = Density(Water,T=T_1,P=P_1)
mu = Viscosity(Water,T=T_1,P=P_1)
A = pi/4*D^2                                     "Flow cross sectional area"
m_dot = rho*V*A

Re = rho*V*D/mu                                  "Reynolds number"
RR = e/D

f = MoodyChart(Re, RR)                           "Friction factor"

k = f*L/D + k_m

h_l = k*V^2/(2*g)                                "Height caused by losses"
```

H = h_s + h_l + P_1/10 "Total height"

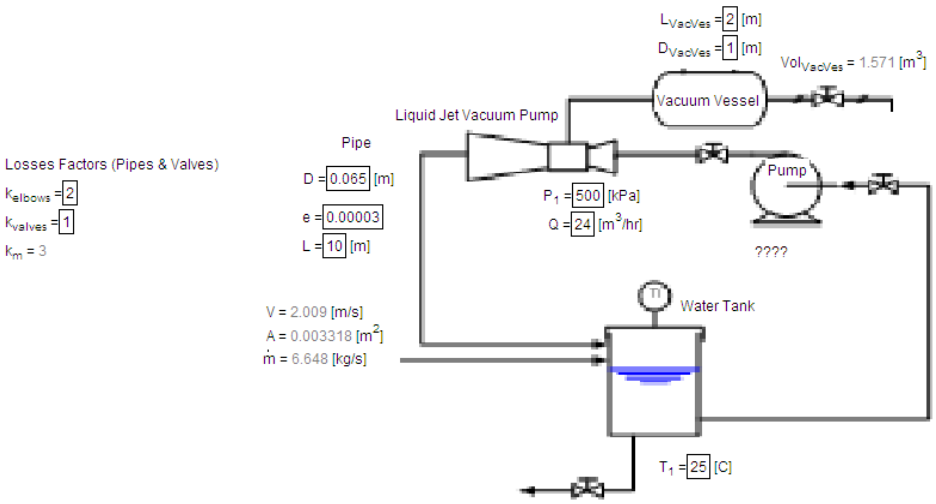

The results of the EES-program are as follows:

Unit Settings: [kJ]/[C]/[kPa]/[kg]/[degrees]

$A = 0.003318$ [m^2]	$D = 0.065$ [m]	$D_{VacVes} = 1$ [m]
$e = 0.00003$	$f = 0.01934$	$g = 9.81$ [m/s^2]
$H = 52.23$ [m]	$h_l = 1.229$	$h_s = 1$ [m]
$k = 5.975$	$k_{elbows} = 2$	$k_m = 3$
$k_{valves} = 1$	$L = 10$ [m]	$L_{VacVes} = 2$ [m]
$\mu = 0.0008904$	$\dot{m} = 6.648$ [kg/s]	$P_1 = 500$ [kPa]
$Q = 24$ [m^3/hr]	$Re = 146256$	$\rho = 997.2$ [kg/m^3]
$RR = 0.0004615$	$T_1 = 25$ [C]	$V = 2.009$ [m/s]
$Vol_{VacVes} = 1.571$ [m^3]		

Annexure D – Data sheets

The following data sheets are contained in this section:

- Data sheet for Liquid Jet Vacuum Pumps with threaded connections
- Data sheet for Liquid Jet Vacuum Pumps with flanged connections

Liquid Jet Vacuum Pumps with threaded connections

Fig. 1

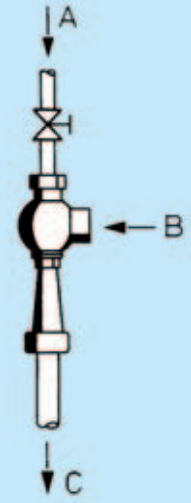

A = Motive liquid
B = Suction connection
C = Liquid outlet

Fig. 2

Liquid jet vacuum pumps generally use water as the motive medium. They are simple in construction, consisting of the head, the diffusor and the motive nozzle. They are safe in operation and maintenance free, whilst the capital outlay is low.

The operation of these liquid jet vacuum pumps is based on the liquid jet from the motive nozzle emerging at a higher velocity, entraining air or gas in the head and compressing it to atmospheric pressure.

Liquid jet vacuum pumps with threaded connections are mainly used in chemical laboratories for the production of vacuum, as for example in vacuum distillation or drying.

They are also used for evacuating syphon lines, suction lines of circulating pumps and condensers; for deaeration of pressure vessels and for producing negative pressures in Nutsch filters.

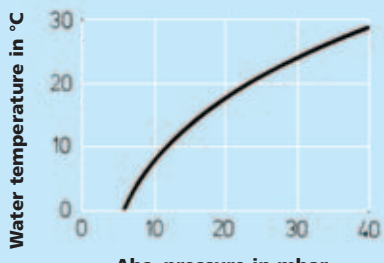

Fig. 3

Liquid jet vacuum pumps, when water is used as the motive medium, can be directly coupled to the water line. If, however, the water consumption has to be as economical as possible, the operating water may be circulated. This is also so for all cases where other liquids are used as the motive medium.

The temperature of the operating liquid may be kept low by the constant addition of a small quantity of fresh liquid. Higher vacuum can be reached by the further cooling of the motive medium. This is particularly expedient when the suction flow contains condensible components, e. g. solvents. In such a case the vacuum pump can be operated by using the condensate as the motive medium.

The lowest suction pressure which can be obtained with a suction capacity of 0 (blind vacuum) corresponds to the vapour pressure of the motive liquid which is dependent upon the temperature of the liquid.

For the motive medium of water the relationship between water temperature and lowest suction pressure is shown in fig. 3.

Capacity Diagram

Diagram fig. 5 gives the mass suction flow in kg/hr air in relation to the suction pressures at various operating water pressures for 4 pump sizes. The curves are based on an operating water temperature of 20 °C. The motive water consumption (circulating water flow) can be read from diagram fig. 7.

Liquid jet vacuum pumps will still operate satisfactorily if the outlet pipe is below the liquid level, or if a reducing piece is connected to the liquid outlet.

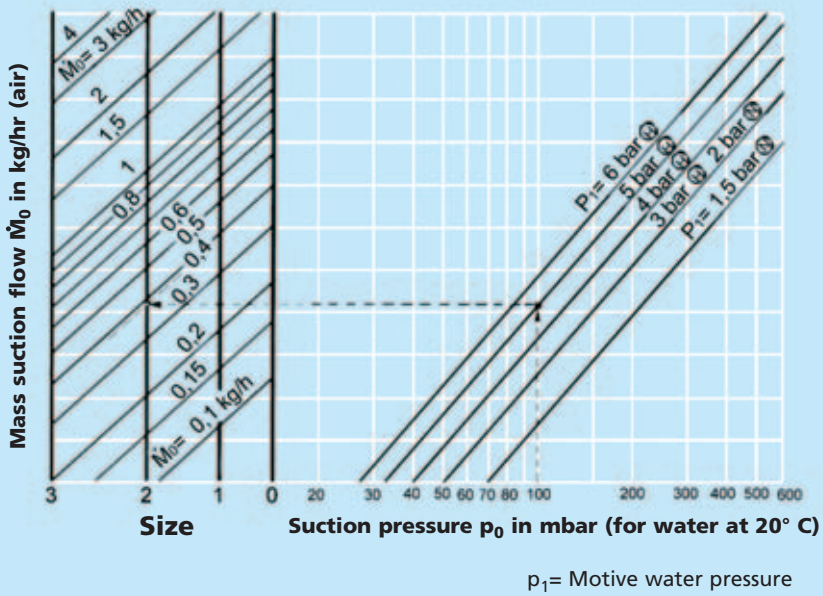

p_1= Motive water pressure

Fig. 5

(N) = Low pressure construction (1.5 – 2 bar)

(H) = High pressure construction (3–6 bar) Pressures stated in bar correspond to gauge.

GEA Jet Pumps GmbH
Einsteinstrasse 9-15
Tel.: +49 (0) 72 43 / 70 50
Email: info@geajet.de
D-76275 Ettlingen
Fax: +49 (0) 72 43 / 70 53 51
Internet: www.geajet.com
Wiegand Technology

Liquid Jet Vacuum Pumps with threaded connection as pre-evacuator

Evacuation time

Diagram **fig. 6** gives the time in minutes which a liquid jet vacuum pump size 2 requires in order to evacuate a vessel volume of 100 litres to a defined suction pressure.
The selection of other sizes is achieved by the following conversion formula:

$$F = \frac{t_{spec.}}{t_{evac.}} \cdot V$$

F = Factor for the selection of the pump size

$t_{spec.}$ = Specific evacuation time in min/100 l (from diagram fig. 6)

$t_{evac.}$ = Expected evacuation time in minutes

V = Volume of vessel to be evacuated, in litres

Size	0	1	2	3
Factor F	0.44	0.68	1	1.5

Example

A vessel volume of 400 litres should be evacuated, in 5 minutes, to 400 mbar. The water pressure is 3 bar. Which pump size is required?

From diagram fig. 6, for 400 mbar and 3 bar, a time of 1.8 minutes/100 litre vessel volume is found. For the evacuation of a vessel volume of 400 litres a liquid jet vacuum pump size 2 requires 4 x 1.8 = 7.2 minutes. As, however, only 5 minutes are available, the above formula is used to calculate the factor for the size of pump required:

$$F = \frac{1.8}{100 \cdot 5} \cdot 400 = 1.44$$

According to the above table factor 1.5 - corresponding to pump size 3 - is the closest to the calculated value. Pump size 3 is therefore selected.

The motive liquid consumption will be influenced by the suction pressure p_0. This is established by means of the curves in fig. 7.

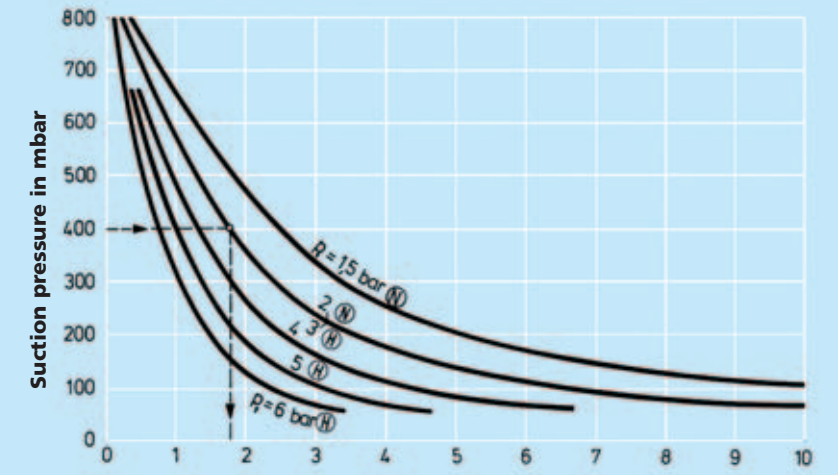

Specific evacuation time $t_{spec.}$ in min/100 l vessel volume for size 2

Fig. 6

Ⓝ = Low pressure construction (1.5 – 2 bar)

Ⓗ = High pressure construction (3 – 6 bar)

p_1 = Motive water pressure

(Pressures stated in bar correspond to gauge)

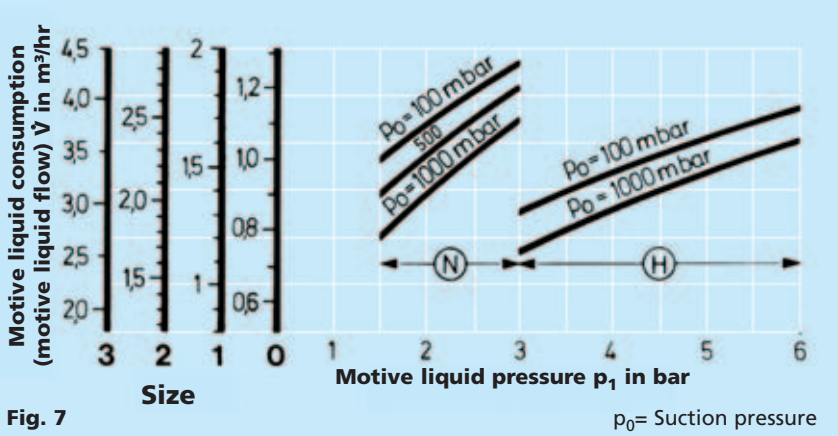

Fig. 7

p_0= Suction pressure

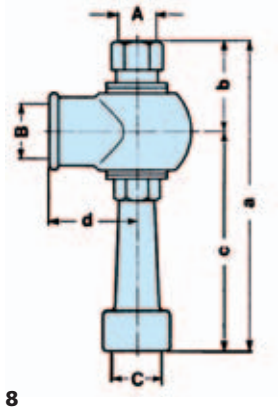

Fig. 8

Connections, Dimensions and Weights

	Size	0	1	2	3
Operating water conn.	A	R ½"	R ¾"	R 1"	R 1½"
Suction connection	B	R ½"	R ½"	R ¾"	R 1"
Pressure connection	C	R ½"	R ½"	R ¾"	R 1"
Length in mm	a	240	260	310	405
	b	65	70	80	105
	c	175	190	230	300
	d	35	40	45	50
Weight kg		0.9	1.4	2.3	3.1

Standard construction:

I Cast iron , motive nozzle: brass

II Cast iron, motive nozzle: stainless steel

III Completely of stainless steel

Special constructions:

Hastelloy, Titanium, Plastic (PVC, PP, PVDF, PTFE) etc.
For standard pumps of porcelain, please see catalogue sheet 2000 fvp 3.

For all inquiries please use our questionnaire on page B 21.

GEA Jet Pumps GmbH
Einsteinstrasse 9-15
Tel.: +49 (0) 72 43 / 70 50
Email: info@geajet.de
D-76275 Ettlingen
Fax: +49 (0) 72 43 / 70 53 51
Internet: www.geajet.com
Wiegand Technology

Liquid Jet Vacuum Pumps with flanged connections

Fig. 1

Liquid jet vacuum pumps generally use water as the motive medium. They are simple in construction, consisting of the head, the diffusor and the motive nozzle. They are safe in operation and maintenance free, whilst the capital outlay is low.

The operation of these liquid jet vacuum pumps is based on the liquid jet from the motive nozzle emerging at a higher velocity, entraining air or gas in the head and compressing it to atmospheric pressure.

Liquid jet vacuum pumps with flanged connections are mainly used for the production of vacuum in technical institutions and in production plants for example for vacuum distillation and vacuum drying.

They are also used for evacuating syphon lines, suction lines of circulating pumps and condensers; for the deaeration of pressure vessels and for producing negative pressure in a Nutsch filter.

Liquid jet vacuum pumps, when water is used as the motive medium, can be directly coupled to the water line. If, however, the water consumption has to be as economical as possible, the operating water may be circulated. This is also so for all cases where other liquids are used as the motive medium.

The temperature of the operating liquid may be kept low by the constant addition of a small quantity of fresh liquid. Higher vacuum can be reached by the further cooling of the motive medium. This is particularly expedient when the suction flow contains condensible components, eg. solvents. In such a case the vacuum pump can be operated by using the condensate as the motive medium.

The lowest suction pressure which can be obtained with a suction capacity of 0 (blind vacuum) corresponds to the vapour pressure of the motive liquid which is dependent upon the temperature of the liquid.

For the motive medium of water the relationship between water temperature and lowest suction pressure is shown in fig. 2.

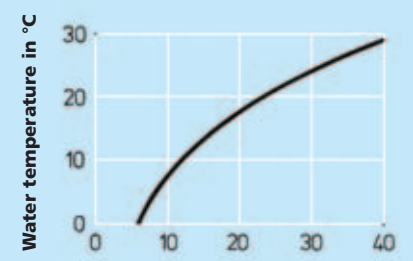

Fig. 2 **Abs. pressure in mbar**

Liquid jet vacuum pumps will still operate satisfactorily if the outlet pipe is below the liquid level (see fig. 3), or if a reducing piece is connected to the liquid outlet.

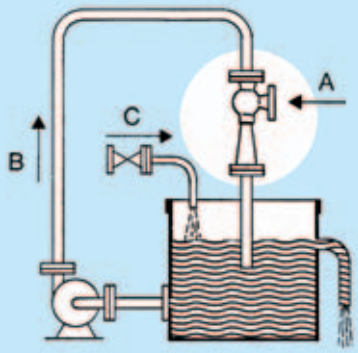

A = Suction connection
B = Operating liquid
C = Fresh liquid

Fig. 3

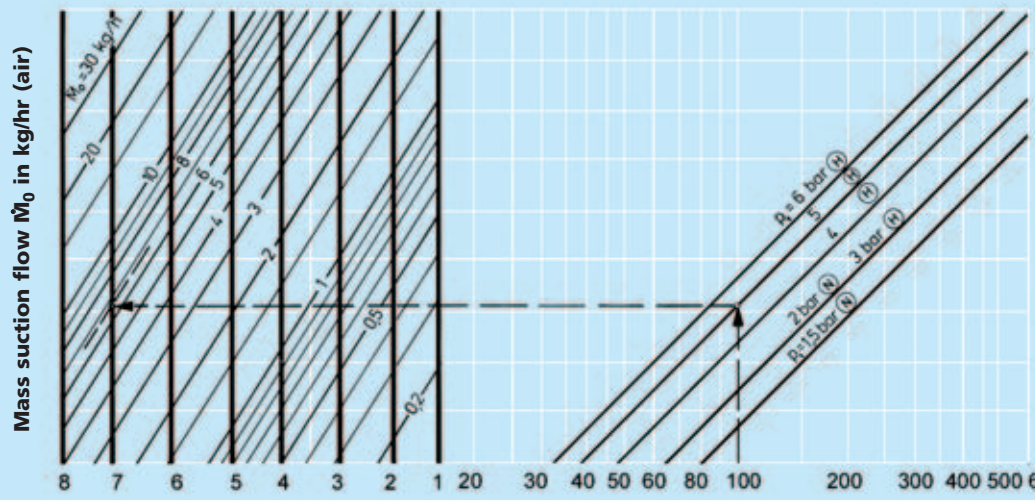

Diagram fig 4 gives the mass suction flow in kg/h air in relation to the suction pressure at various operating water pressures for 8 pump sizes. The curves are based on an operating water temperature of 20 °C. The motive water consumption (circulating water flow) can be read from diagram fig. 5.

Pressures stated in bar correspond to gauge.

Fig. 4

(N) Low pressure construction (1.5 – 2 bar) (H) = High pressure construction (3 – 6 bar)

p_1 = Motive water pressure

GEA Jet Pumps GmbH
Einsteinstrasse 9-15 D-76275 Ettlingen
Tel.: +49 (0) 72 43 / 70 50 Fax: +49 (0) 72 43 / 70 53 51
Email: info@geajet.de Internet: www.geajet.com
Wiegand Technology

Evacuation Time

Diagram **fig. 6** gives the time in minutes a liquid jet vacuum pump size 4 needs to evacuate a vessel volume of 1 m³ to a defined suction pressure.
The selection of other sizes is achieved by the following conversion formula:

$$F = \frac{t_{spec.}}{t_{evac.}} \cdot V$$

F = Factor for the selection of the pump size

$t_{spec.}$ = Specific evacuation time in min/m³ (from diagram fig. 6)

$t_{evac.}$ = Expected evacuation time in minutes

V = Volume of vessel to be evacuated in m³

Example

A vessel of 3 m³ is to be evacuated to 400 mbar in 10 minutes. The water pressure is 3 bar. Which pump size is required?

From diagram fig. 6, for 400 mbar and 3 bar, a time of 8 min/m³ is found. For the evacuation of a vessel volume of 3 m³, a liquid jet vacuum pump size 4 requires 3 x 8 = 24 minutes.

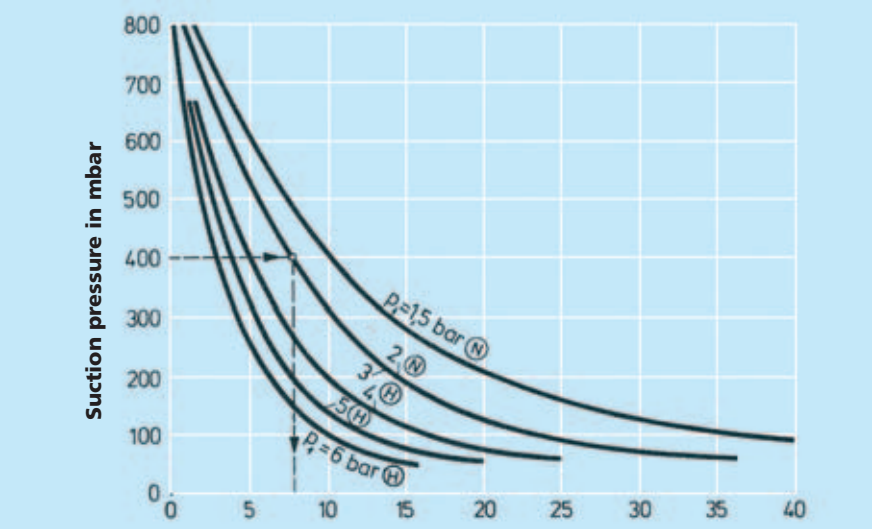

Fig. 6 **Specific evacuation time $t_{spec.}$ in min/m³ vessel volume for size 4**
(N) Low pressure construction (H) High pressure construction p_1 = Motive water pressure

Size	1	2	3	4	5	6	7	8
Factor F	0.28	0.40	0.63	1	1.6	2.5	4	6.3

However, as only 10 minutes are available the above formula is used to calculate the factor for the size of pump required:

$$F = \frac{8}{10} \cdot 3 = 2.4$$

According to the table factor 2.5 corresponding to pump size 6 is closest to the calculated value. Pump size 6 is therefore selected.

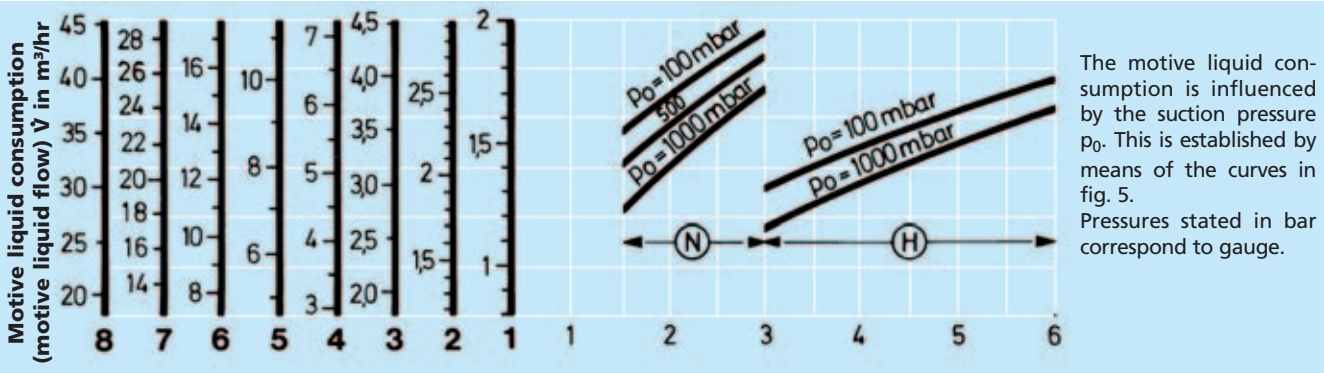

The motive liquid consumption is influenced by the suction pressure p_0. This is established by means of the curves in fig. 5.
Pressures stated in bar correspond to gauge.

Fig. 5 p_0= Suction pressure (abs.) in mbar (N) Low pressure construction (1.5-2 bar) (H) High pressure construction (3-6 bar)

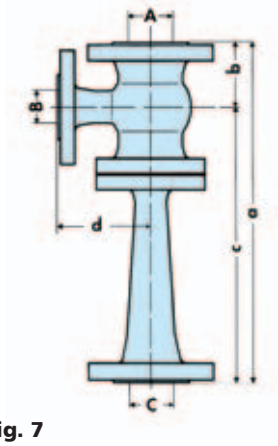

Fig. 7

Connections, Dimensions and Weights

	Size	1	2	3	4	5	6	7	8
Operating water conn.	A	25	25	32	40	50	65	65	80
Suction connection	B	20	20	25	32	40	40	50	65
Pressure connection	C	15	20	25	32	40	50	65	80
Length in mm	a	207	267	347	407	478	608	778	963
	b	60	60	63	68	78	78	78	113
	c	147	207	284	339	400	530	700	850
	d	85	85	100	115	125	125	125	135
Weight		8	10	13	18	26	35	55	65

Standard construction:
I Cast iron , motive nozzle: brass
II Cast iron, motive nozzle: stainless steel
III Completely of stainless steel, loose flanges: steel

Flanges to DIN PN 10

Special construction:
Hastelloy, Titanium, plastic (PVC, PP, PVDF, PTFE) etc.
For standard pumps of porcelain, please see catalogue sheet 2000 fvp 3.

For all inquiries please use our questionnaire on page B 21.

GEA Jet Pumps GmbH
Einsteinstrasse 9-15
Tel.: +49 (0) 72 43 / 70 50
Email: info@geajet.de
D-76275 Ettlingen
Fax: +49 (0) 72 43 / 70 53 51
Internet: www.geajet.com
Wiegand Technology